

**ELECTROMAGNETIC  
COMPATIBILITY IN WIRELINE  
COMMUNICATIONS**

**D. M. Lauder**

*A thesis submitted in partial fulfilment  
of the requirements of the University of Hertfordshire  
for the degree of Doctor of Philosophy*

**October 2007**

**ELECTROMAGNETIC  
COMPATIBILITY IN WIRELINE  
COMMUNICATIONS**

**David Maxwell Lauder**

*A thesis submitted in partial fulfilment  
of the requirements of the University of Hertfordshire  
for the degree of Doctor of Philosophy*

The programme of research was carried out in the School of Electronic, Communication and Electrical Engineering, Faculty of Engineering and Information Sciences, University of Hertfordshire, United Kingdom.

**October 2007**

## **Abstract**

This document is a thesis submitted in partial fulfilment of the requirements of the University of Hertfordshire for the degree of Doctor of Philosophy (Part Time) in 'EMC in Wire-line Communications' in the School of Electronic, Communication and Electrical Engineering at the University of Hertfordshire. It describes a programme of research into the modelling and measurement of radio frequency interference emissions from various communication networks including Power Line (Tele)communications (PLC/PLT) and Digital Subscriber Line (DSL).

An introduction and literature review are followed by the results of practical measurements on installed networks. These measurements include antenna gain and Longitudinal Conversion Loss (LCL). Power line communication networks, splitterless DSL and home phonenumber networks in buildings are studied and modelled and the models are compared with the measured results.

Improved EMC test methods are also described, in particular the modelling and design of four types of portable antennas for use in radiated EMC measurements with improved sensitivity at frequencies up to 30 MHz. The first type is a set of three manually tuned loop antennas covering 100 kHz - 30 MHz. The second is a set of three loop antennas that cover a similar frequency range but with remote tuning via an optical fibre link, under the control of software which also controls an EMC measuring receiver. The third type is a larger (1.6 m diameter) tuned loop covering 1.75 - 10 MHz that allows the measuring system noise floor to be below the typical atmospheric noise floor. The fourth type is an electrically short dipole covering 10 - 30 MHz with improved matching.

The protection requirements for various types of radio communication services are analysed and are compared with emission levels from various types of wireline communication network. A review of existing applicable EMC standards and standards under development is also presented.

## **Acknowledgements**

The support of the following persons and organisations is acknowledged:

- Principal PhD supervisor Prof. Yichuang Sun.
- Professor Reza Sotudeh, Head of School of Electronic, Communication and Electrical Engineering at the University of Hertfordshire for making laboratory and other resources available for research purposes.
- University of Hertfordshire Research assistants James Moritz and Joyce Nyamukapa who assisted in the development of the tuned loop antennas.
- University of Hertfordshire Part time BEng student Alistair Stuart whose final year project included constructing a Macfarlane Network.
- The Radiocommunications Agency of the DTI for loan of a Rohde and Schwarz ZVR network analyser to support the research described in this report and for awarding contracts for the development of tuned loop antennas.
- Schaffner EMC Systems Ltd., for industrial design assistance in connection with the remotely tuned loop antennas and also for performing antenna calibration at their test site.
- The Radio Society of Great Britain EMC Committee for the loan of two types of home powerline networking adaptors for evaluation and for providing regular updates on the current state of EMC standards development.
- Mr A. Talbot of DERA at Portsmouth, Hants for providing spectrum plots of test signals received via ionospheric propagation.
- Mr Ray Brannon of Eastern Electricity for arranging the supply of short off cuts of several types of three-phase cable used in underground low voltage electricity distribution networks.

## **Declaration**

The material contained in the following publications has been pre-published and has been incorporated into this thesis by the author:

D. Lauder and Y. Sun, "Modelling and measurement of radiated emission characteristics of power line communications systems for standards development," presented at 3rd IEEE International Symposium on Power-Line Communications and its Applications, Lancaster, UK, 1999.

D. Lauder and J. Moritz, "Design of a portable measuring system capable of quantifying the LF and HF spectral emissions from telecommunications transmission networks at field strengths of 1 microvolt/metre and below," University of Hertfordshire Report for RA, Ref. AY3430, 1999.

D. Lauder, "Development of Practical Methods and Equipment to Facilitate Detection and Measurement of Radiation From, and Wideband Radio Frequency Currents in, Unstructured Distribution Networks," University of Hertfordshire, report for RA Ref. AY3920, 5 Jan 2003.

D. Lauder, "EMC and Interference Issues Related To Networking Systems Used In The Home - Examining Compatibility Issues and Worldwide Standards That May Impact Home Phoneline And Powerline Networks" presented at 3rd Home Networks Congress, London, 2001.

D. Lauder and Y. Sun, "Radiated emission characteristics of communication systems using unscreened cables," presented at IEE 11th International Conference on Electromagnetic Compatibility, York, UK, 1999.

D. Lauder and Y. Sun, "Prediction and measurement of HF radiated emissions from communication networks that use unscreened cables," presented at HF Radio Systems and Techniques, 2000. Eighth International Conference on (IEE Conf. Publ. No. 474), Guildford, UK, 2000.

Lauder D, Sun Y, "EMC Measurements of Radiated Emissions up to 30 MHz from Installed Communication Cables", IEE Symposium, "EMC - It's Nearly All About the Cabling", IEE Savoy Place, London, UK. 22 Jan 2003.

Lauder D, Sun Y, "Modelling and Measurement of Radiated Emission Characteristics of In-building Power and Telecommunications Cables", IEE Symposium, "EMC and Broadband - The Last Mile" IEE, Savoy Place, London, UK. 17 May 2005

D. Lauder, "EMC - PLT," in Radio Communication, vol. 77, No. 4, 2001, pp. 90.

Lauder, D "EMC - Measuring background noise," in Radio Communication, vol. 83, No. 6, 2007, pp. 45.

Lauder D, Page-Jones R, Robins F and Clayton Smith H "Compatibility between radio communications services and power line communication systems - A position paper prepared by the RSGB EMC Committee for the PLC Workshop in Brussels, 5-Mar-2001," <http://www.rsgb.org/emc/pdfs/plt/emcplc.pdf> (accessed July 2007)

# **CONTENTS**

<b>Abstract</b>	<b>ii</b>
<b>Acknowledgements</b>	<b>iii</b>
<b>Declaration</b>	<b>iv</b>
<b>Table of figures</b>	<b>x</b>
<b>List of tables</b>	<b>xiii</b>
<b>Chapter 1. Introduction</b>	<b>1</b>
<b>1.1. Some EMC aspects of wireline communication networks</b>	<b>1</b>
1.1.1. Power line (tele)communications	1
1.1.2. Broadband over Powerline	2
1.1.3. Digital Subscriber Line (xDSL)	2
<b>1.2. Effect of emissions from wireline networks on radio communications</b>	<b>3</b>
<b>1.3. Aims</b>	<b>5</b>
<b>1.4. Objectives</b>	<b>5</b>
1.4.1. The need for improved EMC measuring antennas	6
1.4.2. Measurement of radiated emission characteristics of various networks	6
1.4.3. Modelling of radiated emission characteristics of wire-line data communication networks	6
1.4.4. Interference potential of emissions from various networks and the protection of radio communication services	7
<b>1.5. Original contributions</b>	<b>7</b>
<b>1.6. Organisation of this thesis</b>	<b>7</b>
<b>Chapter 2. EMC characteristics of power and telecommunications cables</b>	<b>9</b>
<b>2.1. Measurement of Longitudinal Conversion Loss (LCL) using a Macfarlane network</b>	<b>9</b>
<b>2.2. LCL measurements of in-building telecommunications cables and equipment</b>	<b>11</b>
<b>2.3. LCL measurements of in-building power cables and equipment</b>	<b>15</b>
<b>2.4. Emissions from Power Line telecommunication (PLT) systems</b>	<b>21</b>
<b>2.5. Emissions from Digital Subscriber Line (xDSL) systems and home networks</b>	<b>25</b>

<b>2.6.</b>	<b>Emissions from underground power cables</b>	<b>28</b>
2.6.1.	Configuration of test site	29
2.6.2.	Results	31
2.6.3.	Interpretation of results	33
<b>2.7.</b>	<b>Emissions from home powerline networks</b>	<b>33</b>
2.7.1.	Test configuration	34
2.7.2.	Test results (Microlink dLAN)	34
2.7.3.	Test results (SMC EZ-Connect)	37
<b>2.8.</b>	<b>Modelling of potential for radiated emissions from networks</b>	<b>40</b>
<b>2.9.</b>	<b>Other techniques for measuring emissions from networks</b>	<b>42</b>
2.9.1.	Current probe measurements	42
2.9.2.	Non-Contact Current Measurement	43
<b>2.10.</b>	<b>Conclusions</b>	<b>45</b>
<b>Chapter 3.</b>	<b>Antenna modelling of wireline networks</b>	<b>47</b>
<b>3.1.</b>	<b>Antenna modelling of in-building power line networks</b>	<b>48</b>
<b>3.2.</b>	<b>Antenna modelling of underground powerline networks</b>	<b>51</b>
<b>3.3.</b>	<b>Antenna modelling of in-building splitterless DSL and home phoneline networks</b>	<b>52</b>
<b>3.4.</b>	<b>Antenna modelling of BPL powerline networks</b>	<b>52</b>
<b>3.5.</b>	<b>Conclusions</b>	<b>56</b>
<b>Chapter 4.</b>	<b>Development of improved EMC measuring antennas</b>	<b>57</b>
<b>4.1.</b>	<b>Measurement of radiated emissions from networks up to 30 MHz</b>	<b>57</b>
<b>4.2.</b>	<b>Tuned loop antennas</b>	<b>59</b>
4.2.1.	Analysis of tuned loop antennas	61
4.2.2.	Loop antenna parameters	64
4.2.3.	Loop tuning	65
4.2.4.	Loop loading and bandwidth.	66
4.2.5.	Digital control of antenna tuning	68
4.2.6.	Pre-amplifier	70
4.2.7.	Noise floor of measuring system	70
<b>4.3.</b>	<b>Remote control of antennas</b>	<b>71</b>
4.3.1.	Tuning technique	72
4.3.2.	Hardware description	72
4.3.3.	Optical fibre link	76
4.3.4.	Communication protocol	76
4.3.5.	Microcontroller firmware	77
4.3.6.	LabVIEW™ software	78



4.3.7.	Laboratory testing	80
4.3.8.	Pre-calibration of tuned loops	81
4.3.9.	Final calibration	82
<b>4.4.</b>	<b>Further development of measuring antennas</b>	<b>83</b>
4.4.1.	A 1.6 m diameter untuned loop for 1.75 - 10 MHz	83
4.4.2.	A 1.6 m diameter tuned loop for 1.75 - 10 MHz	84
4.4.3.	Loop tuning technique	86
4.4.4.	Loop antenna control logic	86
<b>4.5.</b>	<b>A short dipole measuring antenna for 10 - 30 MHz</b>	<b>88</b>
<b>4.6.</b>	<b>Conclusions</b>	<b>91</b>
<b>Chapter 5.</b>	<b>Antenna modelling of EMC measuring antennas</b>	<b>93</b>
<b>5.1.</b>	<b>Modelling of a loop antenna</b>	<b>93</b>
<b>5.2.</b>	<b>Modelling of a short horizontal dipole antenna</b>	<b>96</b>
<b>5.3.</b>	<b>Modelling of a short vertical monopole antenna</b>	<b>98</b>
<b>5.4.</b>	<b>Conclusions</b>	<b>100</b>
<b>Chapter 6.</b>	<b>Protection of Radio Communication Services</b>	<b>101</b>
<b>6.1.</b>	<b>Protection of various radio communication services</b>	<b>102</b>
6.1.1.	Analogue LF/MF/HF broadcasting	102
6.1.2.	Digital Radio Mondiale	104
6.1.3.	Military HF communications	104
<b>6.2.</b>	<b>Interference models for wireline networks</b>	<b>104</b>
6.2.1.	Home powerline networking	105
6.2.2.	Home phonenumber networking or splitterless xDSL	106
<b>6.3.</b>	<b>Conclusions</b>	<b>109</b>
<b>Chapter 7.</b>	<b>EMC Standards and regulatory issues</b>	<b>110</b>
<b>7.1.</b>	<b>Legislation</b>	<b>110</b>
<b>7.2.</b>	<b>Applicable EMC standards</b>	<b>111</b>
7.2.1.	A review of existing EMC standards	111
7.2.2.	A review of EMC standards development for wireline communications	113
7.2.3.	Recent standards work on PLT/PLC	117
<b>7.3.</b>	<b>Conclusions</b>	<b>118</b>
<b>Chapter 8.</b>	<b>Final analysis of research programme and recommendations for further investigations</b>	<b>120</b>

<b>8.1.</b>	<b>EMC measurements - conclusions</b>	<b>120</b>
<b>8.2.</b>	<b>EMC measurements - suggestions for further work</b>	<b>120</b>
<b>8.3.</b>	<b>Emissions from wireline networks - conclusions</b>	<b>121</b>
<b>8.4.</b>	<b>Emissions from wireline networks - suggestions for further work</b>	<b>121</b>
<b>8.5.</b>	<b>Protection of radio communications - conclusions</b>	<b>122</b>
<b>8.6.</b>	<b>Protection of radio communications - suggestions for further work</b>	<b>122</b>
<b>References</b>		<b>123</b>
<b>Bibliography</b>		<b>131</b>
<b>Appendix A. Remotely tuned loop antenna hardware schematics</b>		<b>134</b>
<b>Appendix B. LabVIEW™ Virtual Instrument (VI) diagram for remotely tuned loop antennas</b>		<b>136</b>
<b>Appendix C. Scattering or ‘s’ Parameters</b>		<b>137</b>
<b>Appendix D. The author's research papers and reports</b>		<b>140</b>

## **Table of figures**

Figure 1. A block diagram of a possible 'Access' PLT network .....	1
Figure 2. Schematic diagram of an LCL probe [44].....	11
Figure 3. Test configuration for cable pair LCL measurements.....	12
Figure 4. Photograph of test configuration for cable LCL measurements. ....	12
Figure 5. LCL test results for a 10 m length of two pair UTP cable. ....	13
Figure 6. LCL test results for two items of telephone equipment. ....	14
Figure 7. LCL test results for a 10 m length of power cable (configuration 'A' & 'B'). ....	16
Figure 8. LCL test for power cable with LCL probe grounded to an independent earth (configuration 'C').....	16
Figure 9. LCL test results for a 10 m length of power cable driven between phase and neutral with neutral and earth grounded at the far end (configuration 'C'). ....	17
Figure 10. LCL test results for two electrical appliances.....	18
Figure 11. LCL test for power cable with LCL probe grounded to protective earth conductor in the power cable (configuration 'D') .....	20
Figure 12. Equivalent circuit of the electrical power network tested.....	22
Figure 13. Measured impedance of house mains wiring .....	23
Figure 14. Effective antenna gain of indoor mains power wiring in dBd for differential mode signals.....	25
Figure 15. Impedance of indoor extension telephone wiring for differential mode signals.....	27
Figure 16. Effective antenna gain of indoor extension telephone wiring in dBd for differential mode signals. ....	28
Figure 17. Configuration of underground cable test site .....	29
Figure 18. Spectrum plots of signals received from buried cable test transmissions.....	32
Figure 19. Conducted emission plot from Microlink dLAN 150 kHz - 30 MHz with peak detection. ....	35
Figure 20. Conducted emission plot from Microlink dLAN 15.0 - 15.025 MHz with QP detection .....	36
Figure 21. Conducted emission plot from Microlink dLAN 15.0 - 15.025 MHz with average detection .....	37
Figure 22. Conducted emission plot from SMC EZ-Connect 150 kHz - 30 MHz with peak detection. ....	38
Figure 23. Conducted emission plot from 16.6 - 16.65 MHz with QP detection.....	39
Figure 24. Conducted emission plot from 16.6 - 16.65 MHz with average detection.....	40

Figure 25. (A) Measurement of differential mode current, (B) measurement of common-mode current.....	42
Figure 26. The use of a 30 cm diameter untuned active loop for non-contact current measurement.....	43
Figure 27. Measured and calculated current transducer factors versus distance from cable. ....	45
Figure 28. Antenna model of a section of in-building power network.....	49
Figure 29. Detail near the origin for a section of in-building power network.....	49
Figure 30. Detail at the far end of a section of in-building power network .....	50
Figure 31. AEC/ARRL antenna model for a BPL network, reproduced from [61] .....	52
Figure 32. Antenna model of a 200 m section of power line with 50 $\Omega$ terminations, showing relative current amplitude.....	53
Figure 33. Far field plots for the antenna in Fig 32 at 10 MHz, with 50 $\Omega$ loads. ....	54
Figure 34. Far field plots for the antenna in Fig 32 at 10 MHz, with 530 $\Omega$ loads. ....	55
Figure 35. Far field plots for the antenna in Fig 32 at 30 MHz, with 50 $\Omega$ loads. ....	56
Figure 36. Noise floor for various radiated field strength measuring systems using QP detection and 9 kHz bandwidth.....	58
Figure 37. Equivalent circuit for an electrically small loop antenna.....	61
Figure 38. Equivalent circuit of an electrically small loop with transformer matching .....	63
Figure 39. Predicted antenna factors of antennas 'A', 'B' and 'C' in passive mode .....	66
Figure 40. Design bandwidth and loaded 'Q' factors of antennas 'A', 'B' and 'C' .....	67
Figure 41. The prototype set of manually tuned loop antennas.....	68
Figure 42. The prototype set of remotely tuned loop antennas during laboratory testing.....	69
Figure 43. Block diagram of a loop antenna with remote tuning. ....	69
Figure 44. Measuring system noise floor, 'E' and 'H' field strength for loops 'A', 'B' and 'C' in active mode (QP and average detection).....	71
Figure 45. Block diagram of an EMC measuring system using a remotely tuned loop antenna.....	72
Figure 46. The assembled microcontroller board mounted in the box.....	74
Figure 47. The assembled switched capacitor board mounted in Loop 'C' box .....	75
Figure 48. Front panel diagram for Swept Measurement R&S ESCS30.vi .....	78
Figure 49. Outdoor pre-calibration of the remotely tuned loop antennas .....	81
Figure 50. RA field trials on a PLT network in Campbeltown using tuned loop 'B'.....	82
Figure 51. A 1.6m diameter untuned loop with balanced series capacitors and a balun:.....	84
Figure 52. A 1.6m diameter tuned loop with 1800 $\Omega$ parallel load resistance.....	86
Figure 53. The prototype 1.6 m diameter loop mounted on a tripod.....	87

Figure 54. The prototype 1.6 m diameter loop folded for transportation.....	88
Figure 55. Short dipole antenna factors, reproduced from CISPR 16-1 [65].....	90
Figure 56. Antenna model of a 1.6 m diameter loop antenna.....	93
Figure 57. Far field horizontally polarised plot of a 1.6 m diameter loop at 1.75 MHz .....	94
Figure 58. Far field vertically polarised plot of a 1.6 m diameter loop at 1.75 MHz.....	95
Figure 59. Far field horizontally polarised plot of a 1.6 m diameter loop at 10 MHz .....	95
Figure 60. Far field vertically polarised plot of a 1.6 m diameter loop at 10 MHz.....	96
Figure 61. Antenna model of a 4.4 m long horizontal dipole.....	96
Figure 62. Horizontally polarised far field plot of a 4.4 m horizontal dipole at 30 MHz .....	97
Figure 63. Horizontally polarised far field plot of a 4.4 m horizontal dipole at 10 MHz .....	98
Figure 64. Antenna model of a 2.5 m vertical monopole with ground radials .....	99
Figure 65. Vertically polarised far field plot of a 2.5 m vertical monopole at 10 MHz.....	99
Figure 66. Vertically polarised far field plot of a 2.5 m vertical monopole at 30 MHz.....	100
Figure 67. The proposed radiated limits from the draft ETSI PLT SRD and CENELEC SC205A (Sec)75 in relation to background noise levels at frequencies up to 30 MHz.....	115
Figure 68. A proposed PLT transmit power limit from the ETSI PLT SRD and CENELEC SC205A (Sec) 75 in relation to EN 55022 Class 'B' conducted emission limits and background noise levels on mains power networks at frequencies up to 30 MHz.	116
Figure 69. Schematic diagram of loop remote tuning microcontroller board .....	134
Figure 70. Schematic diagram of loop remote tuning switched capacitor board .....	135
Figure 71. Block diagram for Swept Measurement R&S ESCS30.vi (version 1.2).....	136

## **List of tables**

<b>Table 4.2.2. Summary of loop characteristics.</b>	<b>65</b>
<b>Table 6.2.1. Worst case parameters for a home powerline network.</b>	<b>106</b>
<b>Table 6.2.2A Worst case parameters for a home phoneline network</b>	<b>108</b>
<b>Table 6.2.2B Worst case parameters for a 'splitterless' VDSL network</b>	<b>108</b>

## Terms and abbreviations

ADSL	Asymmetric Digital Subscriber Line
AEC	Ameren Energy Communications
ARRL	American Radio Relay League
BPL	Broadband over Powerline
BT	British Telecom
CATV	Community Antenna Television
CCIR	Comité Consultatif International de Radio
CENELEC	Comité Européen de Normalisation Electrotechnique (European Committee for Electrotechnical Standardisation)
CEPT	European Conference of Postal and Telecommunications Administrations
CISPR	Comité International Spécial des Perturbations Radioelectriques (International Special Committee on Radio Interference)
CW	Continuous Wave
dBd	Antenna gain in dB relative to a dipole
dBi	Antenna gain in dB relative to an isotropic source.
dB( $\mu$ V)	dB relative to a p.d. of 1 $\mu$ V.
dB( $\mu$ V/m)	Electric field strength in dB relative to an 'E' field strength of 1 $\mu$ V/m.
dB( $\mu$ A/m)	Magnetic field strength in dB relative to an 'H' field strength of 1 $\mu$ A/m.
dB/m	dB per metre. Unit of 'E' field antenna factor, i.e. $20 \text{ Log}_{10}(E_i/V_o)$ where $E_i$ is the incident field strength and $V_o$ is the antenna output p.d. into its designed load.
dBm/Hz	Power spectral density in dB relative to a reference level of 1 mW in 1 Hz bandwidth.
dBS	dB relative to a conductance of 1 siemens
DECT	Digital Enhanced Cordless Telephone
DERA	Defence Evaluation and Research Agency of the UK Ministry of Defence (now separated into two organisations, QinetiQ and DSTL)
DSL	Digital Subscriber Line
EC	European Commission
EMC	Electromagnetic Compatibility
ESR`	Effective Series Resistance
ETSI	European Telecommunication Standards Institute
ISDN	Integrated Services Digital Network

HF	High Frequency (3 MHz to 30 MHz)
ITU	International Telecommunications Union (Formerly CCIR)
ITU-R	ITU-Radiocommunications Sector
LAN	Local Area Network
LCL	Longitudinal Conversion Loss
LISN	Line Impedance Stabilisation Network
LV	Low Voltage
LVEDN	Low Voltage Electricity Distribution Network
MDF	Mains Decoupling Factor
MF	Medium Frequency (300 kHz to 3 MHz)
NEC	Numerical Electromagnetics Code
NPL	National Physical Laboratory
NVIS	Near-Vertical Incidence Skywave
Ofcom	Office of Communications
p.d.	Potential difference
PLC	Power Line Communications
PLT	Power Line Telecommunications
PME	Protective Multiple Earthing
PSD	Power spectral density
QP	Quasi-Peak
R&S	Rohde and Schwarz
RA	Radiocommunications Agency of the DTI (now part of Ofcom)
RA/RTCG	Radiocommunications Agency Radio Technology & Compatibility Group
RF	Radio Frequency
RFI	Radio Frequency Interference
RSGB	Radio Society of Great Britain
TCL	Transverse Conversion Loss
TEM	Transverse Electro-magnetic
TDR	Time Domain Reflectometry
VDSL	Very High Speed Digital Subscriber Line
VI	Virtual Instrument
VSB	Vestigial Sideband
xDSL	Generic DSL, e.g. ADSL, VDSL, etc.



## Chapter 1. Introduction

This chapter introduces EMC aspects of some wireline communication networks and outlines the effect that emissions from such networks may have on radio communications. It also includes the aims and objectives of the programme of research, details of original contributions and the organisation of the thesis.

### 1.1. Some EMC aspects of wireline communication networks

#### 1.1.1. Power line (tele)communications

Power Line (Tele)communications (PLC/PLT) use electrical power wiring for data communications [1]. There are two types of PLT, 'Access' PLT and in-house PLT. Fig 1 shows a block diagram of a possible Access PLT network.

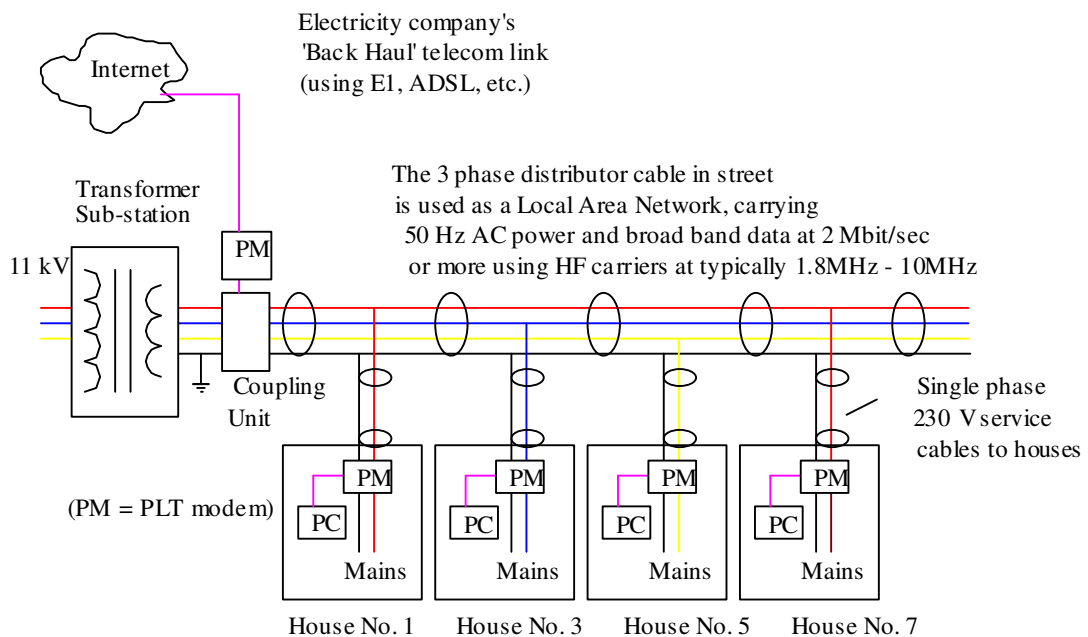


Figure 1. A block diagram of a possible 'Access' PLT network

The network in Fig 1 provides Internet access via the existing 3-phase distributor cable along the street. As the transmission medium is shared, the total data rate available must be shared between multiple users.

In-house PLT systems can be used for home computer networks using electrical power wiring to transmit data. Such networks may be used to allow multiple computers to share a broadband

Internet connection, which could be via access PLT, xDSL or cable TV modem. Another recent application for home powerline networks is digital audio or video streaming for home entertainment systems.

Various 'access' PLT trials have been conducted in the UK and elsewhere and measurements have been made by RA/Ofcom [2], [3] BBC [4] and others [5], [6].

A report by The Smith Group Ltd. for the RA [7] describes a study to develop a model to predict the radiation properties of certain line transmission systems, namely a PLT system that was used by Nor.Web in the North West of the UK and a British Telecom xDSL system. The Smith report includes a detailed analysis and test results for radiated emissions of access PLT signals from lamp posts and also considers radiated emissions from wiring in buildings and from buried cables.

A German language report by the Technical University of Dresden [8] includes results of comprehensive tests of the radiated emission characteristics of PLC networks.

### **1.1.2. Broadband over Powerline**

The term 'Broadband over Powerline' (BPL) originates in the USA where electrical power distribution networks in residential areas typically use overhead wires carrying medium voltage with pole-mounted transformers. BPL networks use the overhead power cables for data transmission in the frequency range 1.7 - 80 MHz, which clearly has significant EMC implications due to cables being unshielded and widely spaced[9], [10]. BPL is being introduced in various countries and limited trials of BPL for a 'back haul' link on a PLT network have been conducted in the UK [11], [12].

### **1.1.3. Digital Subscriber Line (xDSL)**

ADSL uses existing copper telephony cables to transmit data between telephone exchanges and telephone customers at rates of up to 8 MB/s for ADSL or 22 Mbps for ADSL2 [13], [14]. ADSL uses frequencies up to 1.1 MHz and ADSL2 uses frequencies up to 2.2 MHz. EMC issues to be considered include radiated emissions from underground and overhead telephony cables [15], [16]. In the case of 'splitterless' ADSL, there is no filter to isolate the xDSL signals

from in-building telephone wiring, hence radiated emissions from such wiring also need to be considered.

VDSL is a further development of ADSL uses existing copper telephony cables to transmit data between telephone customers and new optical network units over distances of up to approximately 1 km. VDSL can achieve higher data rates than ADSL but may use frequencies up to 10 MHz [17]. DSL systems are generally crosstalk-limited so there is little advantage in increasing the launch power and in any case, launch power is constrained by EMC considerations. Hence in order to increase theoretical maximum data rate as defined by the Shannon-Hartley Law it is necessary to reduce the line length, thereby permitting an increase in the available bandwidth and/or signal to noise ratio.

A paper by Foster of BT on the radio frequency environment for high speed metallic access systems [18] considers emission and immunity aspects of EMC in xDSL systems including VDSL. A report for the RA by York EMC Services Ltd. [19] describes an investigation into impedance and mode conversion of telecommunications cables for xDSL systems. A report for the RA by ERA Technology Ltd [20] describes continuation of investigations into the possible effect of DSL related systems on radio services, specifically the potential for interference from ADSL systems on aeronautical radio beacons operating in the frequency range 255 kHz - 526.5 kHz. The ERA report also gives preliminary consideration to the potential for interference to HF radio services due to unintentional emissions radiated by VDSL lines.

## **1.2.Effect of emissions from wireline networks on radio communications**

The principle of using radio frequency communication via electrical power distribution wiring is not new but previously, the frequencies used have been below those used for broadcasting, i.e. below 150 kHz in Europe where there is a Long Wave broadcast band and below 450 kHz in other regions where there is no Long Wave broadcasting. If such frequencies are used for data communications, the maximum data rate that can be achieved is limited due the limited bandwidth available. This has led to pressure to introduce PLT and xDSL systems that operate above 150 kHz, and up to 30 MHz.

The use of frequencies above 150 kHz for PLT and xDSL needs to take account of EMC standards, whose purpose is to protect radio services from interference from non-radio sources. Such sources include unintentional signals generated by equipment such as switch-mode power supplies and also intentional signals generated by DSL, PLT, DPL and other wire line communication systems.

In principle, PLT or xDSL are no different to television, sound and/or cable TV modem signals distributed via a cable network, where radiated emissions are controlled by existing standards.

PLT requires considerable transmission bandwidth to achieve data rates of the order of megabits per second and various multi-carrier modulation techniques such as OFDM may be used [21]. As mains cables are not generally screened, terminated or filtered, signals cannot be confined to power distribution cables alone and will be radiated by all connected wiring. Unless existing limits such as those for cable TV networks are applied, such emissions have the potential to interfere with other radio services nearby. There is also a possible cumulative effect of many such emissions over considerable distances.

The HF radio spectrum is regarded by many as a valuable natural resource, supporting world-wide analogue and digital broadcasting, commercial and military communication services, aviation, the amateur radio service and other HF services [22]. Radio services require adequate protection from HF PLT. Both the Royal Air Force Signals Engineering Establishment [23] and the Army CIS Engineering Group [24] have produced reports on the possible effect of PLT on military HF communications. Studies have also been performed into protection of 'sensitive' receiving sites such as the BBC Monitoring Site at Caversham and also protection of marine and airborne MF/HF communications [25], [26].

There are some significant new developments that appear likely to ensure continued use of the HF radio spectrum. These involve the replacement of conventional forms of modulation by new digital techniques that are optimised for the propagation characteristics of an HF radio path. These include a new digital broadcasting standard, Digital Radio Mondiale (DRM) that has been developed for high quality international HF broadcasting as well as national MF and HF broadcasting [27], [28], [29]. The protection of DRM broadcasts from interference from PLT has been extensively studied by Stott [30], [31], [32], [33], [34], [35], [36], [37].

Other services such as military communications are using digital modulation techniques to provide reliable and secure long distance communications without reliance on potentially vulnerable communication satellites. A common factor to all such digital communication systems is that although they are resistant to interference from narrow band interfering carriers, they are susceptible to interference from broad-band noise-like interfering sources such as PLT.

### **1.3.Aims**

The overall aim of the programme of research was to improve electromagnetic compatibility in wireline communication networks such as PLC/PLT and xDSL.

Specific aims were as follows:

- To improve methods of EMC measurement of radiated emissions below 30 MHz, particularly with regard to sensitivity.
- To characterise and predict emissions of various data communication systems.
- To determine ways of protecting radio communications services from interference.

### **1.4.Objectives**

The following objectives were identified for the programme of research:

1. Development of EMC measuring antennas for use at frequencies up to 30 MHz, with substantially higher sensitivity than currently available types.
2. Measurement of the radiated and conducted emission characteristics of various wireline networks.
3. Development of a model of the radiated emission characteristics of wire-line data communication networks and verification of the model using measured results.
4. Study of the interference potential of emissions from various networks and derivation of suitable emission limits for protection of radio communication services.

The objectives were achieved as follows:

#### **1.4.1. The need for improved EMC measuring antennas**

Existing EMC measuring antennas for measuring radiated emissions below 30 MHz suffer from poor sensitivity, which results in a relatively high measuring system noise floor. This has led to some claims that emissions from networks such as PLT are 'below the noise floor' at a given distance when such emissions were actually below the noise floor of the measuring equipment but not below the noise floor of radio communications services to be protected.

The need for improved EMC measuring antennas was identified by the Radiocommunications Agency (RA) of the DTI who funded two development contracts related to this programme of research [38] and [39]. This work was followed by further independent development of EMC measuring antennas that allow the measuring system noise floor to be set by HF background atmospheric and/or man-made noise temperature rather than the noise temperature of a measuring receiver or an active antenna.

#### **1.4.2. Measurement of radiated emission characteristics of various networks**

The need for additional work on the development of test methods for measuring radiated emissions from network cables was also identified by the RA and was funded by part of a development contract from the RA [39]. Further independent work on this topic was performed to cover other types of networks and also measurements of Longitudinal Conversion Loss (LCL) in cables.

#### **1.4.3. Modelling of radiated emission characteristics of wire-line data communication networks**

Antenna modelling software was used to model wireline communication networks as unintentional radiating antennas.

#### **1.4.4. Interference potential of emissions from various networks and the protection of radio communication services**

Work on EMC standards and regulatory issues relating to wireline communication networks included consultancy work to the RA to attend field measurements of PLT systems at Crieff [40] and Campbeltown in Scotland and to accompany RA staff at a technical meeting in Berlin with the German telecommunications regulator Reg TP. The RA also sponsored the author of this report to present a paper on EMC at a Home Networking conference [41]

### **1.5. Original contributions**

This thesis includes the following original contributions:

- Measurement of LCL for various types of power and telecommunication wiring
- Measurement of antenna characteristics of various types of power and telecommunication wiring.
- Antenna modelling of various types of power and telecommunication wiring
- Design and development of manually tuned and remotely tuned loop antennas for EMC measurements up to 30 MHz
- Design of a high sensitivity loop antenna for frequencies of 1.75 - 30 MHz and an e-field measuring antenna for 10 - 30 MHz.

### **1.6. Organisation of this thesis**

**Chapter 1. Introduction.** This chapter

**Chapter 2. EMC characteristics of power and telecommunications cables.** This chapter describes LCL measurements of in-building power and telecommunications cables and equipment using a Macfarlane network. It also considers modelling and measurement of radiated emissions from PLT systems, xDSL systems, home networks and underground power cables. Other methods of measurement are also considered including current probe measurements and non-contact current measurement

**Chapter 3. Antenna modelling of wireline networks** applies antenna modelling software in-building power line networks splitterless DSL and home phonenumber networks and BPL powerline networks

**Chapter 4. Development of improved EMC measuring antennas.** This chapter analyses the design of tuned loop measuring antennas for the measurement of radiated emissions from

networks at frequencies up to 30 MHz. It also analyses loop tuning techniques, loading and bandwidth, digital remote control of tuning by software. Measuring system noise floor and antenna calibration are also considered. A design for a higher sensitivity 1.6 m diameter tuned or untuned loop for 1.75 - 10 MHz is also presented together with a design for short dipole measuring antenna for 10 - 30 MHz

**Chapter 5. Antenna modelling of EMC measuring antennas** applies antenna modelling software to a loop antenna, a short horizontal dipole antenna and a short vertical monopole antenna.

**Chapter 6. Protection of radio communication services** studies protection requirements of various HF radio communication services.

**Chapter 7. EMC standards and regulatory issues** reviews existing EMC standards and standards under development in the context of wireline communication systems.

**Chapter 8. Final analysis of research programme and recommendations for further investigations.** Contains the conclusion to this thesis and suggestions for further work.



## **Chapter 2. EMC characteristics of power and telecommunications cables**

This chapter describes LCL measurements of in-building power and telecommunications cables and equipment using a Macfarlane network. It also considers modelling and measurement of radiated emissions from PLT systems, xDSL systems, home networks and underground power cables. Other methods of measurement are also considered including current probe measurements and non-contact current measurement.

For any telecommunication network that uses unshielded cable pairs for transmission, there are two ways in which the signal being transmitted may give rise to a radiated emission. First, the wanted differential-mode signal itself may radiate to a significant extent if the two halves of the cable form a loop with a significant area and if the cable pair is not twisted. This is of particular significance for BPL systems using overhead cables where the conductor spacing may be of the order of 1 m. Secondly, mode conversion may occur where a proportion of the wanted differential mode signal is converted into an unwanted common-mode signal. In such cases, the common-mode signal may be the predominant source of radiated emissions from the cable. Due to the principle of reciprocity, mode conversion also increases susceptibility to external RF fields.

Mode conversion may be caused by imperfect balance in a source, load or cable [42]. Subject to certain limitations, mode conversion can be quantified by measuring longitudinal conversion loss (LCL) or transverse Conversion Loss (TCL) of a wire pair network, a source or load. The general principle of TCL measurement is to launch a differential-mode signal and measure the extent to which it is converted to a common-mode signal. For practical reasons, it is generally preferable to measure LCL which is related to TCL.

### **2.1. Measurement of Longitudinal Conversion Loss (LCL) using a Macfarlane network**

A probe for the measurement of electrical unbalance of networks and devices has been described by Macfarlane in a 1998 contribution to CISPR Subcommittee G Working Group 2 [43], and is further described in [44]. The Macfarlane Probe allows the measurement of longitudinal conversion loss (LCL) and transverse Conversion Loss (TCL) of wire pair

networks and two terminal devices. The method of measuring LCL and TCL is specified in ITU-T Recommendations G.117 [45] or O.9 [46].

In essence, TCL is a measure of the extent to which the wanted transverse mode (differential mode) signal in a cable pair is converted to an unwanted common-mode signal, which increases the potential for radiated emissions. A practical difficulty with the measurement of TCL is that measurement of the common mode signal may be masked by ambient signals, unless the measurement is performed in a shielded enclosure. This problem can be overcome by measuring LCL, which is related to the reciprocal of TCL. The advantage is an LCL measurement compared to a TCL measurement is that the mode conversion of ambient common-mode signals to differential mode is relatively small, being determined by the LCL whereas with a TCL measurement, it is the test signal that undergoes a relatively small amount of mode conversion and this can make it difficult to detect among the ambient common-mode signals.

Fig. 2 shows a schematic diagram of an LCL probe [44] which was constructed as per [47] and was calibrated as specified in [44]. When performing LCL tests, switch S1 is always open. When a network analyser is used, R1 is the source resistance of Port 1 of the analyser. To obtain the reference trace, Port 2 of the network analyser is connected to port *g* of the LCL network via a 'T' piece connector and R2 is the input resistance of Port 2 of the network analyser. Ports *e* and *f* of the LCL probe are both terminated with 50 Ω. A swept measurement of  $|S_{21}|$  provides a relative measurement of  $E_L$ , which is the reference trace (a brief explanation of 'S parameters is included in Appendix 'C'.  $E_L$  is typically close to 0 dB at most frequencies, falling to about -3 dB at frequencies where the common mode impedance of the balanced network under test is low due to resonance.

The 50 Ω termination is then removed from port *e* of the LCL probe and port *e* is connected to Port 2 of the network analyser. A 50 Ω termination R2 is connected via a 'T' piece to port *g*. A swept measurement of  $|S_{21}|$  provides a relative measurement of  $V_p$ . 6dB is then added to  $V_p$  and the result is assumed to be equal to  $V_T$ , the transverse voltage in 100 Ω. LCL is defined as follows [44]:

$$LCL = 20 \log_{10} \left| \frac{E_L}{V_T} \right| \text{ dB} \quad (1)$$

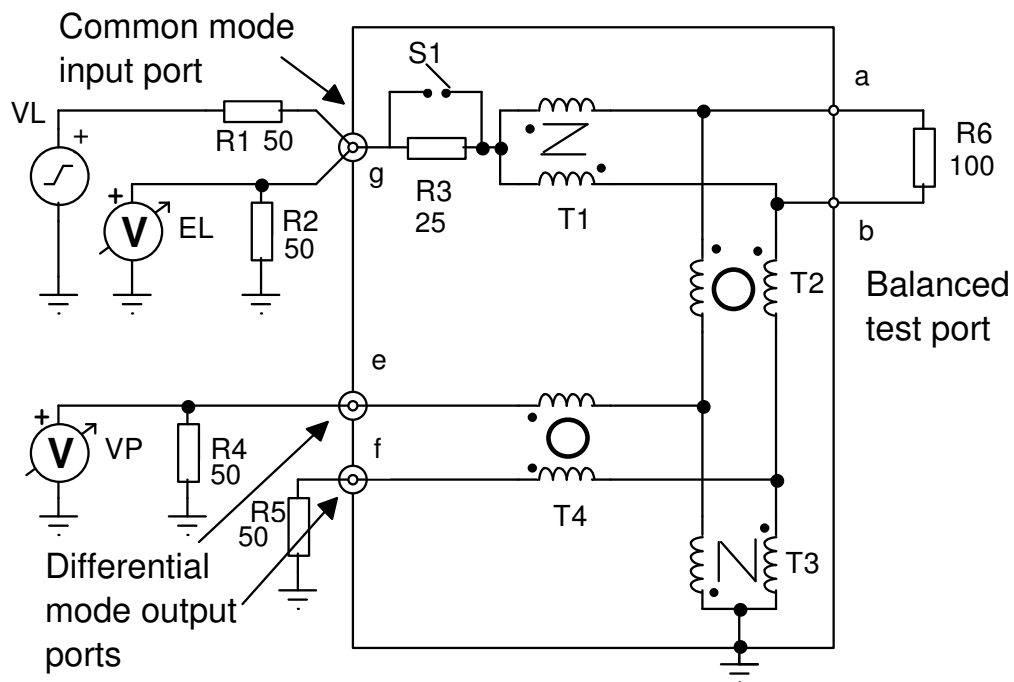


Figure 2. Schematic diagram of an LCL probe [44]

## 2.2. LCL measurements of in-building telecommunications cables and equipment

LCL measurements were performed on various cable samples, each with a length of 10 m, supported 1m above a conductive ground plane consisting of galvanised wire mesh, as shown in Fig. 3. The LCL probe was bolted to a vertical 1 m<sup>2</sup> sheet of 1 mm thick aluminium that was bolted to the mesh ground plane as shown in Fig. 4. The cable was a two pair unscreened twisted pair (UTP) cable of a type used for telephone extension wiring in buildings. Two different cable configurations were used. In configuration *A*, one pair was driven by the LCL probe and was terminated differentially with a 100  $\Omega$  load resistor at the far end. The second pair was not connected. In configuration *B*, one wire of the second pair was connected in parallel with one wire of the driven pair. This models the configuration of indoor telephone wiring that is commonly used in the UK, where a third 'ringer' wire is driven from one side of the line pair via a capacitor in the master telephone socket.

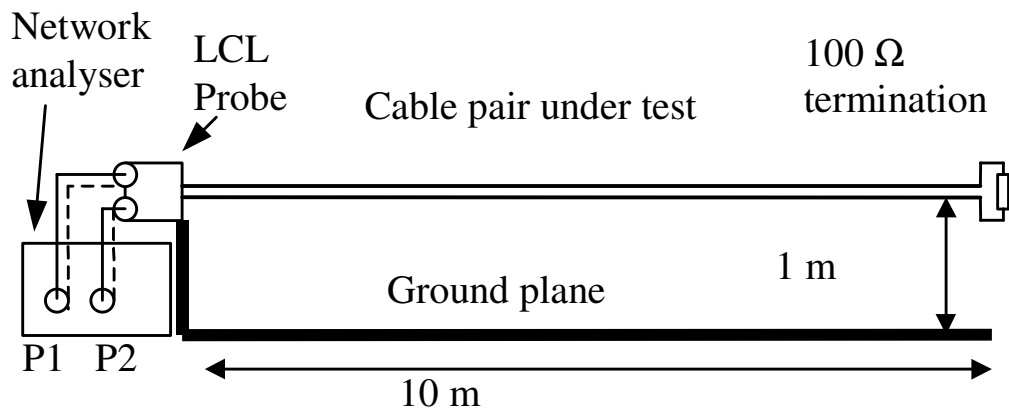


Figure 3. Test configuration for cable pair LCL measurements.

Fig. 4 shows a photograph of the test configuration for cable LCL measurements above a mesh ground plane.



Figure 4. Photograph of test configuration for cable LCL measurements.

The results of the two pair UTP cable test are shown in Fig.5 below. The vertical axis shows -LCL in dB rather than +LCL.

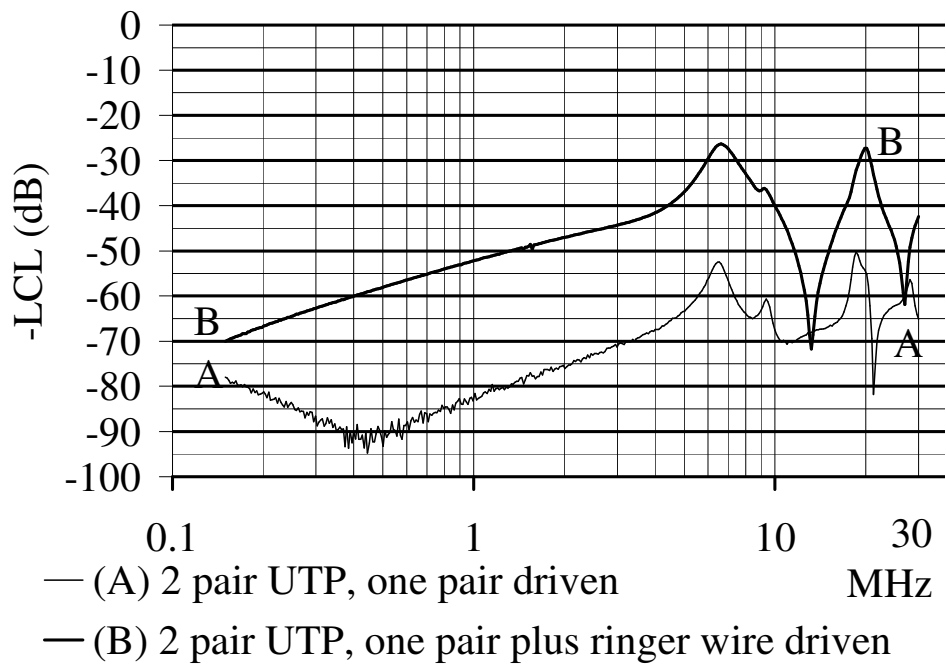


Figure 5. LCL test results for a 10 m length of two pair UTP cable.

In both cases, the peaks (lowest LCL) occur at frequencies where the electrical length of the cable is  $\lambda/4$  or  $3\lambda/4$  as these frequencies correspond to minimum common mode impedance and hence maximum common mode current. Trace *B* shows that the LCL is degraded by over 20 dB at most frequencies when driving an unbalanced pair including the third 'ringer' wire.

The LCL of some typical items of equipment that may be connected to a telephone line was also measured. The first was a relatively old fax machine with a built-in telephone answering machine. This uses the 'ringer' wire and is powered by an internal mains switch-mode power supply via a three core mains cable. The LCL measurement was performed by connecting the telecommunication line port of the fax machine to the balanced test port of the LCL probe and the mains earth wire of the fax machine to the ground of the LCL probe, using the shortest possible cables in both cases.

The second item was a DECT cordless telephone base unit which does not use the third 'ringer' wire. It is powered by an external transformer with no mains earth connection. For this test, the phase and neutral pins of the plug-in transformer were connected to the ground of the LCL probe. The results are shown in Fig. 6 below.

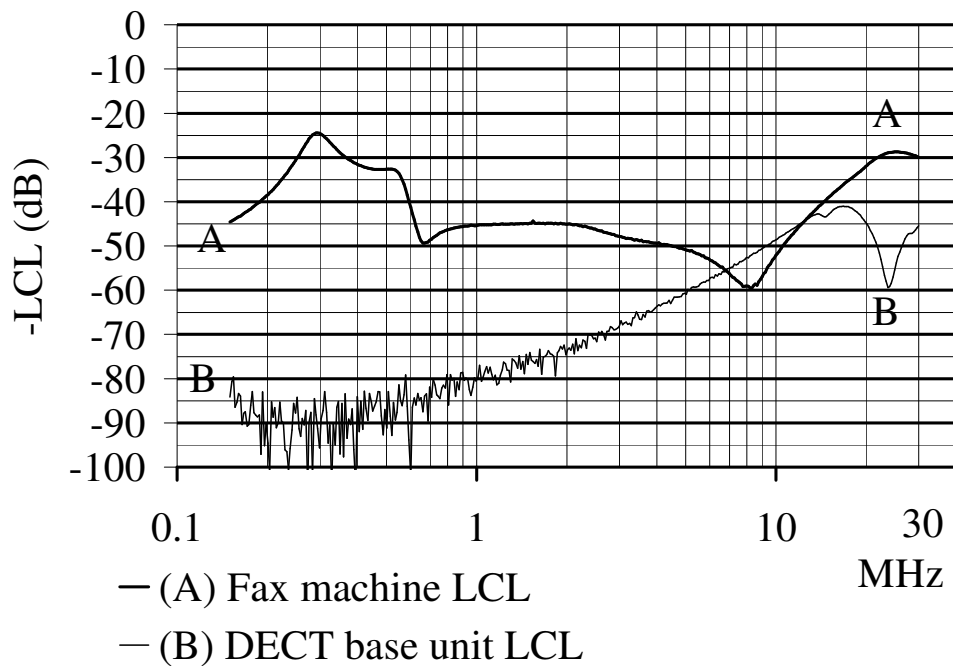


Figure 6. LCL test results for two items of telephone equipment.

Trace *A* in Fig. 6 shows that the fax machine causes a significant degradation in LCL when connected to in-building telephone extension wiring. The improvement in LCL with increasing frequency may be due to a three-turn ferrite ring choke that is fitted to the earth wire inside the fax machine, apparently for reasons of EMC compliance.

Trace *B* in Fig. 6 shows that the DECT base unit is relatively well balanced compared to the cable pair shown in trace *B* of Fig. 5.

The above LCL test results show that when modelling the radiated emission potential of in-building telephone wiring due to signals from splitterless DSL or home phonenumber networking, it is necessary to take account of the unbalance introduced by the third 'ringer' wire that is used in the UK and also the unbalance that may be introduced by certain types of connected equipment. Based on the results of the above tests, it is concluded that due to the combined effect of cable unbalance and connected equipment, a reasonable estimate of the worst-case LCL for a home phonenumber network or the in-building wiring of a splitterless DSL network is 20 - 25 dB from 150 kHz - 30 MHz. Nevertheless, if the cable length exceeds 10 m, a lower LCL may occur at certain frequencies.

### **2.3. LCL measurements of in-building power cables and equipment**

LCL measurements were performed on various power cable samples, each with a length of 10 m, supported 1 m above a mesh ground plane, as shown in Figs. 3 and 4 above.

The cable was a three-core 2.5mm<sup>2</sup> power cable of a type used in the UK for 230 V 'ring main' power circuits in buildings. Two different cable configurations were used. In configuration *A*, the phase and neutral were driven by the LCL probe and were terminated differentially with a 100  $\Omega$  load at the far end. The earth continuity conductor (ECC) of the cable was not connected. It is considered that this configuration shows the inherent balance of the cable when driven in a balanced manner. An alternative configuration *A* would be to use a split termination with 50  $\Omega$  phase to ECC and 50  $\Omega$  neutral to ECC. It is considered likely that this would give similar results to the configuration *A* with the ECC not connected, provided the two 50  $\Omega$  resistors are accurately matched.

In configuration *B*, one terminal of the LCL probe balanced test port was connected to the phase conductor and the other to the earth and neutral connected in parallel. The phase and neutral were terminated differentially with a 100  $\Omega$  load resistor at the far end. This models the normal configuration of power wiring in the UK, where the neutral and earth are connected together at the point where the supply enters the premises. The test configuration shows how a single power circuit would behave if RF signals are injected at or near the consumer unit (fuse box).

The results of the power cable LCL tests are shown in Fig. 7. Trace B shows that the LCL of the cable alone is degraded significantly by driving an unbalanced pair including the earth wire.

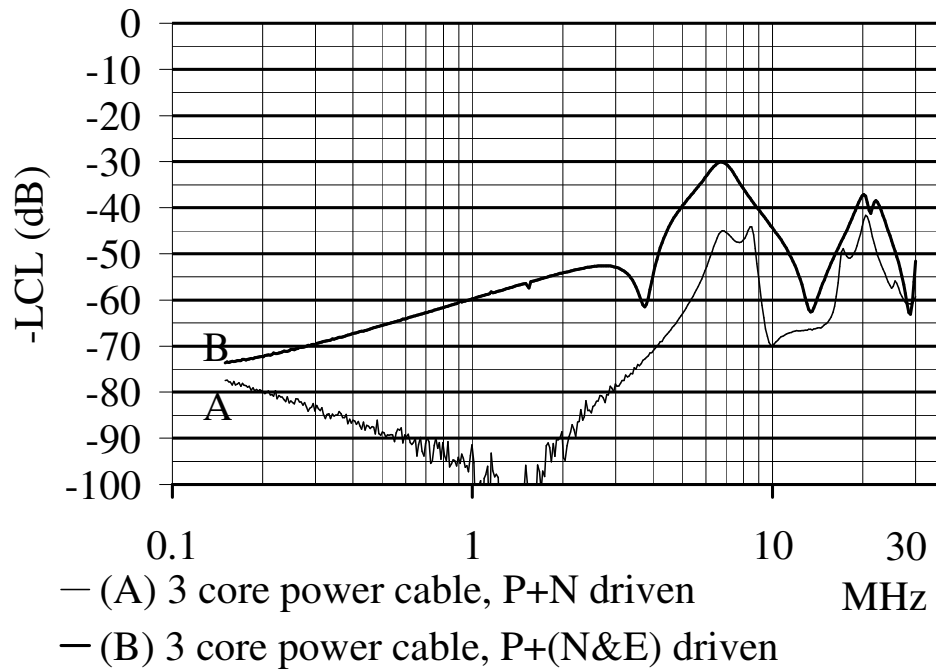


Figure 7. LCL test results for a 10 m length of power cable (configuration 'A' & 'B').

Another test was performed using configuration 'C', which was a modified form of the configuration in Fig. 2. The phase and neutral were driven by the LCL probe and terminated by  $100 \Omega$  load  $R_L$  at the far end where the earth and neutral were also connected together and grounded to the ground plane via a second vertical  $1\text{m}^2$  sheet of aluminium, as shown in Fig 8 below.

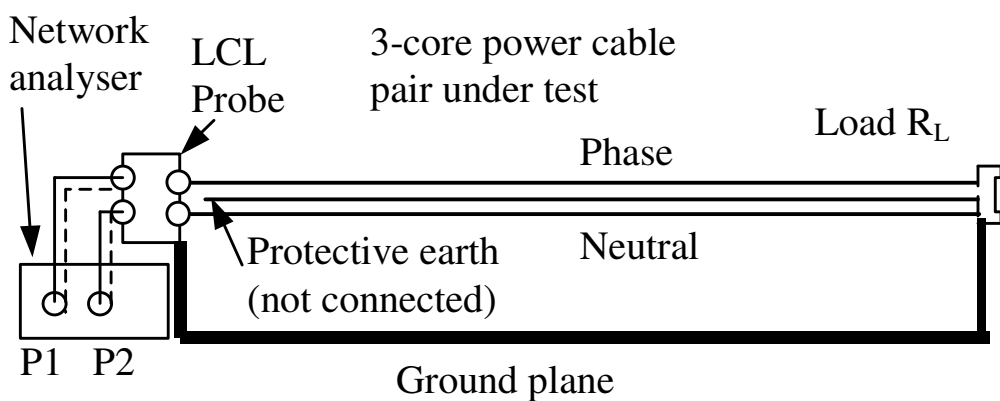


Figure 8. LCL test for power cable with LCL probe grounded to an independent earth (configuration 'C')



Fig. 8 models the situation where an RF signal is injected between phase and neutral at the end of a cable furthest from the consumer unit, e.g. a PLT modem that drives a differential mode signal between phase and neutral at one end of a power circuit. At the other end of the power circuit, earth and neutral are connected together, e.g. at point where the supply enters the building, representing standard UK wiring practice. In Fig 8, a load resistance  $R_L$  between phase and neutral terminates the wire pair in its characteristic impedance although in an actual installation,  $R_L$  would be a lower resistance representing the impedance of other power circuits and loads in parallel with the circuit under test.

Mode conversion due to unbalance in the network results in a common-mode voltage on the non-grounded end of the cable. This leads to radiated emissions with the phase + neutral wire pair radiating against ground. Quantifying this effect is the main purpose of LCL measurements.

The results are shown in Fig. 9 below. It can be seen that the LCL is worst at low frequencies, showing that much of the differential mode signal is converted to common mode.

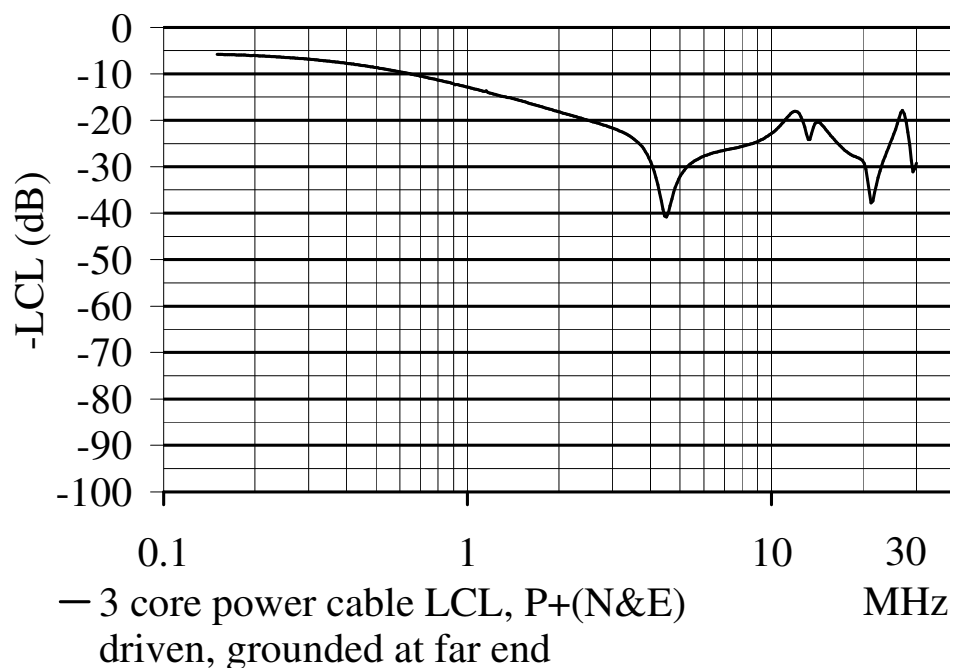


Figure 9. LCL test results for a 10 m length of power cable driven between phase and neutral with neutral and earth grounded at the far end (configuration 'C').

Tests were also performed to assess the unbalance that may be introduced by various types of electrical appliance connected to a mains power network in a building. Two items tested were a refrigerator/freezer and a microwave oven. The phase and neutral conductors of the appliance mains cable were connected to the balanced test port of the LCL probe and the earth conductor of the appliance mains cable was connected to the ground of the LCL probe. Neither appliance was powered during the test. The results are shown in Fig. 10 below.

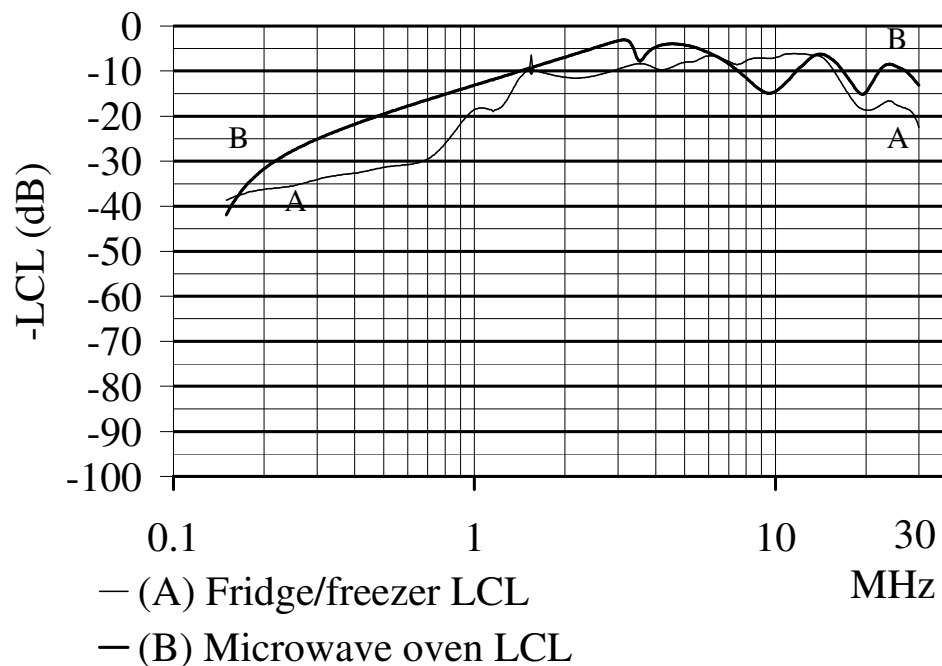


Figure 10. LCL test results for two electrical appliances.

Fig. 10 shows that the LCL of some types of electrical equipment is very poor, particularly above 1 MHz. In the case of the refrigerator, this may be due to the phase and neutral conductors separating inside the case and being of different lengths with significantly different capacitances to the earthed metal case of the appliance.

The above LCL test results show that when modelling the radiated emission potential of in-building power wiring due to differentially driven RF signals from powerline communications, it is important to take account of the unbalance introduced by the direct connection between earth and neutral in most UK installations and also the unbalance introduced by certain types of electrical appliance. Based on the results in Figs. 9 and 10 above, it is concluded that due to the combined effects wiring configuration and connected loads, a reasonable estimate for the

worst-case LCL from 150 kHz - 30 MHz for a section of a ring main on a UK PME installation with connected loads is approximately 5 - 10 dB. Typically, the direct connection between phase and neutral has the most significant effect at frequencies up to approx. 1 MHz while some types of connected appliance have a most significant effect above approx. 1 MHz.

Another factor that contributes to electrical unbalance of in-building power wiring at radio frequencies is lighting circuits where the phase conductor separates from the neutral and goes to light switches. This has two consequences. First, it introduces unbalance, which results in conversion of differential mode signals to common mode. Secondly, the phase conductors to and from the light switches form antennas that radiate in their own right. An LCL test is intended for networks with closely spaced conductors [44], which is not true of lighting circuits. An LCL measurement can only assess the first effect, i.e. mode conversion, not the antenna effect due to the spurs of the phase conductor. Even the mode conversion may not be measured accurately for a lighting circuit that supplies multiple rooms, each with its own light switch. This is because the common mode current at the LCL probe is the vector sum of multiple currents flowing in separate spurs of phase conductor. For example at a frequency where two spurs are spaced a half wavelength apart, the common mode currents at the LCL probe would oppose each other and the potential for radiated emissions due to mode conversion would be under-estimated.

Some researchers have performed in-situ LCL measurements on in-building power wiring [48]. by connecting a MacFarlane probe to electrical power sockets via a length of 3-core cable. This results in a configuration similar to Fig 11 below, which will be called configuration 'D'.

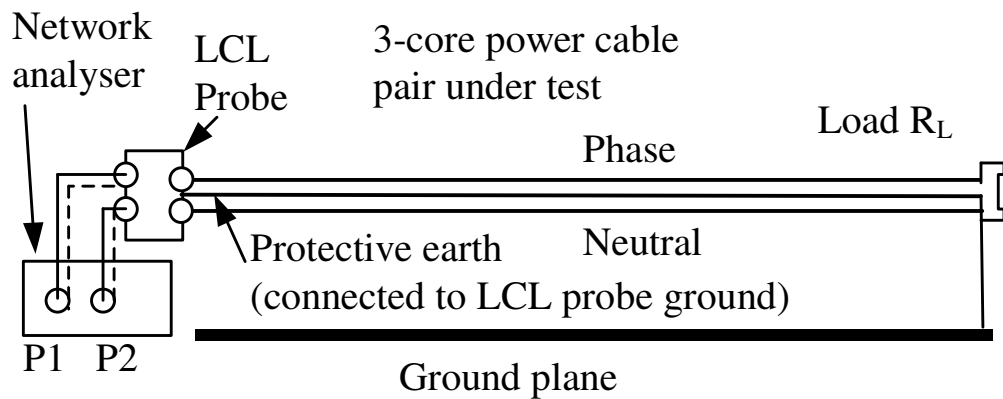


Figure 11. LCL test for power cable with LCL probe grounded to protective earth conductor in the power cable (configuration 'D')

There is an important difference between the method of grounding the LCL probe in Figs 8 and 11. In Fig 8, grounding is via a ground plane and sheets of metal 1 m wide whereas in Fig. 11, grounding is via a 10m length of protective conductor with a typical diameter of 1.35 mm. This raises the following issues:

- The impedance of the protective earth wire is relatively high. For example, it can be shown that the 10 m length of wire mentioned above would have an inductance of approximately  $19 \mu\text{H}$  and hence in isolation it would have an impedance of  $119 \Omega$  at 1 MHz or  $1190 \Omega$  at 10 MHz.
- Due to the close proximity of the protective earth wire to the phase and neutral conductors in the 3-core cable, it forms part of a transmission line so that the two adjacent conductors induce an e.m.f. onto the protective earth conductor.
- The common-mode impedance of the phase + neutral pair driven against a ground plane is likely to be substantially different from the common-mode impedance of the phase + neutral pair driven against the protective earth conductor which is situated between phase and neutral.

It is therefore not clear what a test configuration of the type shown in Fig. 11 is actually measuring but it does not appear to measure LCL as described in [44].

Whatever ground arrangement is used for grounding the LCL probe, the impedance of its ground conductor appears in series with the common mode impedance of the network under

test. The Macfarlane probe [44] works by driving a common-mode signal onto the cable pair under test and measuring the mode conversion to differential mode. Clearly, the impedance of its ground connection is an important consideration, because if this ground impedance is significant compared to the common-mode impedance of the cable under test, then the common-mode voltage driven onto the cable will be reduced. This will result in an error in measuring LCL, with the measured value appearing to show better balance than is actually the case.

It was found from the  $E_L$  traces for the cable measurements described above that the common mode impedance may be as low as  $20 \Omega$  at frequencies where the length of the cable under test is an odd multiple of a quarter wavelength. The impedance of the LCL ground conductor should therefore be substantially smaller than  $20 \Omega$  at RF in order to obtain accurate LCL measurements at frequencies where the common mode impedance is low. It is at these frequencies where the common mode current and hence the potential for radiated emissions is greatest. In practice, it may be difficult to achieve a sufficiently low impedance ground connection for the LCL probe, particularly for in-situ measurements where there is no ground plane. Nevertheless, all possible steps should be taken to minimise the impedance of the LCL probe ground connection, which should be an independent earth back to the protective earth star point for an in-building network (e.g. where the incoming supply cable enters the building). One possible technique for improving LCL probe grounding in the higher parts of the HF band (e.g. 10 - 30 MHz) is to use a local ground plane or elevated ground radials provided these are large enough to have a sufficiently high capacitance to earth and therefore a sufficiently low impedance to earth.

## **2.4. Emissions from Power Line telecommunication (PLT) systems**

Two types of PLC/PLT systems will be considered. So-called 'access' PLT provides data transmission from an electricity sub-station to a user whereas 'In house' PLT provides data communications within a building. Such systems have been developed by the Open PLC European Research Alliance (OPERA) For New Generation PLC Integrated Network and funded under the 6th FWP (Sixth Framework Programme)

In order to assess the interference potential of 'access' PLT systems for a given level of injected RF signal, it is necessary to determine how various configurations of Low Voltage Electricity Distribution Networks (LVEDN) and mains wiring in buildings perform as unintentional

transmitting antennas. Wiring at customer's premises appears to have greater potential for radiated emissions than underground distribution cables as at the majority of locations, 'downstream' signals injected at an electricity sub-station will suffer greater attenuation than the 'upstream' signals injected at the customer's premises.

Furthermore, in order to predict the level of radiated emissions from the 'upstream' signal, it is necessary to determine the load impedance and radiation efficiency of a representative configuration of domestic mains wiring [49].

Measurements were made to determine the RF characteristics of a typical configuration of UK mains wiring over the frequency range 1 - 30 MHz. The configuration tested is typical of UK houses wired in the past 30 years, using PME. An RF equivalent circuit is shown in Fig 12.

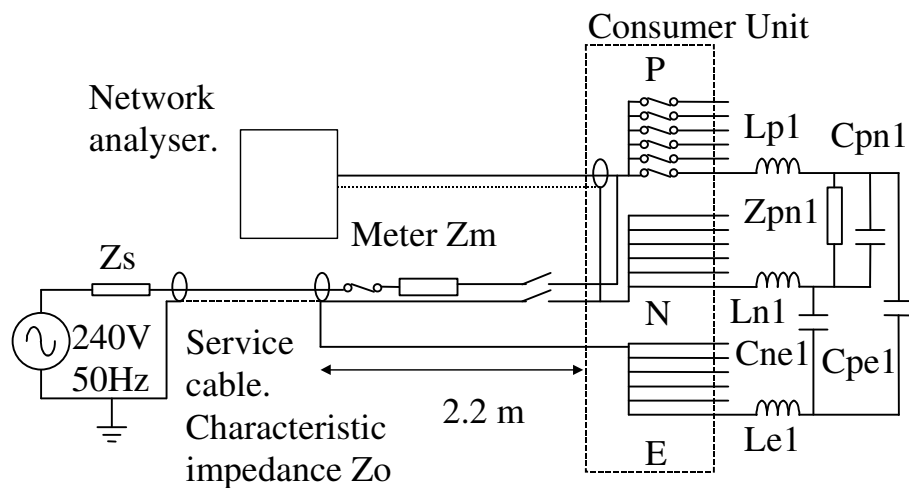


Figure 12. Equivalent circuit of the electrical power network tested

$Z_s$  represents the RF source impedance of the LV supply at the point where the single phase service cable to the house is connected to the three phase distributor cable under the street.  $Z_0$  is the characteristic impedance of the service cable, which is typically  $15 \Omega$  [50].  $Z_m$  represents the impedance of a conventional electromechanical type of electricity meter.

Six power and lighting circuits are connected in parallel at the consumer unit. An equivalent circuit of one of these is shown with  $L_{p1}$ ,  $L_{n1}$  and  $L_{e1}$  representing the series inductance of the phase, neutral and earth conductors respectively.  $C_{pn1}$ ,  $C_{pe1}$  and  $C_{ne1}$  represent the capacitance

between the three conductors and  $Z_{pn1}$  represents the impedance of the load connected to one circuit in Fig. 12.

The impedance was measured at the consumer unit between phase and neutral as shown in Fig. 12. To protect the test equipment, measurements were made with the wiring isolated from the mains supply. Nevertheless, other measurements made in [49] and [50] with the wiring 'live' gave similar results.

The network analyser was powered by a portable generator, because no mains supply was available and also to provide a galvanically isolated mains supply, i.e. a fully 'floating' supply with no connection to the power network under test. The network analyser was set so that it compensated for the length of 50  $\Omega$  coaxial cable from its Port 1 output to the point of measurement, i.e. the reference plane for measurements of  $S_{11}$  was at the consumer unit. Fig. 13 shows the results obtained from the  $S_{11}$  measurement with a reference impedance of 50 $\Omega$ .

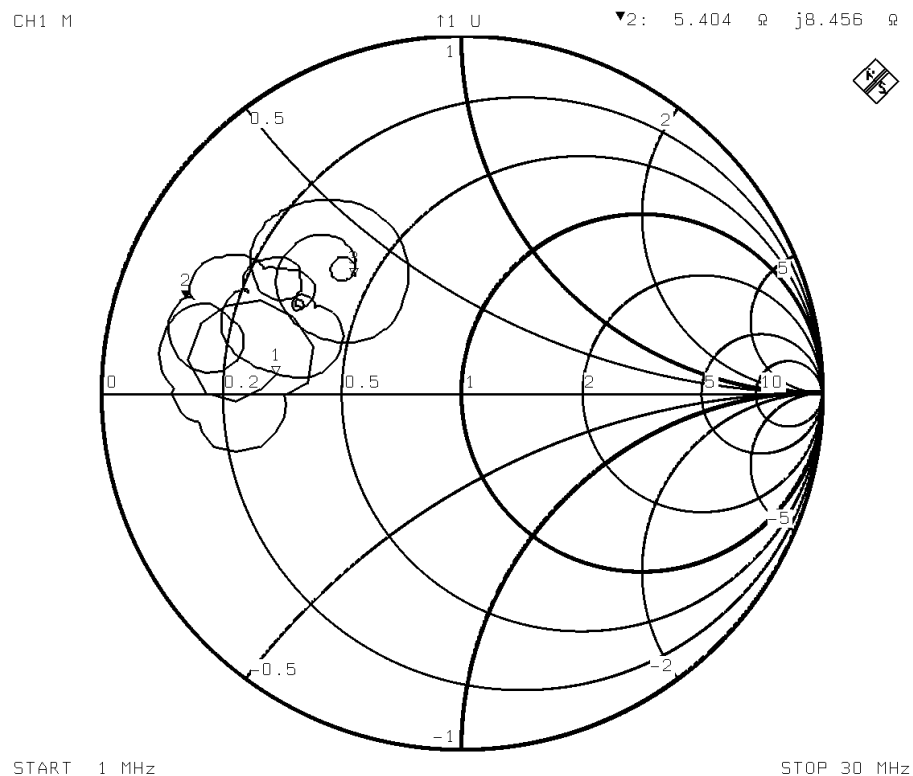


Figure 13. Measured impedance of house mains wiring

The triangular markers 1, 2 and 3 on the trace in Fig. 11 are at 1, 5 and 30 MHz respectively. It can be seen that over most of this frequency range, the real part of the impedance is between

10  $\Omega$  and 30  $\Omega$  and the imaginary part is between  $-j5 \Omega$  and  $+j25 \Omega$ . An approximate average impedance over the range 1 - 30 MHz is  $12 +j12 \Omega$ .

The network analyser was then used to make measurements of  $S_{21}$  where Port 2 was connected to the output of an active H-field measuring loop antenna. The measuring antenna was located 10 m from the rear wall of the house at a height of 1.5m above ground level and was powered using its battery pack. As the house wiring is a distributed source 10 - 20 m from the measuring loop, an effective source distance of 14m was assumed, which is the geometric mean of 10 m and 20 m.

The near field region of a point source or electrically small antenna is normally considered to extend to a distance of at  $\lambda/2\pi$  [51] which is approximately 10 m at a frequency of 4.77MHz. Hence a significant number of measurements are near-field measurements.

After taking account of the antenna factor of the measuring loop antenna, the magnitude of the  $S_{21}$  measurements were converted to an effective gain of the house wiring  $G$ , relative to a lossless half wavelength dipole that is perfectly matched to 50  $\Omega$  [50]. Fig. 14 shows the magnitude of  $G$  with a vertical scale from -60 dB to 0 dB. It should be noted that  $G$  is referenced to a dipole perfectly matched to 50  $\Omega$ , whereas the mains wiring tested is a relatively poor match to 50  $\Omega$ .

It can be seen from Fig. 14 that  $G$  from 1 - 30 MHz varies between -25 dB to -45 dB. Nevertheless, if an arithmetic mean value of  $G$  is required over a particular frequency range, it is necessary to convert  $G$  to linear units before calculating the mean. Other measurements [50] have shown that if the test signal source is well matched to load, values of  $G$  up to 6 dB higher may be obtained for the same wiring configuration.

The term 'K-factor' is also used to quantify the gain of network cabling as an antenna. The K-factor of a system under test is defined as the ratio between the received H-field strength  $H$  at a specified distance and the injected differential mode power  $P$  into the network [48], i.e.

$$K = H/P \tag{2}$$

where the units of  $H$  are dB( $\mu$ A/m) and the units of  $P$  are dBm



Another definition of K-factor that is sometimes found in published literature is the ratio between the received E-field strength  $E$  at a specified distance and the injected differential mode power  $P$ .

As K-factor is defined at a specified distance, it is necessary to know the 'regression rate' of field strength versus distance in order to scale a K-factor to another distance. In cases where the inverse square law applies, the regression rate is -20 dB/decade but the regression rate can be affected by near-field effects.

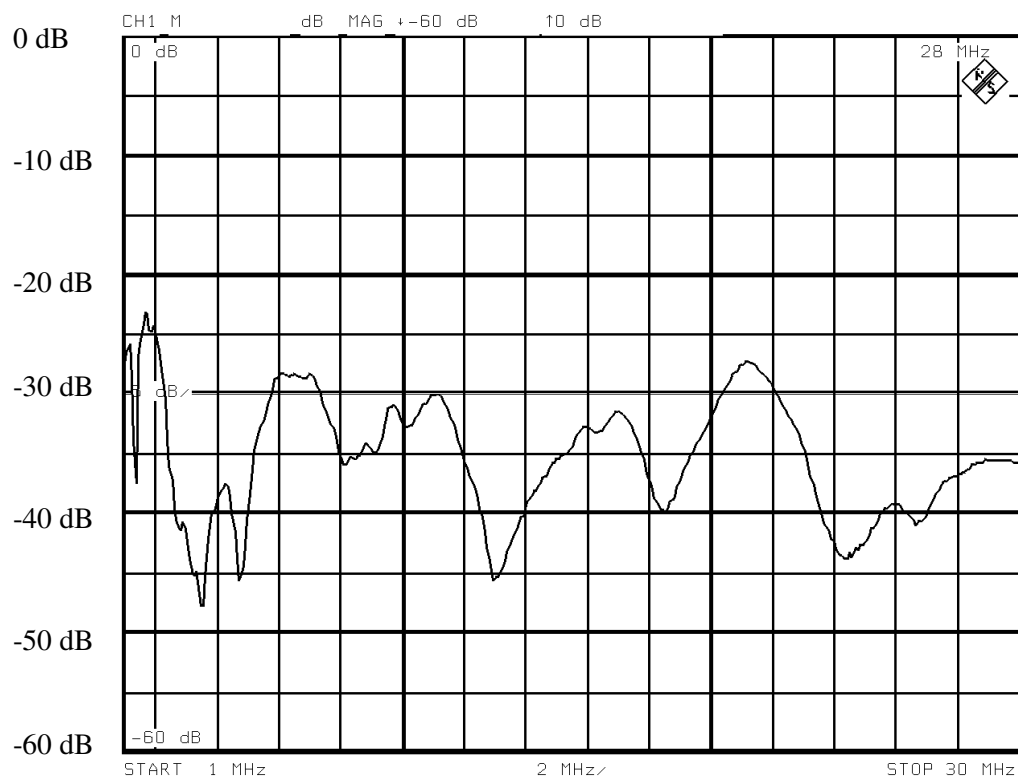


Figure 14. Effective antenna gain of indoor mains power wiring in dBd for differential mode signals.

## 2.5. Emissions from Digital Subscriber Line (xDSL) systems and home networks

The term xDSL covers various types of DSL (Digital Subscriber Line) technology including ADSL (Asymmetric DSL) and VDSL (Very high speed DSL). ADSL typically uses frequencies up to 1.1 MHz or 2.2 MHz for ADSL2 whereas VDSL may use frequencies up to 10 MHz or

higher. Whereas ADSL provides a link from customers' premises all the way to the local telephone exchange, VDSL would only link customers' premises to an intermediate Optical Network Unit (ONU) up to 1 km away. A further development of xDSL is 'xDSL Lite' or 'Splitterless xDSL' where the diplexer to separate base band and RF signals is omitted. Hence RF signals to/from the network can propagate along internal telephone extension wiring at the customers' premises.

A development that is available in the US and the UK is home phonenumber networking [52], which enables existing telephone wiring in a building to be used as a LAN without affecting its use for analogue telephony. One such system transmits 1 Mbit/sec Ethernet type signal using the frequency range 5.5 - 9.5 MHz. As shown below, the use of such a system is likely to result in a significant level of radiated emissions, particularly on existing UK telephone wiring where the third 'ringer' wire increases RF imbalance.

In order to assess the possible level of radiated emissions from 'xDSL Lite' systems or home phonenumber networks, tests were performed on a configuration of UK telephone extension wiring that is considered to represent a near worst case. Two branches run from a point near ground level where they would be connected to the BT master socket. The downstairs branch is 10 m long and is connected to a telephone, an answering machine, a fax machine and a modem. The upstairs branch is 20 m long and feeds three telephones.

The extension wiring was not connected to a BT master socket for the tests. Signals were injected between the 'A' and 'B' wires of the line pair, with a 1.8  $\mu\text{F}$  capacitor connected between the 'B' wire and the 'ringer' wire. This simulates the bell ringing capacitor found in UK master sockets. This capacitor has a significant effect on the RF balance of UK indoor telephone wiring.

The impedance of the extension telephone wiring was measured over the frequency range 1.6 - 30 MHz, using a network analyser. The result is shown in Fig 15. Markers 1, 2 and 3 are at 1.6, 5 and 30 MHz respectively. It can be seen that there are wide variations in the impedance, with the real part varying between less than 10  $\Omega$  up to approximately 150  $\Omega$ . For most installations where there is only one branch of extension wiring, higher impedances are to be expected.

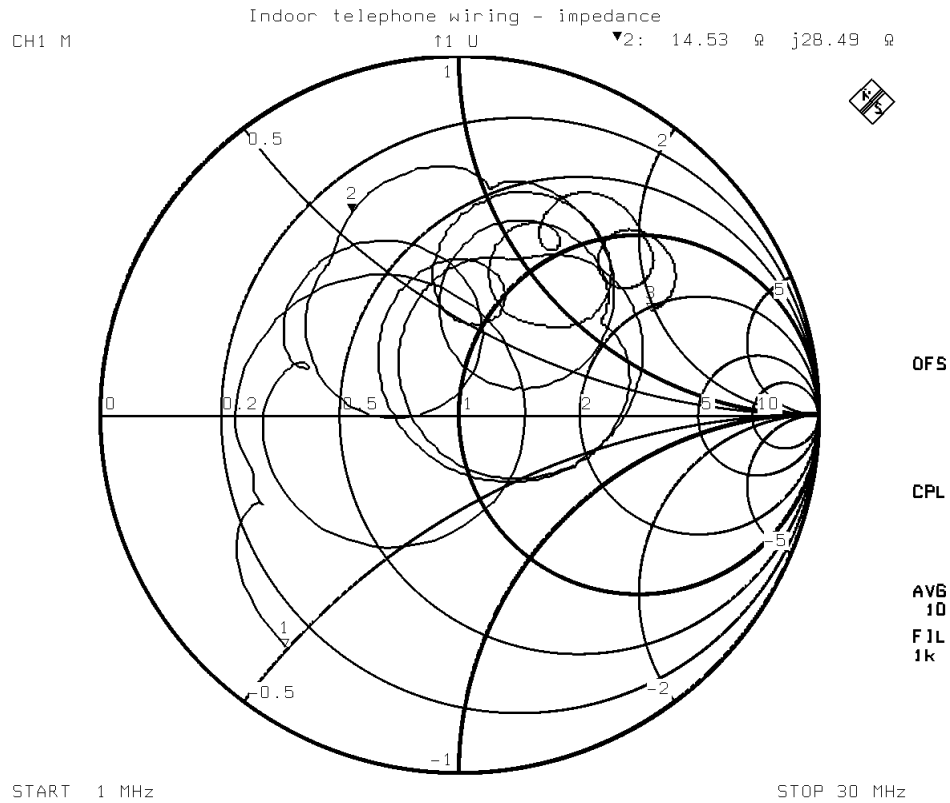


Figure 15. Impedance of indoor extension telephone wiring for differential mode signals.

In order to test the radiated emission characteristics of the wiring, a balun transformer was used. To reduce the residual common mode signal on the balanced output, a common-mode choke was also used. Tests were performed to ensure that this common mode signal was at an insignificant level [50].

RF signals were injected onto the line pair plus the ringer wire, which represents the situation if xDSL Lite or home phonline networking is used with existing UK telephone extension wiring. The H-field strength was measured at a point that was an average distance of 10m from the telephone wiring, using the same method described in Section 2.4 above. Fig. 16 shows the effective gain of the wiring in dBd, as in Section 2.4 above. These results indicate poor RF balance, not only due to the unbalanced three-wire transmission line but also because of connected telephone equipment, particularly mains powered equipment, whose RF balance about earth has been shown to be poor in section 2.2 above.

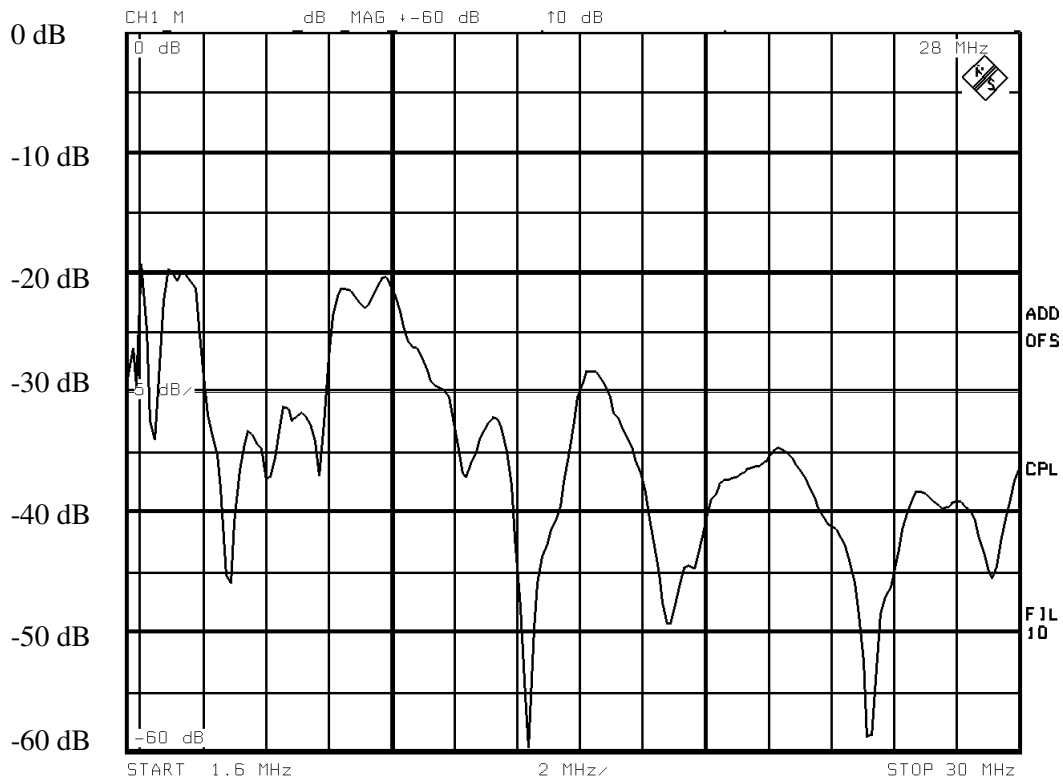


Figure 16. Effective antenna gain of indoor extension telephone wiring in dB for differential mode signals.

## 2.6. Emissions from underground power cables

Although underground cables are generally of a coaxial construction, they are not designed for radio frequency use and they do not necessarily exhibit good shielding effectiveness at radio frequencies. Furthermore, due to the skin depth in typical ground, the shielding effect of the ground may not be particularly significant at frequencies in the MF and HF bands.

In October 1998, a test was performed by RA/RTCG at Whyteleafe in collaboration with the RA Baldock Monitoring Station, DERA Portsdown and RSGB. The primary objective of these tests was to assess the extent to which a buried electricity power cable carrying radio frequency signals may radiate. A secondary objective was to assess the extent to which signals from PLT signals may be propagated via ionospheric propagation modes such as reflection from the 'F' layer.

### 2.6.1. Configuration of test site

The test site is as shown in Fig. 17. The signal source was an RF signal generator set to produce a CW signal of 5.155 MHz, a power of +23 dBm (200 mW). The frequency and power were chosen by the RA who made the transmissions. This frequency is close to the optimum for Near Vertical Incidence Skywave (NVIS) propagation. The RF signal generator was connected to an antenna changeover box designed and constructed by the author, which alternately switched the signal between a half wavelength reference dipole and an underground cable. The period of time on each antenna was initially set to 45 seconds but was subsequently increased to 124 seconds.

The dipole was provided by RA/RTCG and was cut for an electrical half wavelength at the operating frequency. It had a 1:1 balun at the feed point. It was erected 6 m above ground level and 100 m from the underground cable and parallel to it.

The underground cable was a 40 m length of four core steel wire armoured electric power cable type 6944X which had been inserted into a non-conductive underground cable duct 50 cm below the surface. This duct had been in position for more than 5 years allowing the soil above it to become fully compacted. The RF signal was driven onto one core of the cable relative to the steel armouring. The driven core was terminated with a 50Ω termination at the far end. The other three cores were open-circuit at both ends. The cable armouring was earthed via an earth spike at the driven end to minimise radiation from the outside of the braid of the coaxial cable above ground.

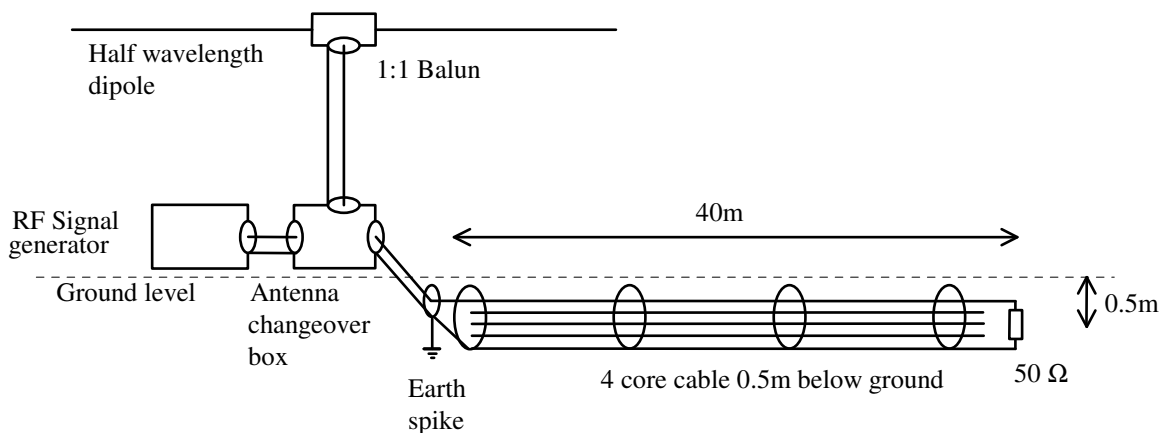


Figure 17. Configuration of underground cable test site

Steps were taken to minimise the possibility of any unwanted radiation from the dipole or its feeder when the dipole was not selected. A double pole relay was used for the antenna switching so that when the dipole was not selected, both the inner and screen were disconnected from the signal source and shorted together. A 100 k $\Omega$  bleed resistor and gas discharge tube surge arrestor were connected between the cable screen and the case of the changeover box to avoid a possible build-up of static charge on the dipole

The characteristic impedance of the four core armoured cable was measured by the author using a Time Domain Reflectometry (TDR) method and by measuring the series inductance and shunt capacitance per unit length. The results were 52 - 54  $\Omega$  with one core driven against the armouring and the other three cores open-circuit. Grounding the unused cores reduced the characteristic impedance but not by a significant amount. The attenuation was too small to measure accurately on the available cable sample at 5 MHz but by extrapolating a measurement made at 30 MHz, the loss at 5 MHz was found to be well under 0.1 dB/m.

The surface transfer impedance (STI) of the 4 core cable was also measured by the author using a test method based on Schelkunoff's method [53]. STI is defined as  $v_{dm}/i_{cm}$  per unit length where  $v_{dm}$  is the differential mode voltage on the inner and  $i_{cm}$  is the common mode current flowing on the outside of the shield. Although STI is normally used to predict the amount of unwanted coupling into a coaxial cable due to an interfering current flowing on the shield, it can also be used to predict the inverse effect.

The measured STI for the 4 core armoured cable was 540 m $\Omega$ /m at 5 MHz. By comparison, the STI of RG 58 coaxial cable was measured at 14 m $\Omega$ /m at 5 MHz. The high STI (i.e. poor RF shielding effectiveness) of the armoured cable can be attributed to the armouring wires being lapped not woven and the contact between wires being uncertain. For thicker cables such as distributor cables from an electricity substation, the strands of armouring may be spaced apart.

The total surface transfer impedance for a 40 m length of the armoured cable tested would therefore be 21.6  $\Omega$  at 5 MHz. With a 50  $\Omega$  termination at the far end, a significant proportion of the return current would flow on the outside of the shield causing a signal to be radiated.

### 2.6.2. Results

The signals from the underground cable and the dipole were monitored at three receiving sites, the RA Monitoring Station at Baldock, Herts, DERA at Portsdown, Hants and Kendal, Cumbria over a period of several weeks. The RA Monitoring Station at Baldock logged the signal on a total of 46 occasions at various times of the day and night on 11 different days. The Baldock Monitoring Station had the capability to measure the absolute field strength of the signal from the dipole as well as its direction and angle of elevation. Although the other two receiving sites were unable to make absolute field strength measurements, they were equipped with Digital Signal Processing equipment which could detect the signal from the underground cable and could measure its power relative to the dipole signal.

The spectral plot in Fig. 18 was provided by Mr A. Talbot of DERA at Portsdown, Hants. The upper trace shows the relative power spectrum of the signal from the dipole with a frequency span of 12.5 Hz. The lower trace shows a 'waterfall' spectrum plot with time on the horizontal axis and graticule marks at 10 minute intervals. The number '19' on the horizontal axis indicates a time of 19:00 hours. The vertical axis represents frequency with a 12.5 Hz span and a resolution bandwidth of 0.1 Hz. Relative power is represented by colour and this indicates that the ratio of field strength from dipole to field strength from underground cable is approximately 30 - 35 dB. The 'waterfall' plot also shows some effects which prove that the signal is being received by ionospheric propagation. In particular, the signal from the underground cable between 19:01 and 19:03 shows two separate peaks 0.35 Hz apart which indicates an ionospheric effect, as explained in [54].

At Baldock, the field strength of dipole signal varied from below the noise level up to +9dB( $\mu$ V/m) depending on time of day and propagation conditions. The apparent direction of arrival of received signals at Baldock was 165 - 190° and the angle of elevation was up to 80°, both angles depending on propagation conditions.

As the distance from Whyteleafe to Baldock is approximately 80 km, the propagation at 5 MHz would be by NVIS which implies that the Maximum Usable Frequency (MUF) of this path is close to the Critical Frequency. According to [54], a signal at 5 MHz is reflected by the 'F' layer at a height of approximately 300 km during day time. Assuming a total path length of approximately 600 km, the calculated received field strength would be 14 dB( $\mu$ V/m) under free

space conditions with perfect reflection from the 'F' layer in the ionosphere and no absorption by lower layers of the ionosphere. The maximum field strength recorded was 9 dB( $\mu\text{V}/\text{m}$ ), which is within 5 dB of the free-space path loss for a 600 km path.

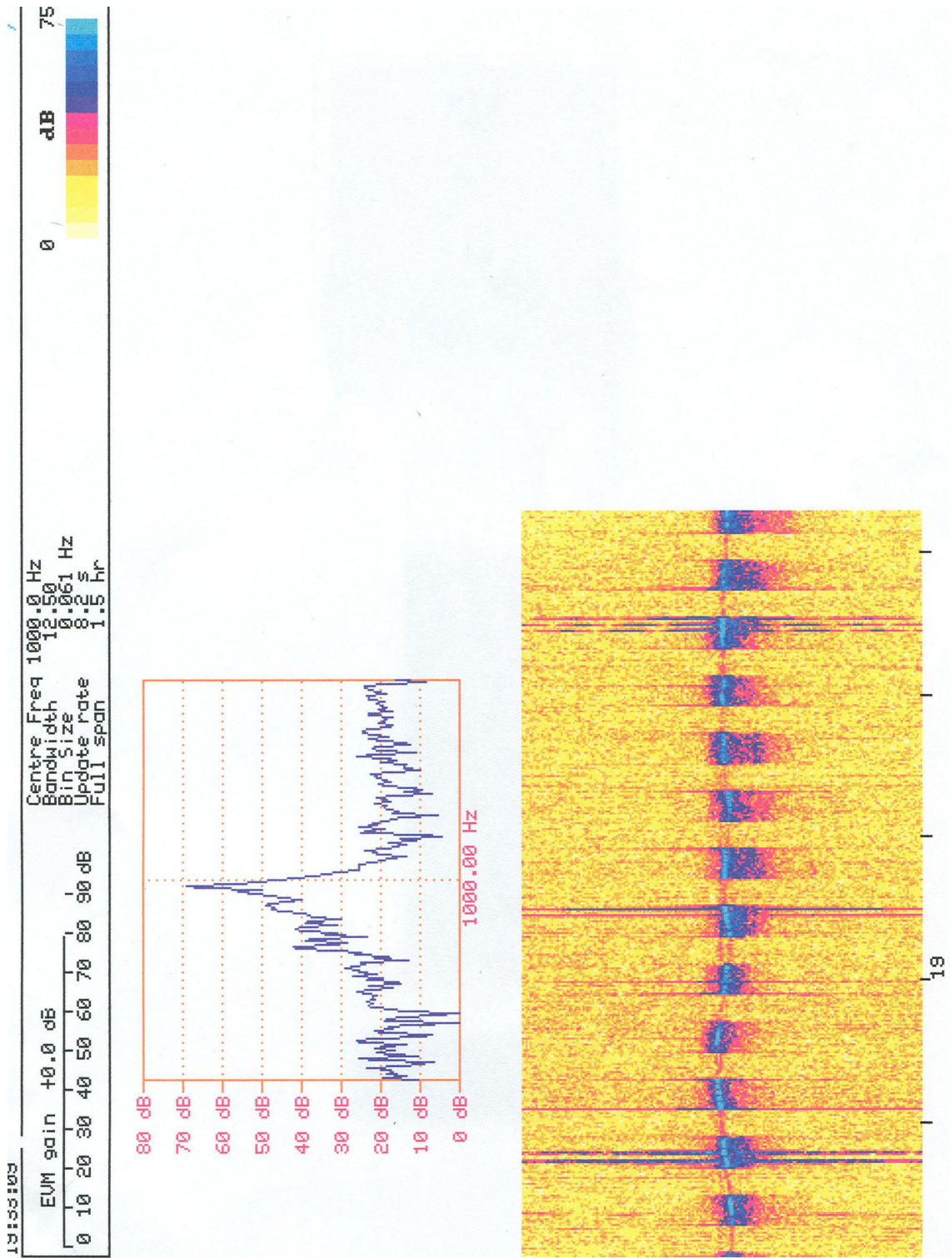


Figure 18. Spectrum plots of signals received from buried cable test transmissions.



### **2.6.3. Interpretation of results**

The radiated emissions from underground cables in an actual PLT installation would depend to a large extent on the type of cable used and the earthing arrangements. Nevertheless, the results for the underground cable tests described above indicate that even if all radiation from cables above ground could be avoided, radiation from underground cables could still be significant, for example for a mobile HF user in a residential street, where an underground cable could be as close as 2 - 3 m from the receiving antenna.

The results of the limited propagation tests performed indicate that a narrow band signal of 200 mW ERP can be received via ionospheric propagation at a site 80 km away, at a field strength which is often above the background noise level even in 9 kHz bandwidth. If PLT systems were deployed extensively, ionospheric propagation would allow a receiver to receive emissions from a large number of distant PLT systems simultaneously. Depending on the number of PLT systems received in this way and the ERP of each, the cumulative effect could increase the background noise level at a distant site due to ionospheric propagation. There are differences between ionospheric propagation of PLT signals at frequencies of 2.9 and 5.1 MHz. At 2.9 MHz, the propagation would be significantly different with a shorter ionospheric path length due to reflection by the 'E' layer at a height of approximately 100 km instead of the higher 'F' layer. HF propagation is also affected by time of day, time of year, sunspot cycle and angles of incidence. Cumulative effects have also been studied by Welsh [55] and Stott [31].

## **2.7. Emissions from home powerline networks**

A specification for home powerline networking products has been issued by HomePlug Powerline Alliance [56]. This specification includes a PSD mask with notches to protect bands by radio amateurs but not other HF users such as broadcasting.

The following items were tested:

- Devolo MicroLink dLAN HS ETH Starter Kit UK, Product Model No. 1154
- SMC EZ-Connect™ 14 Mbps PowerLine to Ethernet Starter Kit

### **2.7.1. Test configuration**

The two MicroLink dLAN Highspeed Ethernet adaptors were plugged into a 2-way 13A mains adaptor that was plugged into an EMCO CISPR 16 Line Impedance Stabilisation Network (LISN). It is only possible to test these Ethernet adaptors when two are communicating with each other but if both are directly connected to the LISN, the emissions measured are from two Ethernet adaptors simultaneously. When transferring large files, it is likely that most of the data is transmitted by the Ethernet adaptor that is connected to the source PC. The Ethernet adaptor that is connected to the destination PC will only transmit acknowledgements as required by the network protocol. If it is required to measure the emissions from a single Ethernet adaptor, it would be necessary to connect the second Ethernet adaptor via a network that passes 50 Hz mains but provides a defined attenuation at RF (e.g. 20 dB), without introducing so much attenuation that the powerline network reduces its data rate.

Each Ethernet adaptor was connected to a PC with a 10/100 Mbps Ethernet card using the 3m long screened twisted pair RJ45 'patch' cables supplied. 12 files of approx. 50 MB each were transferred to the other PC via the powerline network using the supplied SMC or Devolo software as appropriate. This file transfer took approx. 2 minutes to complete. All tests were performed while a file transfer was in progress.

### **2.7.2. Test results (Microlink dLAN)**

It should be noted that the date at the top of each trace is the date when the setup was stored on the memory card, not the date of the trace. The tests were performed in April 2006.

Fig 19 shows a conducted emission plot from 150 kHz - 30 MHz with 9 kHz IF bandwidth, a logarithmic frequency scale, a logarithmic amplitude scale and peak detection. The upper limit line is the EN 55022 Class 'B' Quasi-Peak limit. The lower limit line is the EN 55022 Class 'B' Average limit. The marker position is 14.89 MHz with a level of 86.96 dB( $\mu$ V) using peak detection. In order to assess compliance to EN 55022, it is necessary to make further measurements with a QP and average detector. Due to the relatively long time constant of a QP or average detector, such measurements are usually only performed over a limited frequency range, normally centred on frequencies where peaks are noted on the sweep with a peak detector.

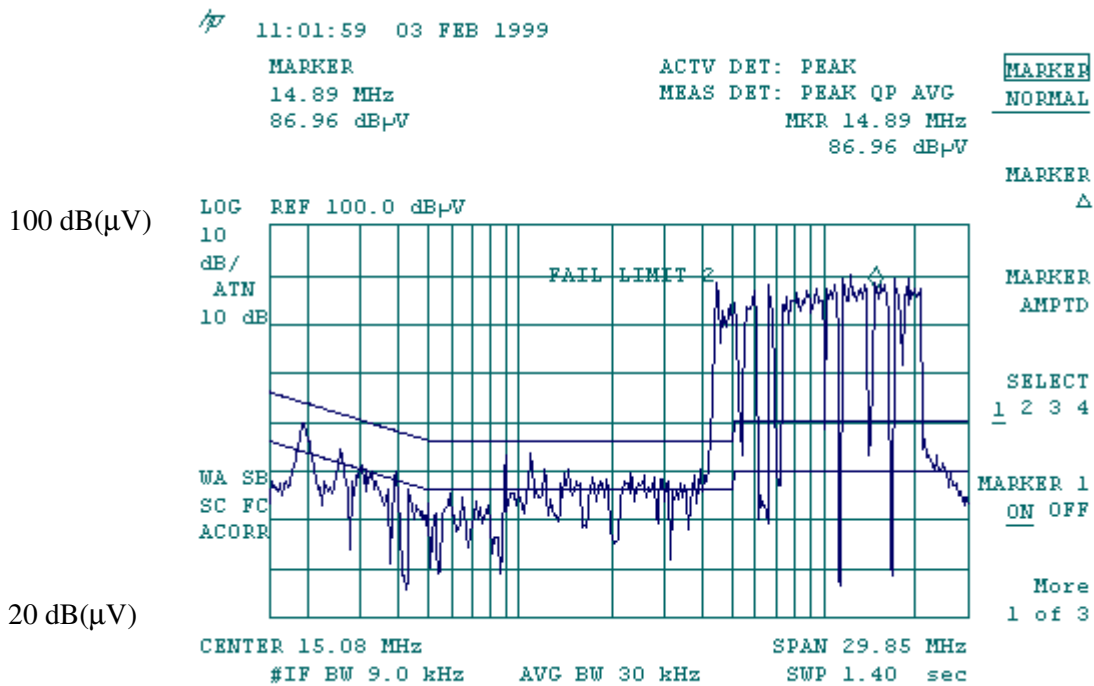


Figure 19. Conducted emission plot from Microlink dLAN 150 kHz - 30 MHz with peak detection.

Fig 20 shows a conducted emission plot from 15.0 - 15.025 MHz with a linear amplitude scale and quasi-peak (QP) detection. The marker position is 15.018 MHz with a level of 84.51 dB( $\mu$ V) using QP detection. This exceeds the EN 55022 Class 'B' QP limit of 60 dB( $\mu$ V) by 24.5 dB and it also exceeds the EN 55022 Class 'A' QP limit of 73 dB( $\mu$ V) by 11.5 dB.

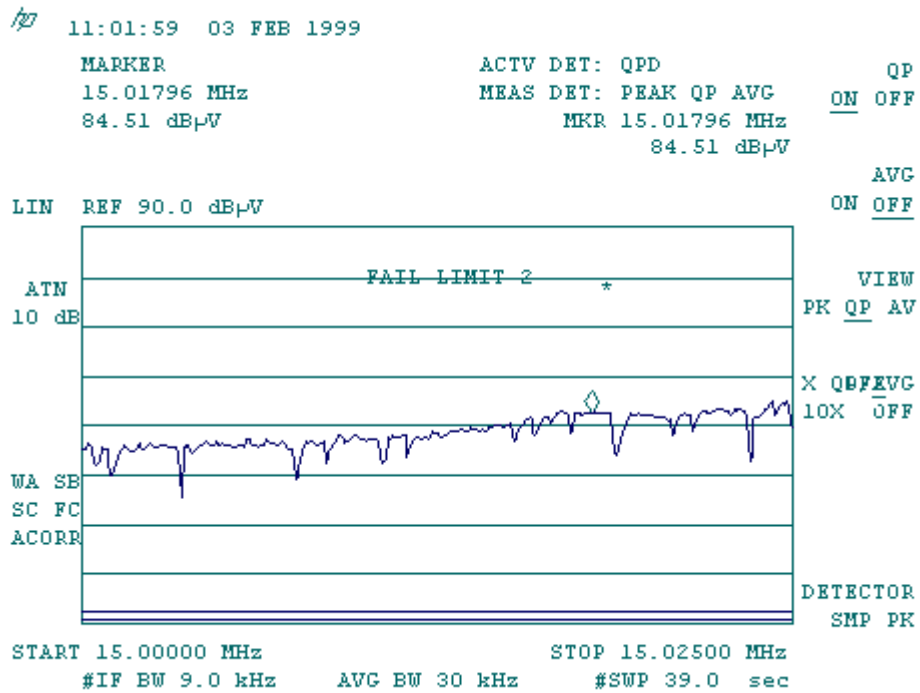


Figure 20. Conducted emission plot from Microlink dLAN 15.0 - 15.025 MHz with QP detection

Fig 21 shows a conducted emission plot from 15.0 - 15.025 MHz with a linear amplitude scale and average detection. The marker position is 15.024 MHz with a level of 77.42 dB(µV) using average detection. This exceeds the EN 55022 Class 'B' average limit of 50 dB(µV) by 27.4 dB and it also exceeds the EN 55022 Class 'A' average limit by 17.4 dB.

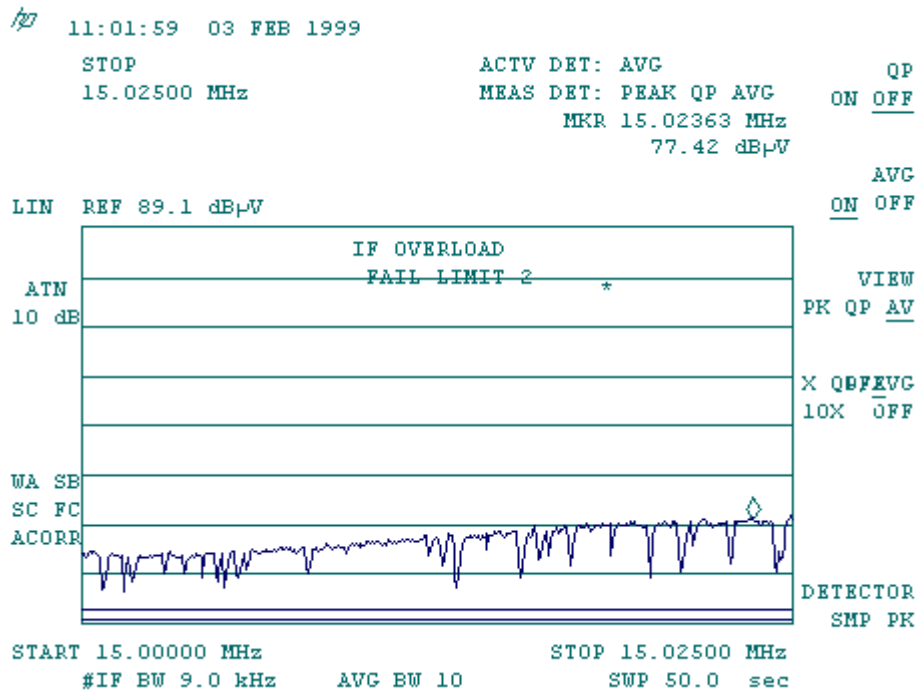


Figure 21. Conducted emission plot from Microlink dLAN 15.0 - 15.025 MHz with average detection

### 2.7.3. Test results (SMC EZ-Connect)

Fig. 22 shows a conducted emission plot from 150 kHz - 30 MHz with 9 kHz IF bandwidth, a logarithmic frequency scale, a logarithmic amplitude scale and peak detection. The upper limit line is the EN 55022 Class 'B' Quasi-Peak limit. The lower limit line is the EN 55022 Class 'B' Average limit.

The marker position is 16.58 MHz with a level of 85.48 dB(µV) using peak detection.

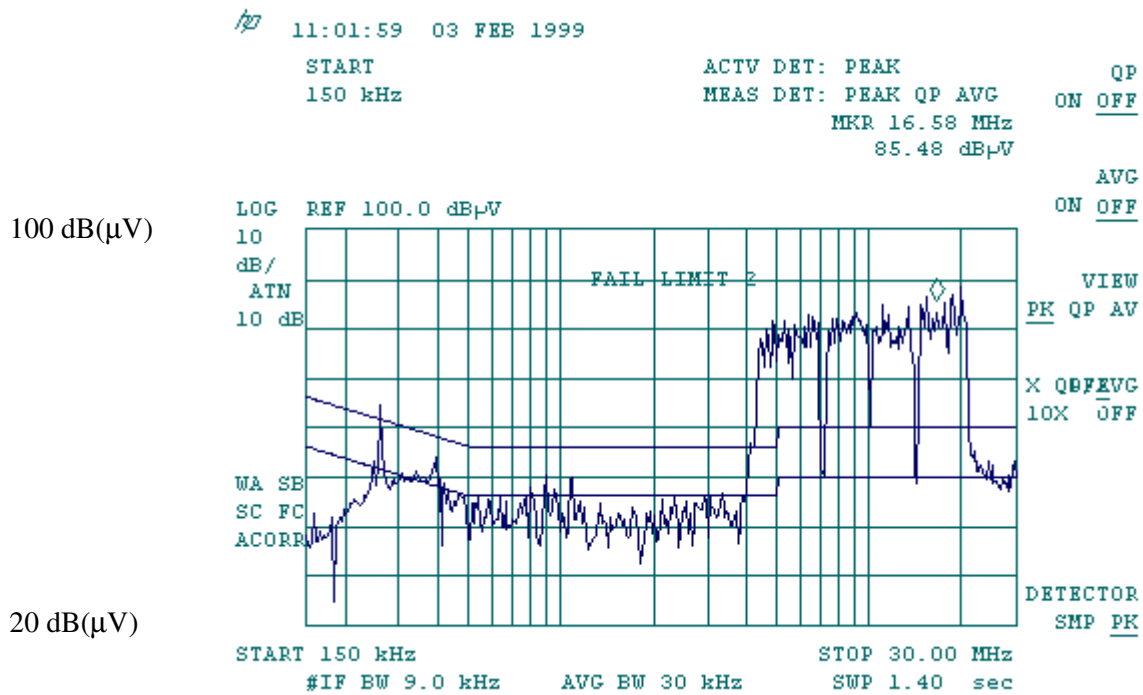


Figure 22. Conducted emission plot from SMC EZ-Connect 150 kHz - 30 MHz with peak detection.

Fig 23 shows a conducted emission plot from 16.6 - 16.65 MHz with a logarithmic frequency scale, a linear amplitude scale and quasi-peak (QP) detection. The marker position is 16.603 MHz with a level of 83.02 dB( $\mu$ V) using QP detection. This exceeds the EN 55022 Class 'B' QP limit of 60 dB( $\mu$ V) by 23 dB and it also exceeds the EN 55022 Class 'A' QP limit of 73 dB( $\mu$ V) by 10 dB.

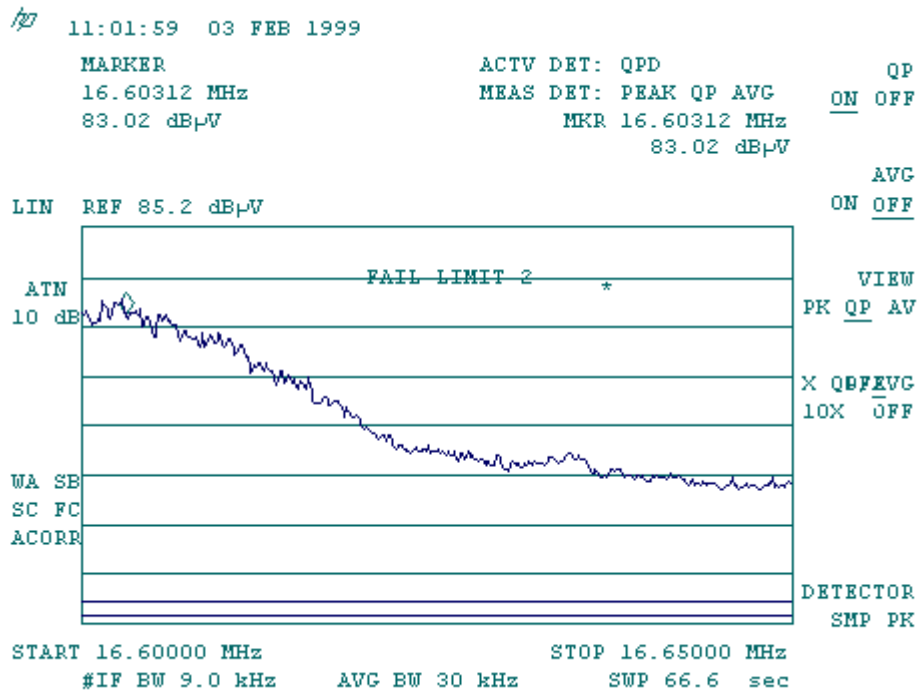


Figure 23. Conducted emission plot from 16.6 - 16.65 MHz with QP detection

Fig 24 shows a conducted emission plot from 16.6 - 16.65 MHz with a linear amplitude scale and average detection. The marker position is 16.6 MHz with a level of 72.28 dB(µV) using average detection. This exceeds the EN 55022 Class 'B' average limit of 50 dB(µV) by 22.3 dB and it also exceeds the EN 55022 Class 'A' average limit by 12.3 dB.

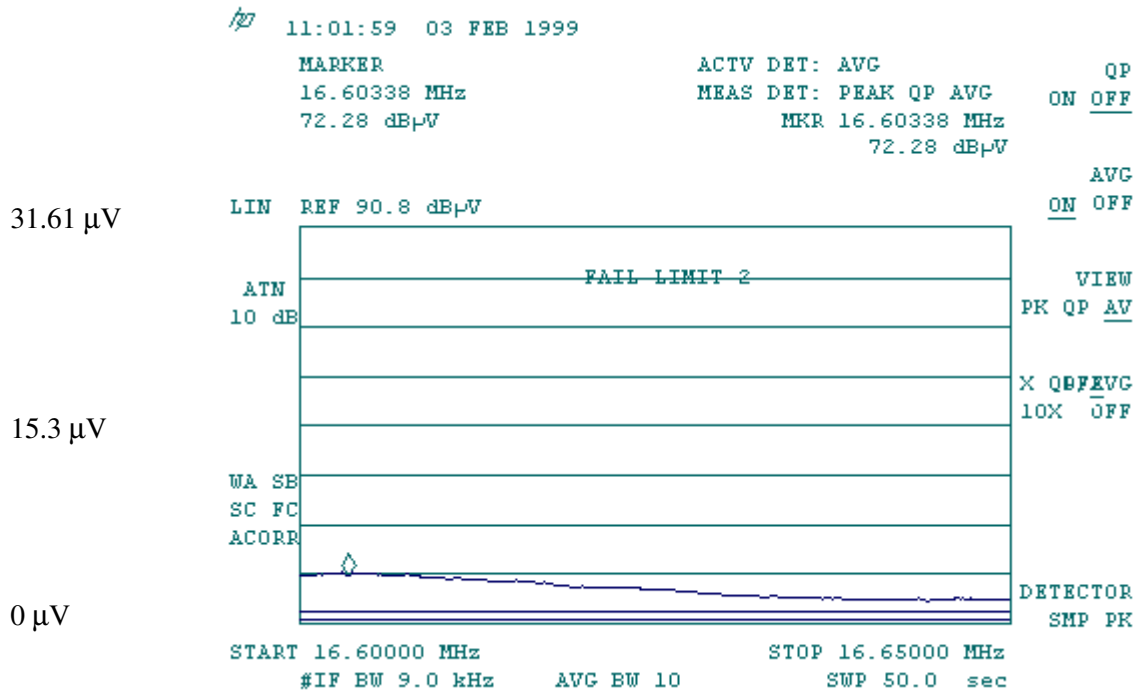


Figure 24. Conducted emission plot from 16.6 - 16.65 MHz with average detection

## 2.8. Modelling of potential for radiated emissions from networks

For telephone wiring in a building, LCL measurements can form the basis of a model to predict the antenna factor of such wiring when used with splitterless DSL or home phoneline networking. Such a model needs to take account of variations in national telephone wiring practice and it also needs to allow for unbalance introduced by connected telephony equipment, particularly mains-powered equipment.

For in-building power wiring, LCL measurements can form the basis of a model that would predict the antenna factor of such wiring. Such a model needs to take account of variations in national wiring practice, for example the connection of neutral to earth in UK installations and the use of a 'ring main' topology for power circuits in the UK. The effect of unbalance introduced by equipment connected to power networks also needs to be considered as it can be very significant.

For any network, in addition to considering the LCL, it is necessary to take account of the common mode impedance of the network under test as this determines the relationship between common mode voltages due to mode conversion and common mode currents that cause radiated



emissions. A poor LCL does not necessarily result in correspondingly high radiated emissions if it occurs at a frequency where the common mode impedance is high. The low frequency portion of the trace in Fig. 9 above is an example of this.

In the case of lighting circuits however, knowledge of the LCL and common mode impedance are not considered sufficient to develop a model of the potential for radiated emissions and the use of other techniques such as antenna modelling would also be required.

The results presented in 2.3 above may be typical of UK domestic mains power installations while those in 2.2 may be near worst-case for indoor telephone extension wiring. Nevertheless, large variations are to be expected between individual installations and repeatability of measurements may be poor. The objective of this aspect of the research was to develop and verify a model that can be applied to any installation if suitable parameters are entered and which yields results that show reasonable agreement with measured results. In order to develop such a model, two phenomena need to be separated. These are:

1. The conversion of differential-mode signal to common-mode due to the unbalance in the network cable.
2. The conversion of common-mode current to radiated field.

The first phenomenon can be measured using Macfarlane's method as described in section 3.1 on page 48.

The second phenomenon requires an unstructured network to be modelled as an antenna. As no two networks will give identical results, a model cannot be expected to predict the frequencies at which maximum and minimum radiation efficiency will occur in any particular case. The objective is therefore to develop a model that takes certain parameters about a network and predicts the mean radiation efficiency versus frequency and also the range of radiation efficiencies that may be expected at any frequency (with 90% confidence for example).

## 2.9. Other techniques for measuring emissions from networks

In addition to measurement of radiated emissions from networks, techniques for direct and indirect measurement of common-mode current have been investigated. This allows the measured emission to be expressed in terms of the total common-mode interfering current flowing in a cable or bundle of cables under test.

### 2.9.1. Current probe measurements

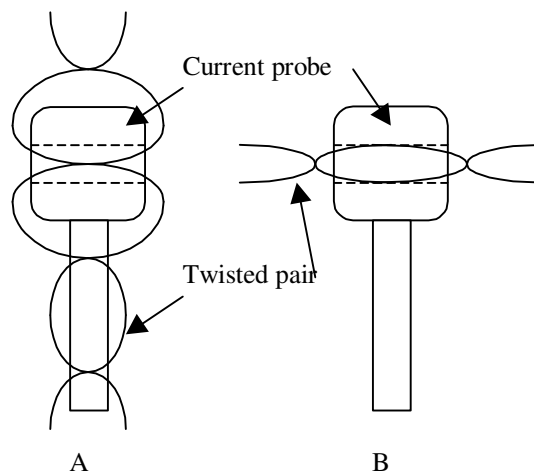


Figure 25. (A) Measurement of differential mode current, (B) measurement of common-mode current

Fig 25(A) shows how a clip-on current probe may be used to measure differential mode current in a twisted pair cable. With the configuration shown, the current measured is twice the actual differential mode current in the cable. This arrangement has the advantage that the impedance added by the current probe is the same in both wires of the pair whereas clipping the current probe around one wire only could introduce some unbalance.

Fig 25(B) shows how a clip-on current probe may be used to measure common mode current in a twisted pair cable. In many cases with installed networks, the cable is inaccessible or too thick for such a measurement so this technique has been used to develop a 'non-contact' current measurement technique.

### 2.9.2. Non-Contact Current Measurement

An alternative approach for measuring common-mode currents in installed networks below 30 MHz is to use an existing type of untuned active loop antenna close to the cable under test.

As part of the RA contact Ref. AY3920 [39], an untuned active loop antenna was purchased from Schaffner EMC Systems as a special order item with a diameter of 30 cm instead of 60 cm. Due to its reduced area, the 30 cm loop has approximately 10 dB less sensitivity than the standard 60 cm type. The antenna factor of the 30 cm loop expressed as an E-field factor is nominally 30 dB/m. The reduced size offers practical advantages when making measurements close to the cable under test and the reduced sensitivity is offset by the close measurement distance.

In order to evaluate the use of a 30 cm loop for common-mode current measurement, a laboratory test using a suspended wire was set up as shown in Fig. 26.

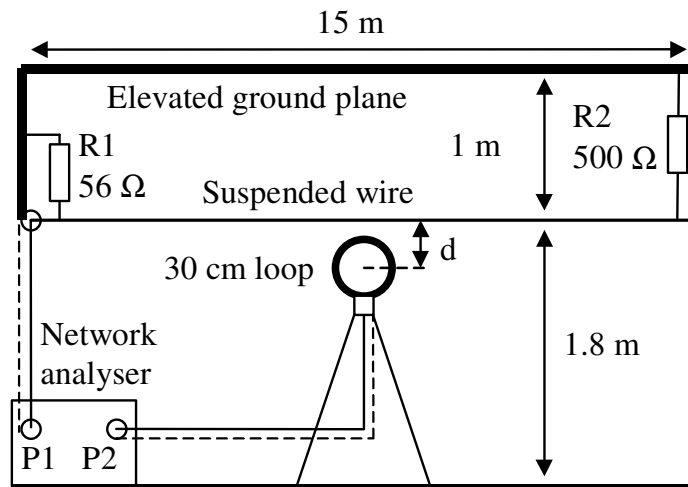


Figure 26. The use of a 30 cm diameter untuned active loop for non-contact current measurement.

The elevated ground plane was a false ceiling 15 m x 9 m consisting of a grid of interconnected metal bars. A 1.5 mm diameter wire was suspended 1 m below the ceiling and 1.8 m above the floor. The wire was terminated by means of 500 Ω resistor R2, which consists of 5 x 100 Ω resistors in series spaced at 100 mm intervals. The impedance of the suspended wire at the feed point without R1 fitted was measured as 500 Ω to 475 Ω at frequencies of 100 kHz - 2 MHz. At 2 MHz, the electrical length of the 15 m wire was one tenth of a wavelength.

With R1 fitted, the wire was driven against the elevated ground plane from Port 1 of a network analyser via a length of 50  $\Omega$  coaxial cable. R1 and R2 in parallel provide a 50  $\Omega$  termination for the source. Port 2 of the network analyser was connected to the output of the loop antenna. The magnitude of the forward transmission coefficient  $S_{21}$  was measured from 100 kHz - 2 MHz and was found to be nearly constant over this range. Moving the loop along the wire showed that the current distribution was relatively uniform.

This current  $i$  in the wire was calculated from the p.d. at the feed point divided by R2. The 'H' field strength  $H$  in amperes/metre at a distance  $r$  from the wire is, by definition, given by[51]:

$$H = \frac{i}{2\pi r} \quad (13)$$

This assumes that the length of the wire is large compared to the distance  $r$  and that the current at all points along the wire is in phase, i.e. that  $r$  is small compared to a wavelength at the highest frequency of interest. It also assumes that the distance  $r$  is small compared to 1 m so that the field due to the return currents in the ground plane is small compared to the field from the suspended wire.

The relationship between the current  $i$  in the cable and the output  $v$  from the loop antenna may be expressed as a current transducer factor  $F_i$  where:

$$F_i = 20 \log_{10} \left( \frac{i}{v} \right) \quad (14)$$

The units of  $F_i$  are dBS, i.e. dB relative to 1 siemens. Hence the current  $i$  expressed in dB( $\mu$ A) may be found by adding  $F_i$  to the output of the loop expressed in dB( $\mu$ V).

The measured values of transducer factor  $F_i$  are shown in Fig. 27 for values of  $r$  in the range 0.25 - 0.65 m. The calculated values are also shown and are based on the calculated 'H' field at the centre of the loop. The corresponding distance  $d$  of the conductor from the perimeter of the loop is also shown.

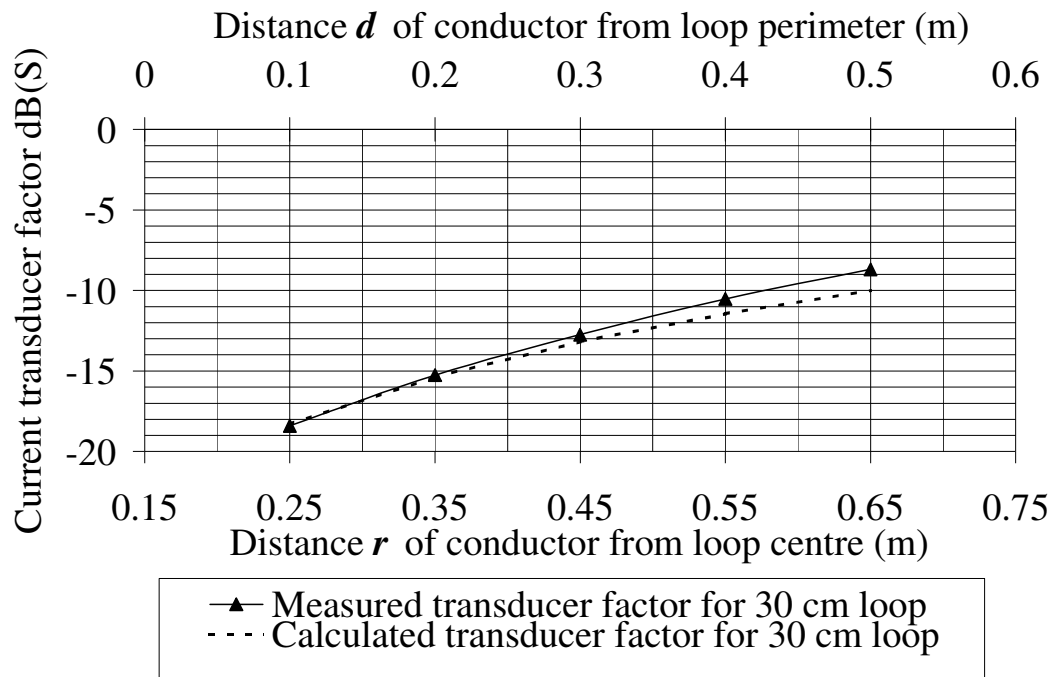


Figure 27. Measured and calculated current transducer factors versus distance from cable.

The calculated values shown in Fig. 27 are based on the assumption that the loop diameter is small compared to the distance  $r$  so that the field at the centre of the loop is equal to the average field over the area of the loop. A more rigorous analysis would take account of the curvature of the field, the non-uniformity of the field over the area of the loop and the effects of the finite distance from the ground plane. Nevertheless, even without taking these factors into account, it can be seen that there is close agreement (within 1 dB) between the measured and calculated values in Fig 27 for the measuring distances used.

## 2.10. Conclusions

Test methods for LCL measurements using a Macfarlane network have been described and results have been presented. It has been shown that cables used for telephone extension wiring and power wiring in buildings are relatively well balanced if driven as a balanced pair but that the balance is degraded substantially when the 'pair' consists of two conductors in parallel on one side and one on the other. It has also been shown that equipment connected to telephone wiring or power wiring can cause a significant degradation of balance, particularly in the case of certain electrical appliances with a very poor LCL that are commonly used in a domestic

environment. A practical difficulty in making LCL measurements in-situ has been identified, namely how to make an effective RF ground connection for the LCL probe.

A limitation of LCL measurements as a modelling technique has been identified in the case of lighting circuits on powerline networks. It is concluded that although LCL measurements appear to be useful in developing a model for the radiated emission characteristics of powerline networks, this technique is only a partial solution.

Measurements have also been made of the efficiency of various networks as unintentional radiating antennas.

The conducted emissions of home powerline networking products have also been measured and compared to the EN 55022 conducted emission limits.

Other test methods have also been described including non-contact current measurements.

### **Chapter 3. Antenna modelling of wireline networks**

This chapter describes the application of antenna modelling software to in-building power line networks, splitterless DSL and home phonenumber networks and BPL powerline networks

In order to determine the characteristics of a wireline network as an antenna, antenna modelling software may be used. Such software models an antenna as a number of wires and divides each wire into segments. It then calculates the current flow on each segment. The accuracy of the model is critically dependent on how the wires are divided into segments and also other factors such as how ground is modelled. In general, the minimum number of segments per half wavelength is about 10 although 20 is preferable for accurate calculation of feedpoint impedance [57]. Smaller segments improve calculation accuracy but the computation time increases with the square of the number of segments.

A technique that can be used to optimise the trade-off between segment length and computation time is called 'tapering'. Segments near the end of a wire are smaller than segments on straight sections of wire. Wires that join at a very acute angle may require smaller segments near the join [57], [58]. Where wires are closely spaced, it is an advantage to align segments in parallel wires.

Some antenna modelling software performs automatic tapering segmentation and it can also perform a segmentation check to warn of unsatisfactory segmentation. In order to evaluate whether segmentation of an antenna model is satisfactory, a convergence test can be performed by increasing and decreasing the segment size and noting whether any significant change in the feed point impedance occurs. It is also advisable to view the antenna model with its current distribution and look for any abrupt variations in current between adjacent segments, as this may indicate poor convergence.

Another important consideration in antenna modelling is modelling of ground. This is of particular significance in cases where the height of any part of the antenna above ground is a small fraction of a wavelength. A real ground model has been used with typical ground characteristics, i.e. relative permittivity  $\epsilon_r = 13$  and conductivity,  $\sigma = 5$  mS/m.

MININEC3 takes account of real ground for the far field calculation but it assumes perfect ground conductivity for the feedpoint impedance calculation. If the antenna height above

ground is relatively small compared to the wavelength ( $<0.2\lambda$ ), or if an antenna with ground radials has ground radials at a height less  $0.05\lambda$  above ground, the use of a perfect ground may result in significant errors in the calculated value of antenna feedpoint impedance, which is likely to be lower than the actual impedance. In such cases, NEC2 was used as it provides more accurate results for gain and feed point impedance than MININEC3. Nevertheless, NEC2 does not model electrically small loops well, e.g. those with a circumference less than 0.1 wavelength, nor very closely spaced wires [58]

NEC4 overcomes various weaknesses of NEC2 and MININEC3 and also includes additional features, including modelling wires that are buried in ground. Unlike MININEC3 and NEC-2, which are in the public domain, NEC4 requires the purchase of a software licence from Lawrence Livermore Laboratories in the US and there are restrictions on its supply to non-US purchasers. Due to these licensing restrictions, NEC4 was not available for use during the current programme of research.

### **3.1. Antenna modelling of in-building power line networks**

The antenna shown in Fig 28 is intended to model a section of in-building power network. The conductor along the 'X' axis represents the outer shield of a 20 mm diameter incoming electricity supply cable entering the building. This models the effect of the supply cable sheath as a counterpoise or 'ground radial' against which in-building power wiring may radiate. In practice this cable is normally buried at a typical depth of 0.5 m but in the model it is 50 mm above ground. As stated in section 3.2 below, the shielding effect of 0.5 m of ground at HF is not considered to be significant.

The vertical conductor along the 'Z' axis consists of a 3 m length three closely spaced conductors representing  $2.5 \text{ mm}^2$  'twin and earth' cable commonly used in power circuits in UK buildings. The phase and neutral conductors have a radius of 0.892 mm and are spaced 4 mm apart between centres. The earth continuity conductor is midway between the phase and neutral conductors and has a radius of 0.673 mm. The conductors are modelled with a PVC dielectric coating. The horizontal conductor above and parallel to the 'X' axis consists of a 5 m length of three closely spaced conductors representing  $2.5 \text{ mm}^2$  'twin and earth' power cable. In both cases, the lengths of the phase, neutral and earth conductors are identical in order to align segments between the closely spaced wires.



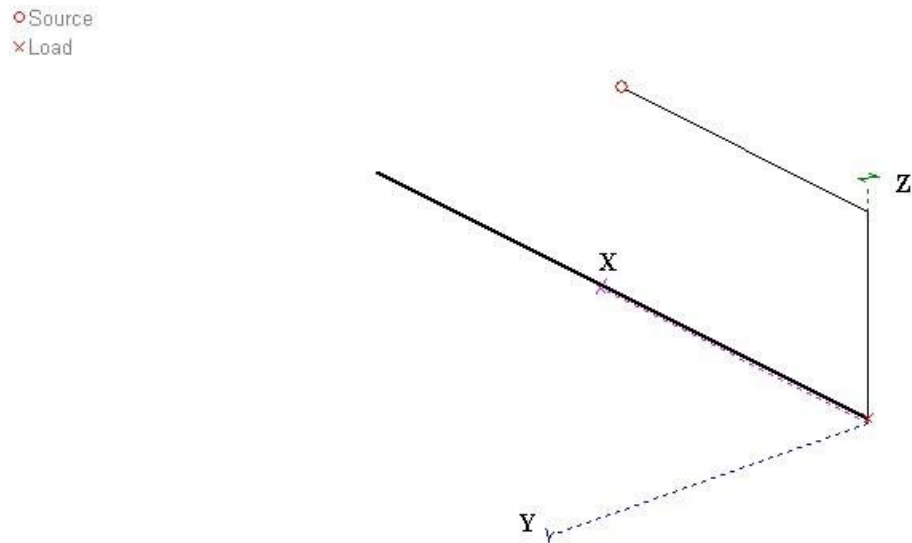


Figure 28. Antenna model of a section of in-building power network.

Fig 29 shows the detail near the origin in Fig 26. The neutral and earth conductors are connected together, as in modern UK PME installations. The phase conductor is joined to earth/neutral via a load that is set to  $12 + j0 \Omega$  to represent the RF impedance of other power and lighting circuits connected in parallel. This load is representative of measured impedances given in Section 2.4 above.

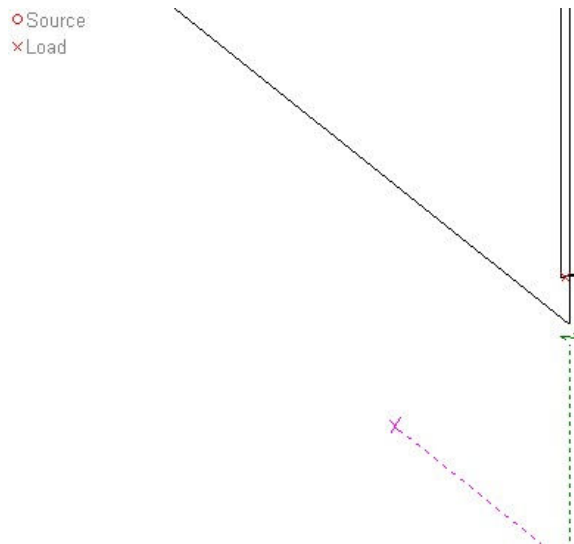


Figure 29. Detail near the origin for a section of in-building power network

Fig 30 shows a detail at the far end of the horizontal section of 3-core cable. A source is connected differentially between the phase and neutral conductors but the earth wire is not

connected. This is intended to represent the situation where a PLT transceiver is located on the first floor of a building.

○Source  
×Load

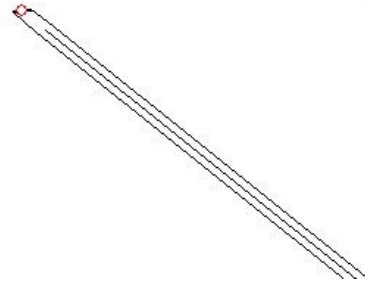


Figure 30. Detail at the far end of a section of in-building power network

When a convergence test of model adequacy was performed, the MININEC3 results were showing signs of instability as changes in segment size resulted in large variations on feedpoint impedances, with negative reactances in some cases. The NEC-2 results were as follows:

NEC-2 result with 165 pulses:

```
FINITE GROUND. SOMMERFELD SOLUTION
RELATIVE DIELECTRIC CONST.= 13.000
CONDUCTIVITY= 5.000E-03 MHOS/METER
Source in wire N 4:  Z=18.420 - j 12.636  SWR(50+j0)=2.91
Elevation angle: 20.0 deg
Max Gain: -52.48 dBi at azimuth: 233 deg, F/B: 3.88 dB
Azimuth angle: 0.0 deg
Max Gain: -49.88 dBi at elevation 75 deg
***
```

NEC-2 result with 987 pulses:

```
Frequency: 14.15 MHz
Antenna environment:
FINITE GROUND. SOMMERFELD SOLUTION
RELATIVE DIELECTRIC CONST.= 13.000
CONDUCTIVITY= 5.000E-03 MHOS/METER
Source in wire N 4:  Z=18.048 - j 12.754  SWR(50+j0)=2.98
Elevation angle: 20.0 deg
Max Gain: -12.42 dBi at azimuth: 216 deg, F/B: 1.77 dB
Azimuth angle: 0.0 deg
Max Gain: -9.53 dBi at elevation 82 deg
```

The above results indicate convergence of the feedpoint impedance but not the gain, which has changed by 40 dB. It was therefore concluded that modelling in-building power cables as three closely spaced conductors with mode conversion from differential mode to common mode currents may not be practicable using currently available antenna modelling software, due to the close spacing of the conductors ( $< 2$  mm) relative to a wavelength and relative to the length of the conductors.

An alternative approach to antenna modelling of in-building power cables is to use a common-mode model with all three conductors being treated as a single conductor that is fed at various points with the common-mode signals resulting from mode conversion. The amount of mode conversion could be determined from LCL measurements or LCL models.

Some common mode antenna modelling is described by Womersley et al in section B.2.5 of [7], by Flintoft et al in [59] and by Catrysse and Vantomme in Appendix 'C' of [48] and by Hockanson, et. al.[60].

### **3.2. Antenna modelling of underground powerline networks**

The NEC4 calculating engine can model wires buried in the ground and would be useful for modelling radiated emissions from underground power cables, but as explained in section 3 above, it was not available due to licensing restrictions.

An approximate analysis of radiation from an underground power cable can be performed by considering skin depth for propagation in a conductive medium. It can be shown that the minimum skin depth in the MF/HF bands for various types of ground is significantly greater than the typical 0.5 m depth at which underground power cables are normally buried. Hence, the shielding effect of ground is generally insignificant and the radiation at MF/HF from a cable buried at a depth of 0.5 m is approximately equal to a cable on the surface of the ground.

Radiation from underground cables has also been considered in section B.2.6 of [7].

### 3.3. Antenna modelling of in-building splitterless DSL and home phoneline networks

Antenna modelling of in-building DSL and home phoneline networks is subject to similar practical constraints as in-building power networks described in section 3.1 above. In the case of in-building telephone wiring, the constraints are more severe due to the smaller spacing of the conductors in the cable.

As stated in 3.1 above, an alternative approach to antenna modelling of in-building telephone cables is to use a common-mode model that is fed at various points with the common-mode signals resulting from mode conversion. The amount of mode conversion could be determined from LCL measurements or LCL models.

### 3.4. Antenna modelling of BPL powerline networks

Hare [61] and [62] has modelled the radiated emissions from a section of BPL network using antenna modelling software. The model is based on a section of overhead power line as shown in Fig. 31.

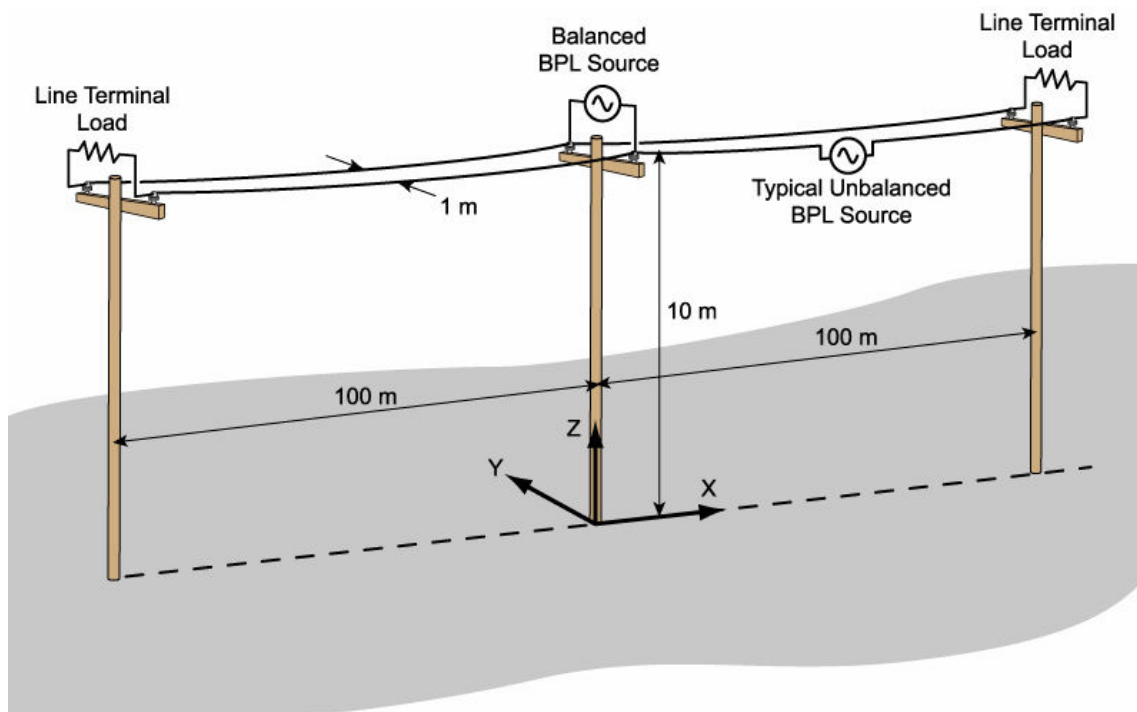


Figure 31. AEC/ARRL antenna model for a BPL network, reproduced from [62]

If field strength measurements are made near the centre of the 200 m section of power line in the model, and the measurement distance is small compared to 200 m (e.g. 30 m or less), then modelling a 200 m length should provide a reasonable approximation to an infinite length of power line. Hare [62] states that the unbalanced source is more representative of the way unbalanced couplers feed a single phase in practice.

Fig 32 shows an antenna model based on the configuration in Fig 31. As the wires are 200 m long with 1 m separation, the two separate wires appear to be a single wire when the whole antenna is viewed. An unbalanced source has been used and the feed point has been placed at an arbitrary position on one of the wires, offset 50 m in the X direction from the centre of the wire. The wire radius is 12.7 mm and the material is aluminium. Resistive loads have been placed at each end of the wire pair, as used by Hare [62].

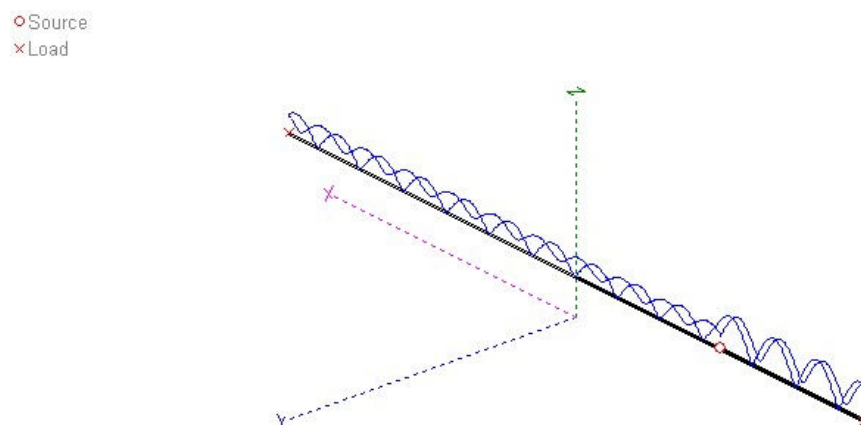


Figure 32. Antenna model of a 200 m section of power line with 50  $\Omega$  terminations, showing relative current amplitude.

The terminating resistors model the situation that occurs in practice where the power line is generally much longer than 200 m and it may have loads such as transformers connected. If the power line is long and has no power transformers or other loads connected then the resistance of the termination should be equal to the characteristic impedance of the transmission line. For a two-wire transmission line with a conductor diameter of 25 mm and a spacing of 1 m, the characteristic impedance is 530  $\Omega$  according to [63]. When power transformers or other loads are connected, it appears likely that the 50  $\Omega$  loads used by Hare [62] are a reasonable representation of the RF impedance of connected loads in practice.

Fig 33 shows the far field radiation pattern for the antenna in Fig 32 at a frequency of 10 MHz, with 50  $\Omega$  loads at each end of the power line pair. It exhibits a multi-lobe polar diagram that is characteristic of an antenna that is many wavelengths long. It also produces 'end fire' radiation in the 'X' direction, i.e. parallel to the axis of the power line pair. The maximum predicted gain is 6.52 dBi. This shows that a section of overhead power line operates as quite an efficient unintentional radiating antenna and has a greater gain than a dipole in certain directions.

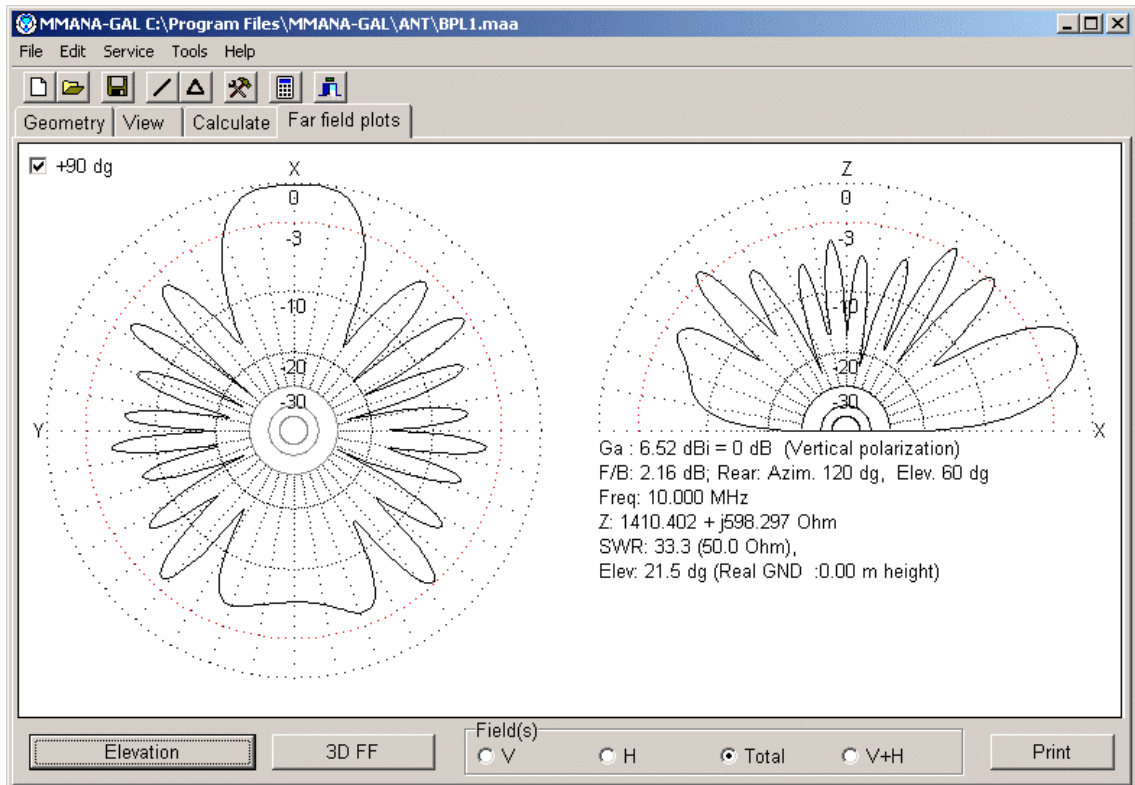


Figure 33. Far field plots for the antenna in Fig 32 at 10 MHz, with 50  $\Omega$  loads.

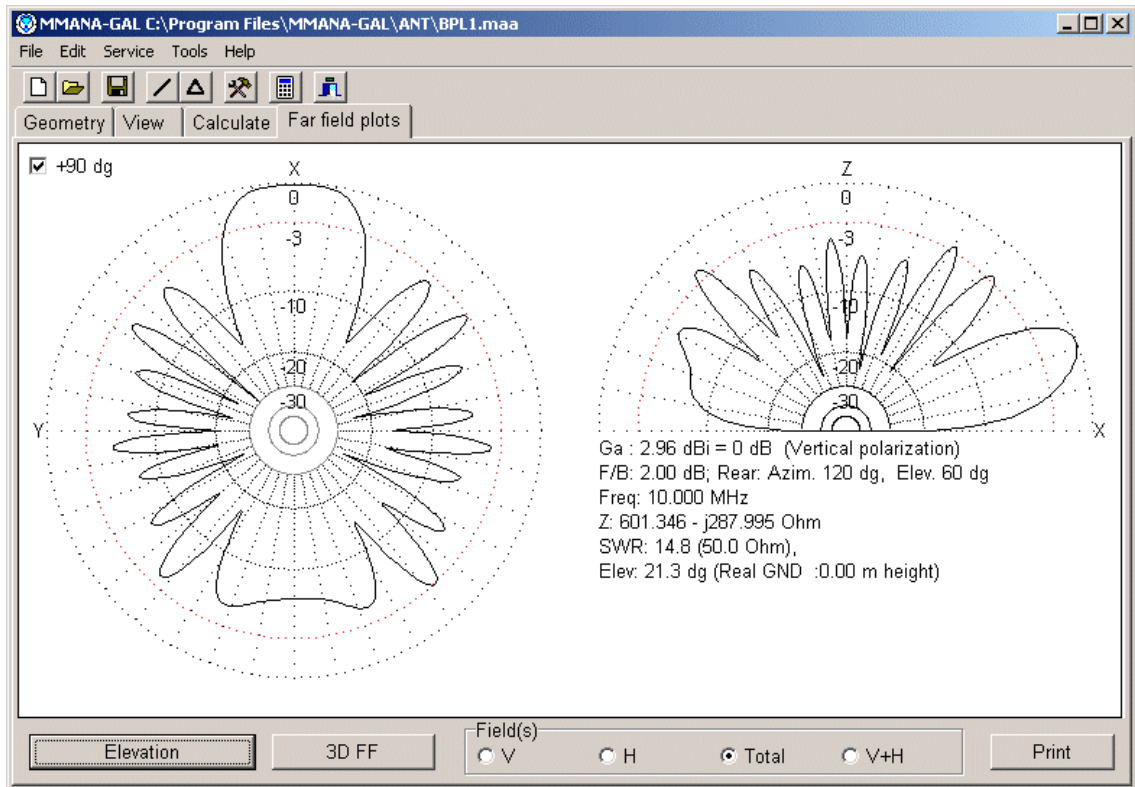


Figure 34. Far field plots for the antenna in Fig 32 at 10 MHz, with 530  $\Omega$  loads.

Fig 34 shows that with the 530  $\Omega$  terminating resistors, the maximum gain of the antenna is reduced to 2.95 dBi. It is concluded that the 50  $\Omega$  load is likely to be a better model for the worst-case situation in practice.

Fig 35 shows far field plots for the antenna in Fig 32 at 30 MHz, with 50  $\Omega$  loads. It can be seen that the maximum gain is increased slightly to 7.12 dBi and the number of lobes is increased.

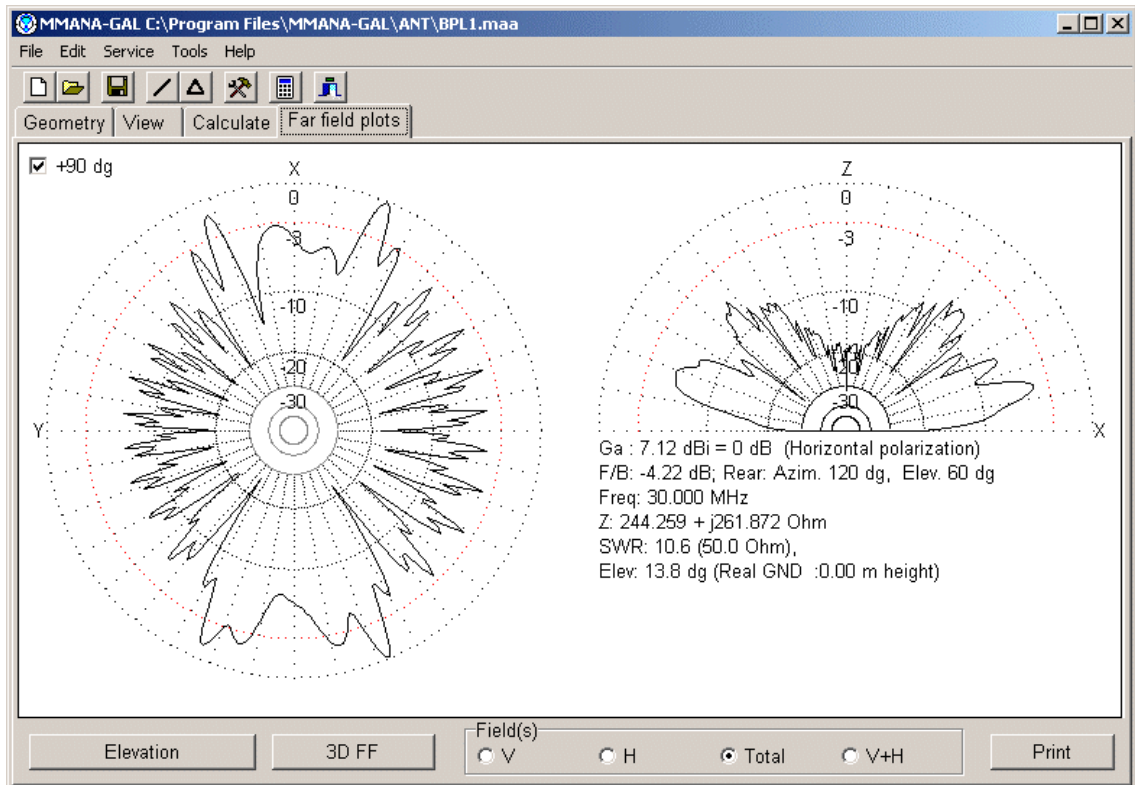


Figure 35. Far field plots for the antenna in Fig 32 at 30 MHz, with 50  $\Omega$  loads.

### 3.5. Conclusions

Antenna modelling has been applied to several types of wireline network. A model of in-building power wiring that was intended to model radiated emissions due to conversion of a differential mode source to common mode was found to suffer from convergence problems, which may be due to the close spacing of the conductors in a 3-core cable. Similar considerations apply to modelling in-building telephone wiring.

Antenna modelling of underground power cables required NEC4 antenna modelling software but this was not available for this programme of research due to licensing restrictions for non-US users.

Antenna modelling of a section of overhead line for BPL was performed successfully although with relatively long computation times at 30 MHz due to the large number of segments. It was shown that such networks can radiate BPL signals with a gain greater than a dipole in certain directions.



## **Chapter 4. Development of improved EMC measuring antennas**

This chapter analyses the design of tuned loop measuring antennas for the measurement of radiated emissions from installed communication networks at frequencies up to 30 MHz. It also analyses loop tuning techniques, loading and bandwidth, digital remote control of tuning by software. Measuring system noise floor and antenna calibration are also considered. A design for a higher sensitivity 1.6 m diameter tuned or untuned loop for 1.75 - 10 MHz is also presented together with a design for short dipole measuring antenna for 10 - 30 MHz

Measurement of H-fields below 30 MHz using an 'electrically small' loop is specified in standards such as CISPR 11/EN55011. An electrically small loop responds primarily to the H-field component of the incident electromagnetic field and this type of measurement is generally considered to be more satisfactory in practice than an E-field measurement in the LF/MF/HF bands because H-field measurements are less affected by the proximity of conductive objects. A set of three high sensitivity remotely tuned loop measuring antennas has been developed to allow measurement of lower field strengths than is possible with existing untuned H-field loop antennas.

Antennas have also been developed that provide a further increase in sensitivity in the range 1.6 - 30 MHz whilst still being reasonably portable. These are a 1.6 m diameter loop antenna for 1.6 - 10 MHz and a 2.5 m vertical antenna for 10 - 30 MHz.

### **4.1. Measurement of radiated emissions from networks up to 30 MHz**

The use of conducted rather than radiated emission tests for EMC emission measurements below 30 MHz is based on the assumption that as wavelength increases, the predominant source of radiated emissions is from connected cables rather than direct radiation from the Equipment Under Test (EUT) itself. This principle was originally applied to power ports only but more recently, it has been extended to telecommunication ports.

The CISPR 22 amendment of 18th April 1997 has been incorporated in an amendment to the Harmonised European EMC Standard for Information technology Equipment (ITE), EN 55022 [64]. This amendment specifies conducted emission limits from 0.15 - 30 MHz for telecommunication ports. These limits are derived from the mains power port limits but a

minimum value of Longitudinal Conversion Loss (LCL) is assumed for the twisted pair cable connected to the telecommunication port. LCL is the reciprocal of Transverse Conversion Loss (TCL) [44].

Where the communication cable is a type not specifically designed for radio frequency use, for example, in the case of Digital Subscriber Line (DSL) or Power Line Telecommunication (PLT) networks, the minimum TCL is poorly defined. In the case of multi-pair cables, there may be multiple sources all contributing to radiated emissions from such cables. In order to quantify radiated emissions from installed networks and to protect LF, MF and HF radio services adequately, it is becoming necessary to perform in-situ measurements of radiated emissions from cable communication systems at frequencies below 30 MHz.

An important consideration for radiated emission measurements below 30 MHz is the type of antenna used and its effect on the overall noise floor of the measuring system consisting of the antenna and measuring receiver. Fig. 36 shows the typical noise floor for three types of radiated field strength measuring systems, each using a measuring receiver with CISPR Quasi Peak (QP) detection and a bandwidth of 9 kHz.

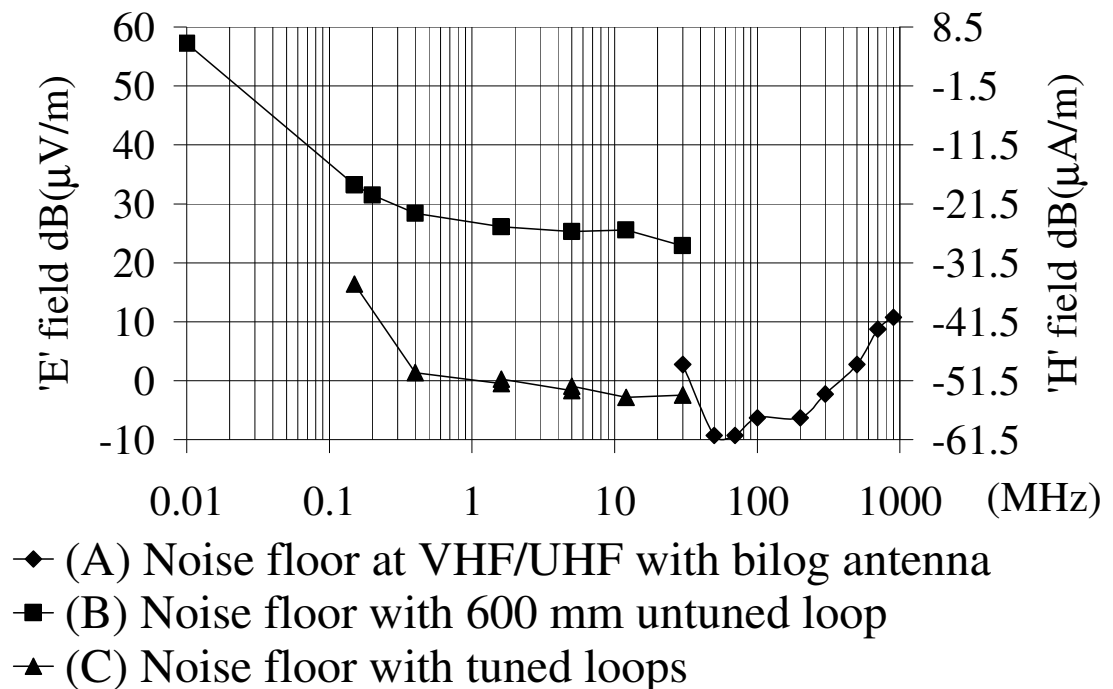


Figure 36. Noise floor for various radiated field strength measuring systems using QP detection and 9 kHz bandwidth.

Curve (A) in Fig. 36 is for a Schaffner CBL6111C 'Bilog' type of EMC measuring antenna commonly used for VHF/UHF radiated emission measurements at 30 - 1000 MHz and beyond. Although a bandwidth of 120 kHz is normally used above 30 MHz, curve (A) has been scaled to the equivalent field strength in 9 kHz bandwidth to allow direct comparison with the curves below 30 MHz.

Curve (B) is for a commercially available Schaffner HLA6120 600 mm diameter untuned loop antenna covering a frequency range of 9 kHz - 30 MHz. This is intended for CISPR 11 measurements and contains a built-in pre-amplifier. Although this is an 'H' field antenna, it is useful to consider its equivalent E-field antenna factor which is nominally 20 dB/m (i.e. an output from the antenna of 0 dB( $\mu$ V) corresponds to a field strength of 20 dB( $\mu$ V/m)).

Compared to an E-field antenna factor of 6 - 22 dB/m for a 'Bilog' type of antenna, this may appear reasonable but the noise contributed by the integral pre-amplifier in a typical untuned active loop needs to be considered. When referenced to an incident 'H' field strength, the pre-amplifier noise is equivalent to -18 to -28 dB( $\mu$ A/m) over the range 150 kHz - 30 MHz in 9 kHz bandwidth with QP detection. This is equivalent to an E-field strength of approximately +33 to +23 dB( $\mu$ V/m) under 'far field' conditions. It can be seen from Fig 36 that for the same measurement bandwidths, the noise floor of an LF/MF/HF measuring system using an untuned active loop antenna is substantially poorer than for a VHF/UHF measuring system using a passive antenna.

## 4.2. Tuned loop antennas

The performance of 'H' field loops for LF/MF/HF can be improved substantially by using a tuned loop, as shown by curve (C) in Fig 36. From 400 kHz - 30 MHz, a tuned loop can achieve an equivalent E-field antenna factor of approximately 20 dB/m without the use of a pre-amplifier. When referred to the incident field strength, the typical noise floor of the overall measuring system can be +1 dB ( $\mu$ V/m) or less over the range 400 kHz - 30 MHz, in 9 kHz bandwidth with QP detection. This represents an improvement of approximately 23 dB compared to an untuned loop antenna.

A set of three tuned loop measuring antennas was developed by the University of Hertfordshire under contracts from the Radiocommunications Agency of the DTI under contract, Ref. Electromagnetic Compatibility In Wireline Communications, Rev. 3

AY3430, "Design of a Portable Measuring System Capable of Quantifying the LF and HF Spectral Emissions From Telecommunications Transmission Networks at Field Strengths of  $1 \mu\text{V}/\text{metre}$  and Below." [38]. These loop antennas met the design requirement but required manual tuning and were therefore only suitable for measurements at spot frequencies. A further development was to make the antennas remotely tuned with control via an optical fibre communications link. The remote tuning development was funded by the Radiocommunications Agency under contract Ref. AY3920 [39]. Remote tuning allows automated swept measurements to be performed under software control.

It is not considered feasible to use the conventional design of 'shielded loop' which is normally used for untuned loops because the capacitance inherent in the conventional 'shielded' loop design would restrict the tuning range unduly. Furthermore, according to Collin and Zucker, [65] the type of antenna normally known as a 'shielded loop' is not truly shielded. The outer 'shield' is actually the antenna and the conductor inside the shield is the inner conductor of the coaxial transmission line leading to the load. The conventional 'shielded loop' design moves the effective feed point to the top of the loop and allows significant 'E' field rejection to be achieved without the use of a balun.

For the tuned loops, the 'E' field response is minimised by making the loops electrically balanced with balanced loads and by ensuring that they are 'electrically small'. The design target is for the ratio of electric dipole current to magnetic dipole current to be such that the response is primarily to the 'H' field component with at least 20 dB less sensitivity to the 'E' field under 'far field' conditions where  $E/H = 120\pi$  [51].

For the tuned measuring loops, an unscreened design is used because the capacitance inherent in the conventional 'shielded' loop design would restrict the tuning range unduly. Unlike the conventional 'shielded' loop design which normally uses an unbalanced feed to the actual loop conductor, the tuned loops are electrically balanced about earth to minimise 'antenna effect'. As a result of the research work under RA contract AY3430, a proposal was submitted to the IEC CISPR/A Committee to amend Clause 5.5.3.2 of CISPR 16-1:1999 [66], to include the use of tuned, electrically balanced loop antennas. This proposal was accepted and the 2004 edition of the CISPR 16 standard [67] has been amended.

#### 4.2.1. Analysis of tuned loop antennas

Kanda [68] gives the following equivalent circuit for an electrically small loop antenna.

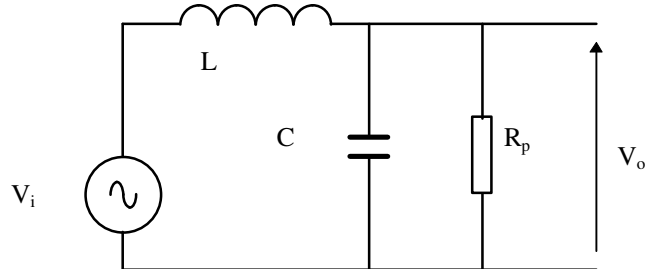


Figure 37. Equivalent circuit for an electrically small loop antenna

$L$  is the self-inductance of the loop,  $C$  is the total capacitance in parallel with the loop and  $R_p$  is the parallel load resistance.  $V_i$ , the voltage induced in the loop by the incident electromagnetic wave is determined by the rate of change of magnetic flux and is given by:

$$V_i = j\omega\mu H_i N S \quad (3)$$

where  $\mu$  is the permeability of the loop core,  $H_i$  is the component of the magnetic field normal to the plane of the loop,  $\omega$  is the angular frequency of  $H_i$ ,  $N$  is the number of turns and  $S$  is the area in  $m^2$ . Kanda states that at angular frequency  $\omega$ ,

$$\frac{V_o}{V_i} = \frac{-j\frac{1}{\delta}}{\frac{1}{Q} + j(\delta - \frac{1}{\delta})} \quad (4)$$

Where

$$Q = \frac{R_p}{X_0} \quad X_0 = j\omega_0 L \quad \delta = \frac{\omega}{\omega_0} \quad \omega_0 = \frac{1}{\sqrt{LC}} \quad (5)$$

If  $\omega = \omega_0$ , i.e. when the loop is at resonance,  $\delta = 1$  and (4) reduces to:

$$\frac{V_o}{V_i} = -jQ \quad (6)$$

Combining equations (3) and (6) yields the following transfer function at resonance:

$$\frac{V_o}{H_i} = \omega\mu NSQ \quad (7)$$

If far field conditions are assumed where  $E/H = 120\pi$ ,  $E_i/120\pi$  may be substituted for  $H_i$  so that:

$$\frac{V_o}{E_i} = \frac{\omega\mu NSQ}{120\pi} \quad (8)$$

Substituting  $\mu = \mu_0 = 4\pi \times 10^{-7}$  and taking the reciprocal yields the following expression for the inverse transfer function  $E_i/V_o$ :

$$\frac{E_i}{V_o} = \frac{120\pi}{\omega \cdot 4\pi \times 10^{-7} \cdot NSQ} = \frac{3 \times 10^8}{\omega NSQ} \quad (9)$$

It is also desirable to maintain a constant value of  $E_i/V_o$  over a relatively wide range of frequencies. One way to achieve this is to make the load resistance  $R_L$  much less than the inductive reactance  $X_L$  at all frequencies of interest, i.e.  $Q \ll 1$ . Hence the increase of  $V_i$  with frequency is compensated by the increasing reactance  $X_L$ . This is known as a 'short-circuit current loop' but does not yield sufficient sensitivity for this application.

An alternative approach is to use a 'Q' factor substantially greater than 1 and to maintain a constant  $\omega Q$  product, i.e. to make Q inversely proportional to frequency. Increasing Q as frequency decreases compensates for the decreasing rate of change of magnetic flux at lower frequencies. This can be achieved if C in Fig 37 is variable and R is constant and large compared to  $X_L$ .

As  $Q = R_p/X_L$  and  $X_L$  is directly proportional to frequency, Q is inversely proportional to frequency.

Although Kanda's analysis [68] is in the context of 'Q' factors less than 1, it appears to be valid for larger 'Q' factors. The maximum loaded 'Q' factor which can be achieved in practice is limited by series losses. These are ohmic losses which swamp the radiation resistance of the loops. The calculated radiation resistance of the loops ranges from  $2.5 \times 10^{-2} \Omega$  at 30 MHz to  $6 \times 10^{-9} \Omega$  at 100 kHz. The series losses in the resonant circuit can be represented by an equivalent parallel load resistor connected in parallel with  $R_p$  in Fig. 37.

Equation (7) only represents the antenna factor if  $R_p = 50 \Omega$ . As  $L$  is determined by the geometry of the loop and  $Q$  is determined by the required antenna factor, making  $R_p = 50 \Omega$  will not generally give the required 'Q'. Hence, it is necessary to match the parallel load resistance  $R_p$  to the required load resistance  $R_L$  (e.g.  $50 \Omega$ ) using a transformer with  $N:1$  turns ratio as shown in Fig. 38. The transformed load resistance  $N^2 R_L$  therefore defines the loaded 'Q'. A consequence of this is that the antenna factor depends on  $R_L$  and if the loaded 'Q' is small compared to the unloaded 'Q',  $R_L$  is driven by a constant current source.

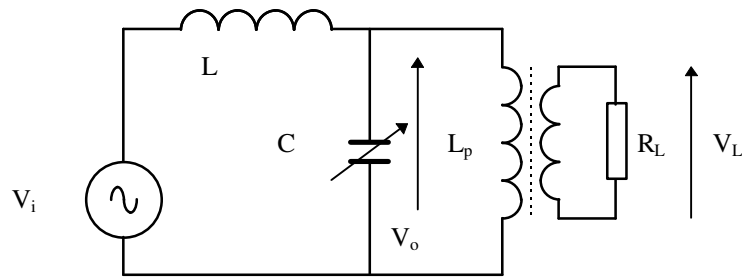


Figure 38. Equivalent circuit of an electrically small loop with transformer matching.

If the primary inductance  $L_p$  is large compared to  $L$  so that primary magnetising current is insignificant, then:

$$\frac{V_o}{V_L} = \sqrt{\frac{R_p}{R_L}} \quad (10)$$

where  $V_L$  is the p.d. across load  $R_L$ . Hence by substituting for  $V_o$ , the 'E' field antenna factor for a load  $R_L$  is given by:

$$\frac{E_i}{V_L} = \frac{3 \times 10^8}{\omega N S Q} \sqrt{\frac{R_p}{R_L}} \quad (11)$$

$R_p$  can be eliminated by substituting  $R_p = Q\omega L$

$$\frac{E_i}{V_L} = \frac{3 \times 10^8}{\omega N S Q} \sqrt{\frac{Q\omega L}{R_L}} = \frac{3 \times 10^8}{S} \sqrt{\frac{Q\omega L}{N^2 \omega^2 Q^2 R_L}} = \frac{3 \times 10^8}{S} \sqrt{\frac{L}{N^2 \omega Q R_L}} \quad (12)$$

It is required to maximise  $V_L$  for a given value of  $E_i$ , hence the ratio  $E_i/V_L$  should be as small as possible. The inductance of a single turn loop is determined by the loop geometry and wire diameter. The inductance of an  $N$  turn loop is directly proportional to  $N^2$ , hence  $L/N^2$  is constant. This shows that at a given frequency, changing the number of turns does not change

the antenna factor nor the required  $Q$ . Changing the number of turns does not change the amount of power captured by the loop. Nevertheless, it is desirable to minimise the inductance of each turn in order to reduce the required  $Q$ .

#### 4.2.2. Loop antenna parameters

$E_r/V_o$  is required to be of the order of 10 to achieve the required sensitivity. The design is subject to the following constraints:

- (A) The antenna factor should be substantially constant with frequency.
- (B) The largest practicable size of loop for portable use is considered to be approximately 1 m square or diameter.
- (C) The total conductor length should not exceed approximately 0.1 wavelength at the highest frequency of operation, for two reasons. First, to ensure that the loop is 'electrically small', i.e. the current is in the same phase all round the loop and the response is primarily to the 'H' field. Secondly, the self-resonant frequency (SRF) should be significantly higher than the highest frequency of operation to minimise proximity effects which occur near SRF where the loop resonates with stray capacitance.
- (D) Tuning should be by means of variable or switched capacitors with practical values of capacitance and ESR.
- (E) The unloaded 'Q' factor should be significantly higher than the loaded 'Q' but must be achievable in practice.
- (F) The loaded 'Q' should be such that the -3 dB bandwidth of the loop is always significantly greater than the 9 kHz -6 dB bandwidth of the measuring receiver.
- (G) The impedance transformation ratios for matching to 50  $\Omega$  should be achievable in practice with acceptably low loss.

The required frequency range of 100 kHz - 30 MHz can be covered using a set of three measuring antennas designated 'A', 'B' and 'C'. Four switched frequency ranges are required for loop 'A' and two for loop 'B'.

The design characteristics of the three original square loops are summarised in Table 5.2.2 below.



Loop:	A	B	C
Dimensions:	1 m x 1 m	0.6 m x 0.6 m	0.3 m x 0.3 m
No. of turns:	4	1	1
Inductance:	65 $\mu$ H	2.6 $\mu$ H	1.3 $\mu$ H
Maximum tuning capacitance:	730 pF	730 pF	182 pF
Conductor length:	16 m (0.094 $\lambda$ at $f_{\max}$ )	2.4 m (0.096 $\lambda$ at $f_{\max}$ )	1.2 m (0.12 $\lambda$ at $f_{\max}$ )
Frequency ranges:	100 kHz - 220 kHz 200 kHz - 440 kHz 400 kHz - 880 kHz 800 kHz - 1.76MHz	1.6 - 5.2 MHz 4.5 - 12 MHz	11 - 30 MHz
Self-resonant frequency:	>2 MHz	>18 MHz	>45 MHz
Minimum bandwidth: (See also Fig 40)	15 kHz.	45 kHz.	275 kHz.
Loaded Q (max):	30	33	40
Parallel load:	4000 $\Omega$ above 400 kHz	800 $\Omega$	3200 $\Omega$
Series load:	6 $\Omega$ below 400 kHz		

Table 4.2.2. Summary of loop characteristics.

#### 4.2.3. Loop tuning

The solution adopted for Loop 'A' is to use a 4 turn loop, 1 m square with a step-up transformer. The loop can then be resonated from 100 kHz upwards using up to 720 pF of variable capacitance. For 100 - 220 kHz, a 1:8.6 step up transformer is used between the loop and the variable capacitor. This effectively transforms a 4 turn loop into a 34.4 turn loop. The capacitor resonates with an inductor whose effective inductance is transformed up by a factor of  $8.6^2$  from approximately 65  $\mu$ H at the loop terminals to 4.6 mH at the capacitor terminals. The turns ratio is switched between 1:8.6, 1:4.3, 1:2.15 or 1:1.08 to select one of four ranges.

The required ratios and 'Q' factors can be realised in practice using two separate ferrite cored transformers, one for 100 kHz - 440 kHz and one for 400 kHz - 1.76 MHz.

For loop 'B', a step-up autotransformer wound on a ferrite ring core is used to resonate the single turn loop on the 1.6 - 5.2 MHz range using a 3:1 turns ratio. On the 4.5 - 12 MHz range, the variable capacitance is connected directly across the loop.

Loop 'C' has a single range covering 11 - 30 MHz. For the original mechanically tuned loops, a dual gang 365 pF variable capacitor was used with the two gangs in series so that the wiping contact is not in series with the resonant. This ensures a high unloaded 'Q' for loop 'C' at frequencies where the effect of series resistance of the wiping contact would be more significant than for loops 'A' or 'B'.

#### 4.2.4. Loop loading and bandwidth.

From 400 kHz - 30 MHz, the loops are loaded with parallel load resistances as listed in Table 2.2.2 above. This results in a substantially constant antenna factor as is shown in Fig 39. The antenna factors shown in Fig 39 are calculated and take account of the effect of finite unloaded 'Q'.

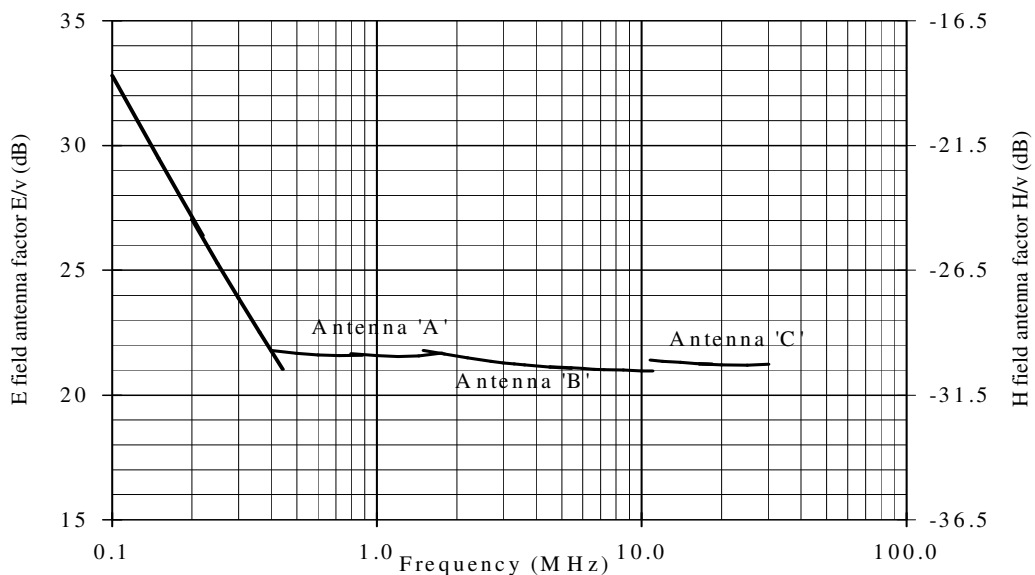


Figure 39. Predicted antenna factors of antennas 'A', 'B' and 'C' in passive mode

Although a near constant antenna factor could be maintained down to approximately 200 kHz before unloaded 'Q' becomes a limiting factor, the bandwidth at 200 kHz would be 9 kHz or less which is considered too narrow for EMC measurements using a 9 kHz measuring receiver bandwidth. The loading is therefore changed from parallel to series below 400 kHz. This results in a 'Q' which is directly proportional to frequency so that as frequency is reduced, the bandwidth remains constant but the sensitivity is reduced. Even if a constant antenna factor could be maintained down to 100 kHz without unduly narrow bandwidth, there would be little need for such high sensitivity in practice due to atmospheric noise levels. The -3 dB bandwidth of the loop antennas and the target loaded 'Q' factors are shown in Fig 40.

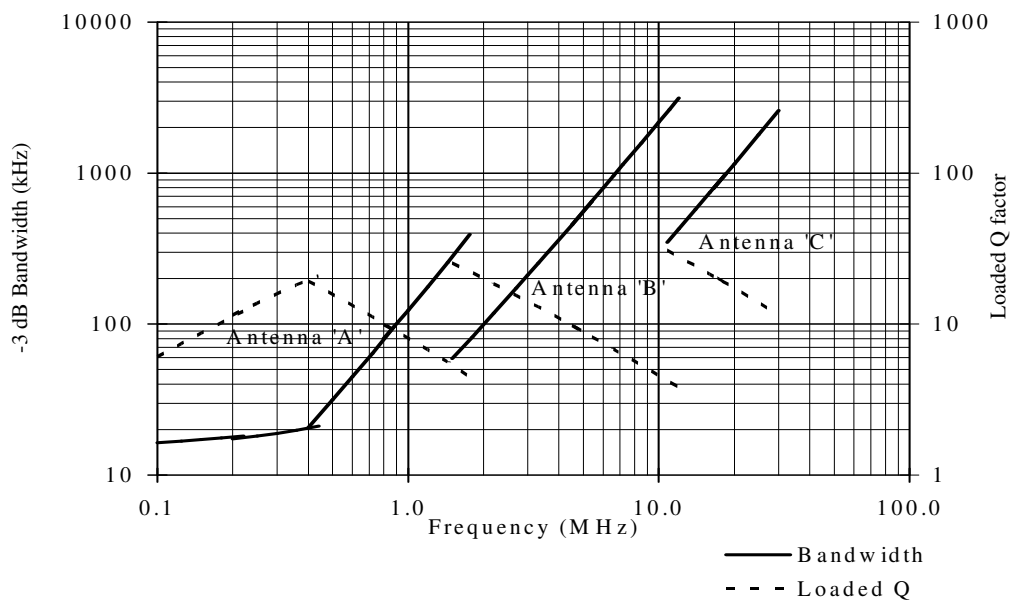


Figure 40. Design bandwidth and loaded 'Q' factors of antennas 'A', 'B' and 'C'

Fig 41 shows the prototype set of manually tuned loop antennas.

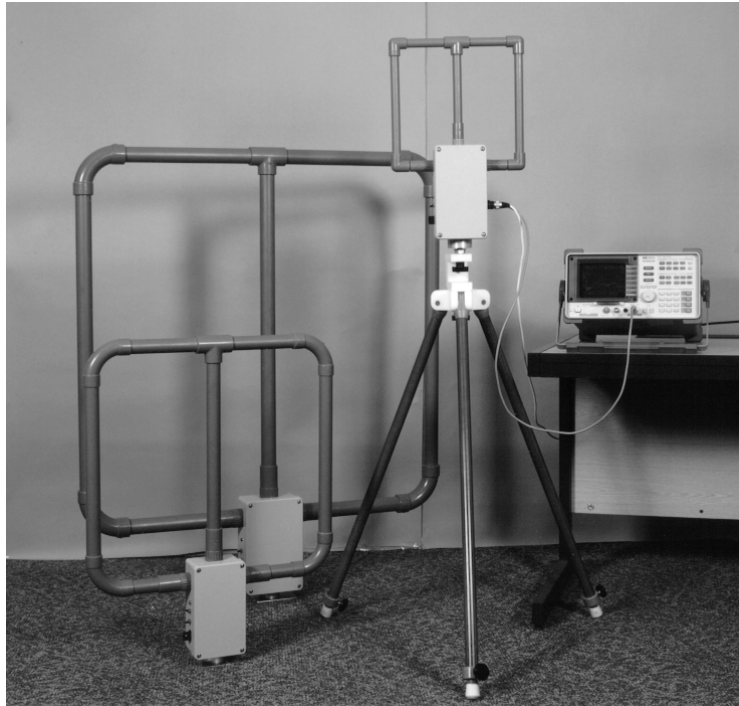


Figure 41. The prototype set of manually tuned loop antennas.

#### **4.2.5. Digital control of antenna tuning**

The manually tuned antennas were further developed into remotely tuned antennas, where the mechanical variable capacitors are replaced by a network of switched capacitors. A small proportion of the total capacitance is provided by variable capacitance (varicap) diodes for fine-tuning between steps. The switched capacitors, varicap diode bias voltage and range switching are all digitally controlled. The square loop conductors of the original tuned loops are replaced by circular loops as shown in Fig 42. The reduced inductance of the loops requires an increased capacitance of up to 1023 pF. The reduced area results in a slight reduction in sensitivity.



Figure 42. The prototype set of remotely tuned loop antennas during laboratory testing.

The largest loop, 1 m diameter covers a frequency range of 80 kHz - 1.7 MHz. The 600 mm diameter loop covers a frequency range of 1.5 - 13 MHz and the smallest 300 mm diameter loop covers a frequency range of 12.2 - 30 MHz.

Fig. 43 shows the principle of the remotely tuned loop antennas.

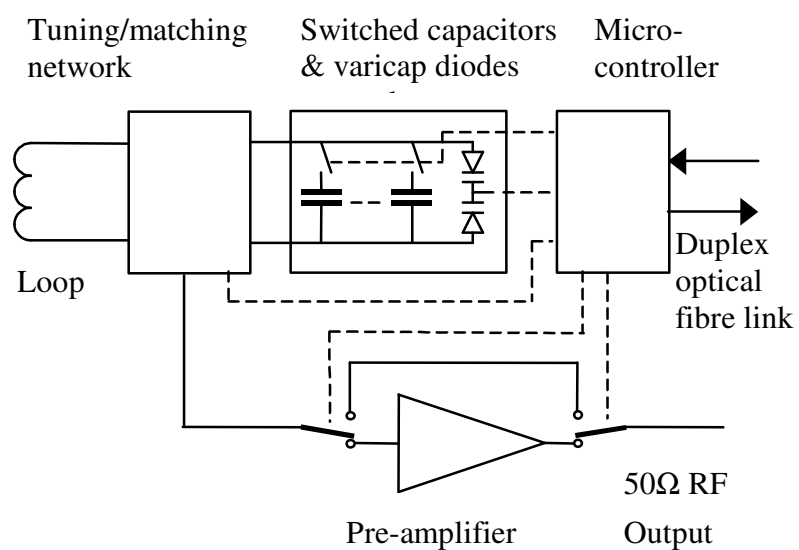


Figure 43. Block diagram of a loop antenna with remote tuning.

#### 4.2.6. Pre-amplifier

Each tuned loop antenna contains a built-in low noise pre-amplifier to compensate for the relatively poor noise figure of some measuring receivers or spectrum analysers which may have a noise figure of 12 dB or more. A broad band pre-amplifier module, Mini Circuits ZFL 500LN is used. The gain of 24 - 27 dB is sufficient to ensure that the overall measuring system noise floor is largely independent of the noise figure of the measuring receiver or spectrum analyser. The pre-amplifier can be switched out to enable the antenna to be used in passive mode if required, for example to increase dynamic range.

#### 4.2.7. Noise floor of measuring system

When using antennas 'A', 'B' and 'C' in active mode with their built-in pre-amplifiers and an EMC measuring receiver or spectrum analyser, the predicted system noise floor expressed as an equivalent field strength is as shown in Fig. 36. This is based on a measuring receiver noise floor of -22 dB( $\mu$ V) (Average) and -16 dB( $\mu$ V) (QP). Tests in a shielded enclosure showed that a lower noise floor could be achieved in practice.

Although the system noise floor increases below 400 kHz, the atmospheric noise field strength also increases at lower frequencies. Details of atmospheric noise levels are provided by ITU-R [69]. There are substantial variations with season, time of day and geographical location. The man-made and atmospheric noise curves in [69] are for a lossless vertical monopole antenna and have been converted to RMS field strength in 9 kHz bandwidth using equation (7) in [69].

Fig 44 shows two atmospheric noise levels plotted in terms of median r.m.s. 'E' field strengths in 9 kHz bandwidth. The 50% confidence curve is comparable to night time atmospheric noise levels in the UK whereas the 20% confidence curve is comparable to UK atmospheric noise levels at 08.00 - 12.00 UTC. At 200 kHz for example, the atmospheric noise level does not exceed +7 dB( $\mu$ V/m) with 20% confidence and does not exceed +21 dB( $\mu$ V/m) with 50% confidence. Hence if a measuring system noise floor of 0 dB( $\mu$ V/m) could be maintained from 400 kHz down to 100 kHz, this would be below the background atmospheric noise level for much of the time.

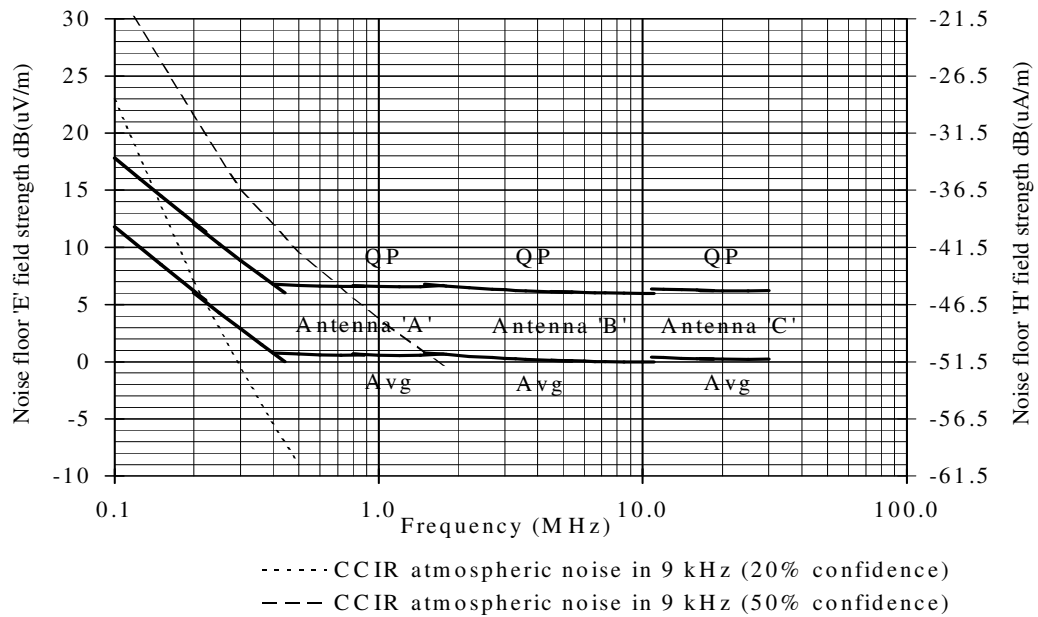


Figure 44. Measuring system noise floor, 'E' and 'H' field strength for loops 'A', 'B' and 'C' in active mode (QP and average detection)

### 4.3. Remote control of antennas

As stated in Section 4.2.5. above, the original manually tuned loop antennas were developed to provide digital control of tuning. This allowed a further development, which was to implement remote tuning via an optical fibre link so that automated swept frequency measurements could be made.

In the remotely tuned loop antennas, digital control of the switched capacitors, range switching and pre-amplifier is performed by a microcontroller in each of the antennas. The microcontroller receives commands and provides responses via a duplex optical fibre communication link. When measurements are being made, the microcontroller can be set into a 'sleep' mode which stops the clock oscillator to avoid generating RF interference.

When the tuned loop antennas are used with a measuring receiver for swept measurements, both instruments can be controlled by means of a portable computer and LabVIEW™ software. Fig. 45 shows a block diagram of a system for performing swept measurements using the tuned loop antennas.

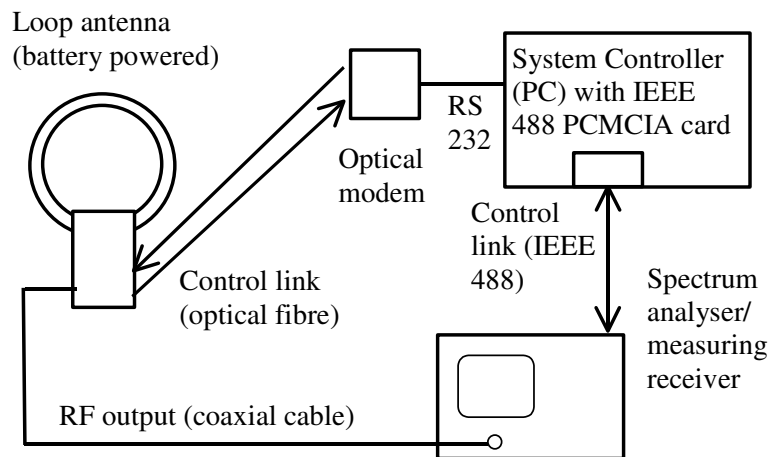


Figure 45. Block diagram of an EMC measuring system using a remotely tuned loop antenna.

#### 4.3.1. Tuning technique

A combination of switched capacitors and varicap diodes was used. For switching the capacitors, various solid state switching devices were evaluated but none had both a sufficiently low ESR and a sufficiently low shunt capacitance.

The final design of the digitally controlled switched capacitor consists of 6 relays which switch capacitors in a binary sequence. Each switched capacitor consists of two halves with one half switched by each pole of the double pole relay. This halves the ESR but doubles the stray capacitance. The steps are interpolated by means of varicap diodes which provide 16 linear capacitance steps. Hence the overall switched capacitance resolution is 10 bits. The 16 steps are derived from an 8 bit D/A converter which is driven via a software lookup table to linearise the square law characteristic of the varicap diodes.

#### 4.3.2. Hardware description

Fig 69 in Appendix A shows the schematic diagram of the microcontroller board in the remotely tuned loop antennas. The microcontroller board is mounted in the battery compartment of the loop antennas. U5 is an Atmel AT89S8252 single chip microcontroller with 8 kBytes of Flash electrically erasable and reprogrammable program storage and 2 kBytes of EEPROM non-volatile data memory.



Port pins P0.0 - P0.7 are buffered to control six relays on the radio frequency and the band selection function. Port pin P1.1 is an output that is buffered to control the pre-amplifier. Port pin P1.0 can be programmed to generate a 'comb' frequency for confidence testing purposes. Port pin 1.2 is an input used to set Normal or Calibration mode according to the position of a 'jumper' link on the pins of J3.

Port pins P1.5, 1.6 and 1.7 are used for the in-circuit programming function, which allows the microcontroller program to be loaded or erased and reloaded without removing the microcontroller from its socket.

Port pins 2.0 - 2.7 provide an 8 bit parallel output to drive then varicap fine-tuning voltage via a Digital to Analogue Converter (DAC). The DAC output is amplified by U9A to give a swing of approximately 0.5 - 13 V. This is the varicap tuning voltage but the lower part of the range below 3.5 V is not used.

Ports 3.0 and 3.1 of U5 are the serial port receive input and transmit output respectively. The received serial data signal on P3.0 is also connected to P3.2 input (Interrupt 0) in order to generate an interrupt to wake the microcontroller up from sleep mode when a character is received. U1C - U1F buffer and invert the transmit data line and can provide up to 16 mA of current source or sink capability to drive an optical fibre transmitter.

Port 3.4 is an input that is connected to the overload detector in the existing loop antenna circuitry. Port 3.3 is an input that is connected to the low battery warning indicator in the existing loop antenna circuitry via R12 and R14 which reduce the 15 V swing to 5 V.

The microcontroller clock frequency is 11.059 MHz. This frequency is required by the internal baud rate generator. To avoid generating RF interference, the processor clock is stopped when the microcontroller goes into 'sleep' mode and can be restarted by means of an interrupt on port pin P3.2.

A photograph of the assembled microcontroller PCB mounted in the box is shown in Fig 46 below.

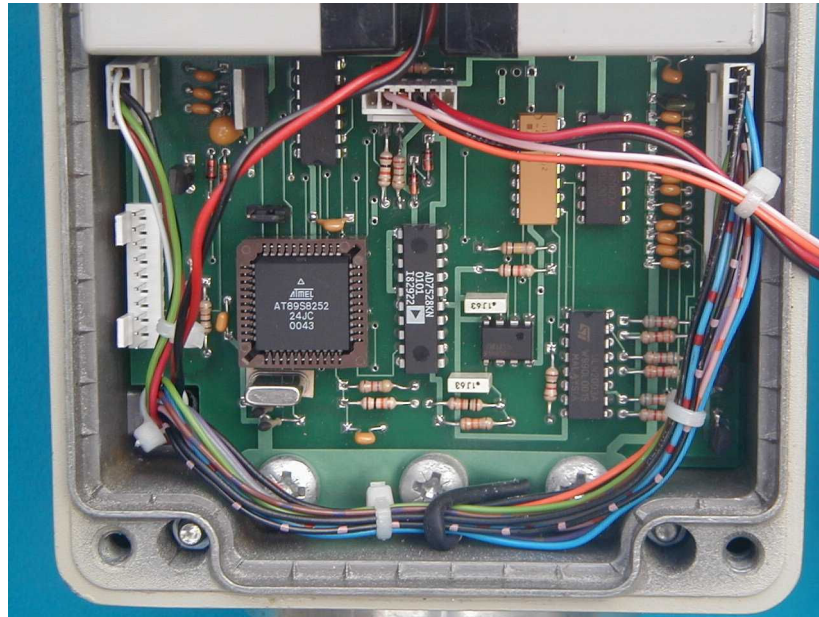


Figure 46. The assembled microcontroller board mounted in the box

Fig 70 in Appendix A shows the schematic diagram of the switched capacitor board. This consists of six relays that switch a binary sequence of capacitors.

For loops 'A' and 'B', the sequence of switched capacitors is nominally 16, 32, 64, 128, 256 and 512 pF. This allows capacitance values of 0 - 1008 pF to be selected in 64 steps of 16pF. The 16 pF steps are interpolated by means of varicap diodes D5 and D6 which provide a resolution of 1 pF steps using a bias voltage of approximately 3.5 - 11.5 V. The possible effect of varicap diode non-linearity on strong signal handling performance is minimised by making the varicap diode capacitance a small proportion of the total, by using 'back-to-back' varicaps and by avoiding low bias voltages. The overall result is that 10 control bits allow the selection of 0 - 1023 pF in 1 pF steps for Loops 'A' and 'B'. For Loop 'C', all capacitances are divided by 4 so that the relays switch 4 pF steps and the varicap works in 0.25 pF steps giving an overall range of 0 - 255.75 pF in 0.25 pF steps.

Silver-mica capacitors are used for the larger fixed capacitance values where close tolerance, low temperature coefficient and low RF loss are required. Miniature trimmer capacitors are also provided to compensate for the capacitor tolerances and also the switched stray

capacitances, so that a monotonically increasing sequence of capacitance values can be achieved.

Due to the stray capacitance of the relays, PCB tracks and the minimum capacitance of the varicap diodes, the minimum capacitance is approximately 40 pF. This is substantially larger than for a mechanical variable capacitor and although this is not a significant issue for Loops 'A' and 'B', it was necessary to reduce the inductance of Loop 'C' to allow a maximum frequency of at least 30 MHz to be reached.

U10 and U11 are varicap diodes connected in a balanced 'back to back' configuration with bias voltage supplied via R20.

J9 is the output of the 'Comb Generator' test signal. To implement the 'Comb generator' requires further development of a means of coupling the signal into the main loop.

A photograph of the assembled PCB mounted in a box (Loop 'C') is shown in Fig 47 below.

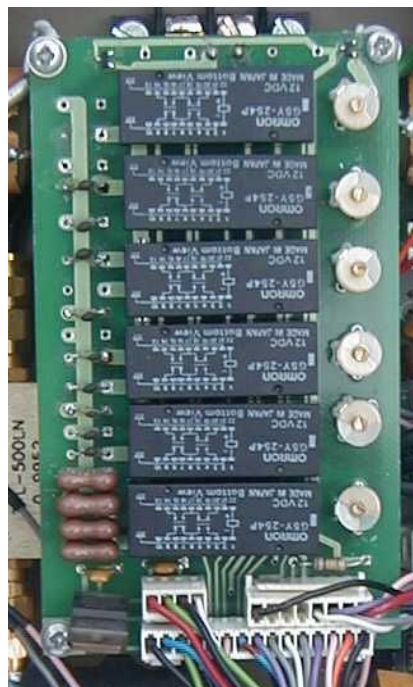


Figure 47. The assembled switched capacitor board mounted in Loop 'C' box

### **4.3.3. Optical fibre link**

An optical fibre communication link is used in preference to a copper cable to avoid the possibility of RF signals reaching the antenna via the control cable. The link operates at 9600 bits/s. The optical fibre used is a duplex 62.5/125µm glass fibre terminated with ST type connectors. The length of the fibre used is 10 m but the opto-electronic devices used could operate with a very much longer fibre if required.

A commercial RS-232 to optical fibre line driver is used at the PC end of the optical fibre cable. Each loop antenna has its own built-in optical fibre transmitter and receiver operating at 850 nm wavelength.

### **4.3.4. Communication protocol**

Full details of the Loop Antenna Serial Communication Protocol are given in [39]. The loop antenna communicates with the system controller using a pair of optical fibres that carry 9600 bits/s asynchronous serial data with no flow control.

The protocol includes messages that request the antenna to report its type, minimum and maximum frequency, serial number, firmware version and date. There is also a message to request the antenna status which includes the status of the overload detector, battery condition, pre-amplifier and test signal ('comb') generator.

There is also a message to instruct the antenna to tune to a specific frequency. The antenna responds with a message indicating that it is ready or that the requested frequency is out of range. There are messages to control the state of the pre-amplifier and the test signal (comb) generator.

There is a message to get the antenna factor from the antenna factor lookup table that is stored in non-volatile memory in the microcontroller. If the frequency requested does not coincide with one of the points stored in the antenna factor table, the microcontroller interpolates between the two nearest stored points.

The antenna can be instructed to enter and leave a 'sleep' mode where the clock oscillator is stopped to avoid generating RFI while measurements are being taken. It can also be set to a standby mode where it de-energises all relays to minimise battery current

There are further messages that are only accepted when the antenna is set to 'Calibration' mode by setting an internal jumper link. These include direct setting of the switched capacitors, the band and the DAC code. Other Calibration mode messages are available to set, clear and list the varicap voltage look-up table, the frequency to capacitance look-up table and the antenna factor table in non-volatile memory.

There is also one error message and one warning message that the antenna may send at start-up. No other messages are initiated by the antenna.

#### **4.3.5. Microcontroller firmware**

The program for the microcontroller is written in the 'C' programming language. Some public domain functions are used with modifications for interrupt driven serial I/O and a command interpreter. The total program size is approximately 8100 bytes.

An algorithm for frequency interpolation has been developed which calculates the required capacitance  $C_x$  for a frequency  $f$  in between two frequencies  $f_1$  and  $f_2$  where the required capacitances  $C_1$  and  $C_2$  respectively are known. In order to do this, the apparent stray capacitance  $C_s$  must be known but this cannot be measured directly so it must be calculated. It may be expected that  $C_s$  would be constant across the frequency range covered by each antenna but there is some variation with frequency in practice.

$$C_s = ((k_3.C_2) - c_1)/(1 - k_3) \quad (13)$$

$$C_x = ((C_1+C_s)/k_2) - C_s \quad (14)$$

$$\text{where } k_2 = (f/f_1)^2 \text{ and } k_3 = (f_2/f_1)^2$$

This algorithm uses 32 bit floating point arithmetic but the rest of the program uses 8 or 16 bit integer arithmetic wherever possible.

### 4.3.6. LabVIEW™ software

The software to control the loop antennas and the measuring instruments was implemented using LabVIEW™ version 6. This allows 'virtual instruments' (VI) to be produced which run on a computer.

A LabVIEW™ VI consists of a graphical front panel, which is the user interface and a diagram which is the means of programming the VI. A top level VI can invoke 'sub-VIs' which can in turn invoke further sub-VIs, each with their own diagrams and panels. LabVIEW™ also provides a library of 'VISA' Input/Output functions which can be used to control instruments such as an EMC measuring receiver or spectrum analyser via an IEEE488 interface or instruments with a serial interface such as the remotely tuned loop antennas.

The front panel diagram for the Swept Measurement R&S ESCS30.vi is shown in Fig. 48 below. This was used to control the ESCS30 EMC measuring receivers used by the RA.

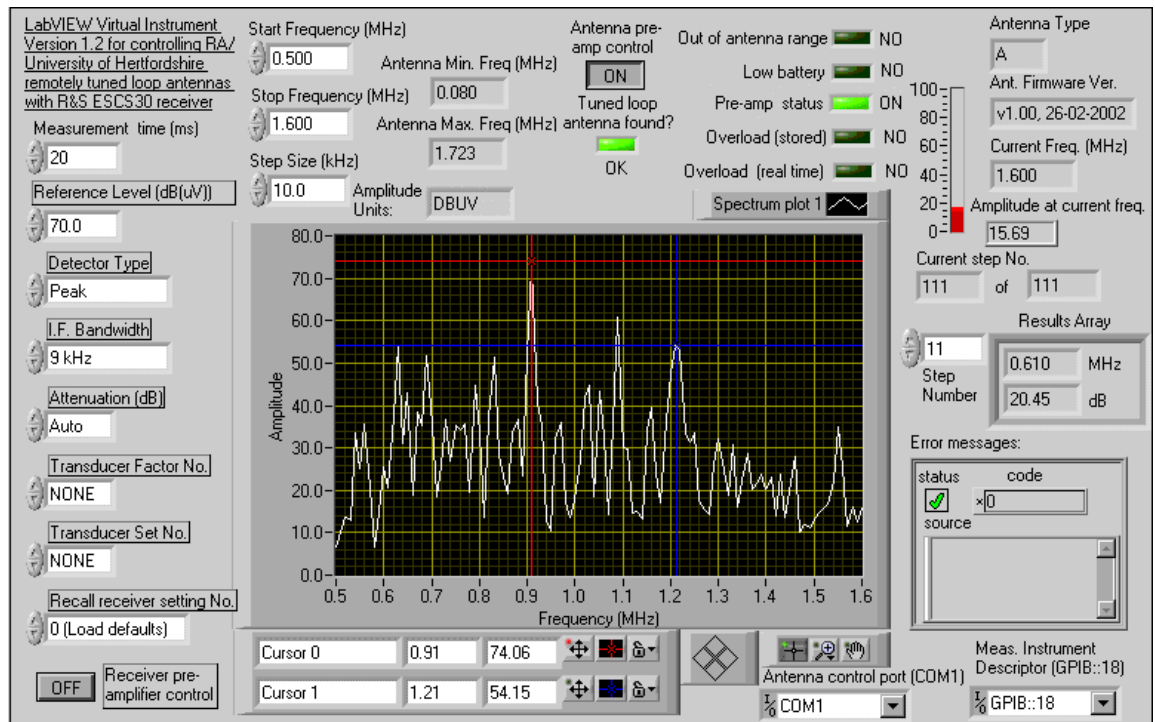


Figure 48. Front panel diagram for Swept Measurement R&S ESCS30.vi

This VI is the user interface for swept measurements using the tuned loops with an R&S ESCS30. It allows the user to control the following settings of the ESCS30:

- Measurement time (in addition to the time required for the selected detector to settle).
- IF bandwidth (200 Hz, 9 kHz, 120 kHz or 1 MHz)
- Attenuation, (0 - 60 dB or automatic)
- Detector type (Peak, Quasi-Peak or Average)
- Transducer factor and set
- Optional recall of stored settings
- Receiver pre-amplifier state (On or Off)

This VI displays the following information from the tuned loop antenna:

- Antenna found or not found
- Antenna type, serial number, firmware version, maximum and minimum frequencies
- Antenna pre-amplifier status (On or Off), overload status and battery status.

It also allows the user to control the following Antenna pre-amplifier state

This VI allows the user to control the following settings of the swept measurement:

- Start, stop frequencies and step size
- GPIB address of measuring receiver and COM port number for loop antenna

This VI displays the following information when a swept measurement is in progress:

- Current step number and amplitude at current step (with bar graph)
- Total number of steps (currently limited to 2000 steps but could be increased)
- Out of antenna range (if sweep start or stop frequency is outside antenna range)
- LabVIEW error status box with any error messages or warnings

When a swept measurement has been completed, the user is prompted for the name of a file in which to store the results in CSV (Comma separated value) format compatible with Microsoft Excel and other spreadsheets. Measurement points are then displayed by the VI as a spectrum

plot with automatic horizontal and vertical scaling and a zoom function. The user can also step through the array of results and display the frequency and amplitude at each point.

The diagram of the Swept Measurement R&S ESCS30.vi is shown in Fig 71 Appendix B. The diagrams for this and other associated VIs are contained in [39]. The top-level VI calls a number of sub-VIs to initialise the ESCS30, configure its amplitude, detector type and bandwidth, set transducer factors and perform a measurement at a specified frequency.

Other sub-VIs are provided to perform various functions related to the tuned loop antenna. These include initialising the antenna, getting its status and information, setting the pre-amplifier state, tuning the antenna to a specified frequency and entering or leaving the 'sleep' mode.

The LabVIEW software was initially developed using an HP8591EM spectrum analyser as the measuring instrument because the ESCS30 measuring receivers are property of the RA and one was not available for the duration of the software development phase of the project. A top level VI and a set of sub-VIs was developed to drive the HP8591EM as a measuring receiver to make a series of spot-frequency measurements. Although these are broadly similar to those that control the R&S ESCS30 receiver, there are significant differences between the two instruments.

A third set of VIs was derived from the set for the HP8591EM. These VIs drive a Rohde & Schwarz type ZVR network analyser which was used for performance verification and pre-calibration of the loop antennas.

#### **4.3.7. Laboratory testing**

The switched capacitor network needs to be adjusted so that it generates a monotonic sequence of capacitance values with near uniform step sizes. Details of how this was performed are given in [39]. In practice, this was found to be a difficult procedure. Various resonant frequencies were then stored in the antenna frequency-to-capacitance lookup tables. This resulted in between 17 and 25 points per antenna, depending on how many bands the antenna has. A comprehensive frequency setting accuracy test was then performed and the maximum



frequency setting error was found to be  $\pm 0.5\%$  at isolated frequencies and substantially less at other frequencies.

#### 4.3.8. Pre-calibration of tuned loops

Pre-calibration was performed to verify performance before submitting the antennas for final calibration by an EMC test laboratory. An outdoor pre-calibration set-up is shown in Fig 49 below. A Rohde and Schwarz model ZVR network analyser was used to perform swept measurements of path loss between a radiating loop and the tuned loop under test. The resolution bandwidth of the ZVR analyser was set to 100 Hz, which minimised interference from ambient signals and allowed the radiating loop to be driven with only the 10 mW output power available from Port 1 of the ZVR analyser. Antenna calibration was performed using a substitution method where a calibrated Schaffner-Chase HLA6120 untuned loop antenna was substituted for the tuned loop antenna under test.



Figure 49. Outdoor pre-calibration of the remotely tuned loop antennas

Some difficulties were encountered during calibration as the polar diagram and polarisation of the radiating and receiving loops appeared to vary with frequency, leading to increased measurement uncertainties. The radiation pattern of a loop was subsequently analysed using antenna modelling software and are described in section 5.1 below.

#### 4.3.9. Final calibration

Enquiries were made with NPL about antenna calibration but their test method used a TEM cell and could not accommodate a loop antenna with a diameter larger than 600 mm.

Final calibration was performed by Schaffner EMC Systems Ltd on their open area antenna test site at Capel near Dorking. This required some software development by Schaffner EMC Systems Ltd to drive the loops and enable automatic swept measurements to be performed using their test equipment.

To avoid unwanted coupling via earth loops, a separate signal generator and measuring receiver were used with the measuring receiver powered by batteries. The readings from the measuring receiver were communicated via an optical fibre link to ensure full galvanic isolation between the radiating and receiving antennas, thereby avoiding any unwanted coupling path by conduction. The antennas were calibrated both with the pre-amplifier on and again with the pre-amplifier off giving two sets of antenna factor data.

After calibration, the loop antennas were delivered to the RA who used them in field trials of PLT networks at Crieff and Cambeltown in Scotland, as shown in Fig 50 below.



Figure 50. RA field trials on a PLT network in Campbeltown using tuned loop 'B'

## **4.4. Further development of measuring antennas**

Based on the knowledge gained in developing the remotely tuned loop antennas [39], various design improvements were identified, including improved sensitivity and method of tuning. There are benefits in increasing the sensitivity so that the limiting factor for the noise floor of the field strength measuring system becomes atmospheric noise rather than receiver noise or pre-amplifier noise.

### **4.4.1. A 1.6 m diameter untuned loop for 1.75 - 10 MHz**

Although the tuned loop antennas designed above achieved a substantial improved antenna factor compared to untuned antennas, a need for a further increase in sensitivity was identified. This could be achieved by increasing the 'Q' factor of the loop or increasing the area. Due to the practical difficulties of increasing the 'Q' factor, the area has been increased while still maintaining a portable antenna.

Applying the calculations in section 4.2.1 above shows that with an untuned 1.6 m diameter loop, a 23dB/m E-field antenna factor can be achieved. Although this antenna factor is 3dB poorer than a Rohde and Schwarz HFH-Z2 loop, the former is passive whereas the latter uses a pre-amplifier. Hence the noise floor of the measuring system with a passive loop is approximately 20dB lower. With a tuned loop, an equivalent E-field antenna factor of 5 to 8 dB/m can be achieved.

The inductances of a 1.6 m diameter loop with a conductor diameter of 10 mm is approx. 5 $\mu$ H. There would be some advantage in using 100 mm wide metal strip conductor, which can reduce the inductance to approx. 4 $\mu$ H but due to the practical difficulties involved in construction of a folding loop, a strip was not used.

The antenna factor at 1.75 MHz can be improved by introducing a series capacitor of 1.6 nF in series with the loop. This resonates with the inductance of the loop so that the mismatch loss due to the inductance of the loop at 1.75 MHz is minimal (approx 0.14 dB) and a constant antenna factor of 22.8 dB/m can be achieved from 1.75 MHz - 10 MHz. It should be noted however that the above matching technique does not provide conjugate impedance matching, i.e. the 50  $\Omega$  load resistance is much higher than the real part of the source impedance of the loop, which consists of radiation resistance plus loss resistance. Below 1.75 MHz, there is a

relatively rapid second order, 40 dB/decade roll-off. Fig 51 shows a 1.6m diameter untuned loop with balanced series capacitors and a balun.

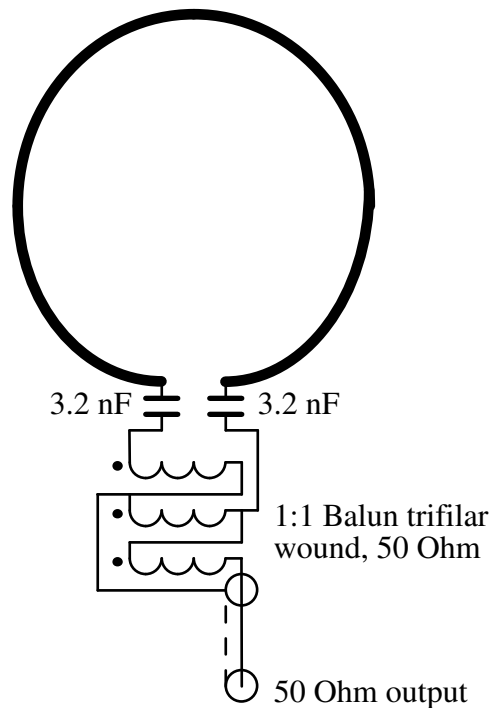


Figure 51. A 1.6m diameter untuned loop with balanced series capacitors and a balun:

Inclusion of the balun is desirable otherwise the braid of the coaxial cable would become part of the antenna which distorts the radiation pattern and increases measurement uncertainty.

This 1.6m diameter untuned loop gives a useful antenna factor as it is entirely passive with no pre-amplifier noise. It is adequate for many EMC emission measurements but it does not allow the atmospheric noise floor to be detected. For this a tuned loop is required (see 4.4.2. below).

#### 4.4.2. A 1.6 m diameter tuned loop for 1.75 - 10 MHz

For higher sensitivity to measure background radio noise levels at HF, a tuned loop is required although swept measurements cannot then be made except over a relatively narrow bandwidth unless the loop is remotely tuned and automatically tracks the measuring receiver's tuned frequency. Although the 'Q' factor is low compared to transmitting loops, it is well defined in order to provide a well-defined antenna factor.

Using the analysis in section 4.2.1 above, it can be shown that with a loaded Q of 37,  $R_L = 50 \Omega$ ,  $S = 1.99 \text{ m}^2$ ,  $f = 3.5 \text{ MHz}$ ,  $E_i/v_o = 1.66 = 4.4 \text{ dB}$  antenna factor. This would be a very effective EMC measuring antenna, allowing atmospheric noise level to be measured from 1.75 - 10 MHz.

A 'Q' of 37 at 3.5 MHz requires a parallel load resistance of  $4070 \Omega$  which can be achieved using two cascaded transformers each with a turns ratio of 3:1 (9:1 impedance ratio each) to give a total of 81:1 impedance transformation. For a loaded Q of 37 at 3.5 MHz, an unloaded 'Q' of at least 100 would be desirable. This requires variable capacitors, fixed capacitors and any switches or relays to have a low series loss resistance and is probably the highest practical 'Q' for operation down to 3.5 MHz. For 3.5 - 10 MHz, the constant parallel load resistance results in a loaded 'Q' which falls with frequency, hence the unloaded 'Q' also becomes less critical at higher frequencies. Conversely, for operation at lower frequencies down to 1.75 MHz with a constant antenna factor, the loaded 'Q' would need to rise to 74 so an unloaded Q of >150 at 1.75 MHz would be desirable. This may be difficult to achieve in practice so for operation down to 1.75 MHz with constant antenna factor, a lower loaded 'Q' was selected.

A lower 'Q' design uses an  $1800 \Omega$  parallel load resistance using two cascaded transformers with a turns ratio of 2:1 and 3:1 respectively to give a 36:1 impedance transformation. This results in a loaded 'Q' of 16 at 3.5 MHz, hence  $E_i/v_o = 2.52 = 8 \text{ dB}$ . This is still a good antenna factor for a passive antenna and it is less critical on loss resistance and tuning accuracy as it has a wider -3dB bandwidth (219 kHz at 3.5 MHz and 109 kHz at 1.75 MHz). Fig 52 shows a 1.6m diameter tuned loop with  $1800 \Omega$  parallel load resistance.

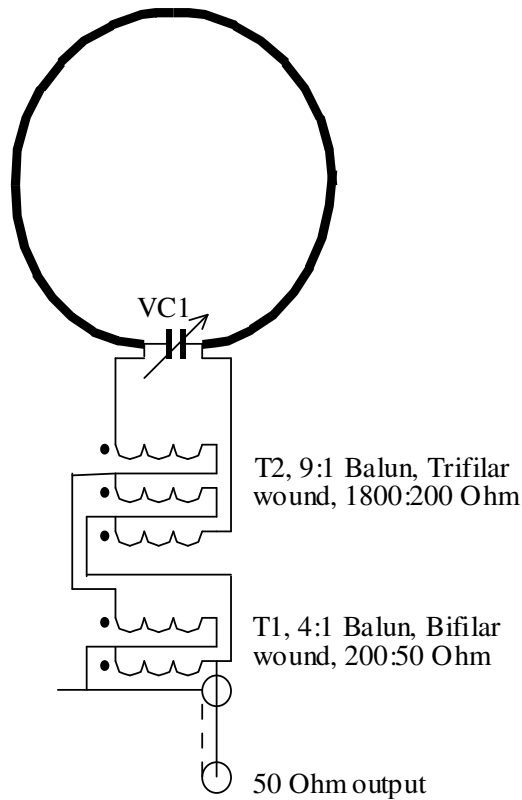


Figure 52. A 1.6m diameter tuned loop with 1800  $\Omega$  parallel load resistance.

#### 4.4.3. Loop tuning technique

The switched-capacitor technique with varicap diode fine-tuning was implemented successfully in the previous remotely tuned antennas but it required careful setting-up to achieve a monotonic sequence of steps from 0 - 1023 pF. It also results in small step changes in antenna factor at certain frequencies. An alternative approach is to dispense with the preset capacitors and avoid the need for a monotonic sequence by using a much larger look-up table stored in the PC rather than in the antenna (see 4.4.4 below).

#### 4.4.4. Loop antenna control logic

The use of a microcontroller in the previously developed remotely tuned loop antenna has the advantage that the frequency calibration data is stored inside the antenna and the antenna can report its status. A significant disadvantage is that in order to avoid RF interference, the microcontroller clock must be stopped before measurements are made. It must then be restarted by means of a 'wake up' message or preamble before subsequent serial communications messages can be received.

An alternative approach has therefore been adopted for the 1.6 m diameter tuned loop which is to minimise the functionality of the control circuitry built into the loop. Control is still via an optical fibre but the microcontroller in the antenna is replaced with digital logic that performs a 16 bit serial-to-parallel converter function and does not require a continuously running clock. All processing is therefore performed in the PC, including tuning look-up tables. As the tuning look-up tables can be larger and more complex, it is possible to avoid the need for critical adjustments as it is not necessary to make the switched capacitor and varicap diodes tune in a monotonic sequence.

The variable capacitor VC1 in Fig 52 above is implemented using a combination of low loss capacitors switched by means of low loss RF relays together with varicap diodes. The prototype 1.6 m diameter loop, which can operate in tuned or untuned mode and can tune from 1.75 - 10 MHz, is shown in Fig 53 below [70]. It can also be folded in half for easier transportation by vehicle, as shown in Fig 54 below.



Figure 53. The prototype 1.6 m diameter loop mounted on a tripod



Figure 54. The prototype 1.6 m diameter loop folded for transportation

#### **4.5.A short dipole measuring antenna for 10 - 30 MHz**

A practical difficulty with increasing the sensitivity of the set of three tuned loop antennas described in Section 4.2 above was that Loop 'C' for a frequency range of 11 - 30 MHz, had to be relatively small so that the loop inductance was low enough to allow the loop to tune up to 30 MHz with the stray capacitances of the tuning circuitry. For the remotely tuned antennas, the stray capacitance was larger than for the manually tuned loops, which necessitated a further reduction in loop area. In order to achieve the required antenna factor with the available loop area, it was necessary to use a relatively high loaded 'Q' factor, which resulted in other practical difficulties [39]. Any further increase in sensitivity of a remotely tuned loop antenna covering 11 - 30 MHz was therefore not considered feasible.

In order to produce an EMC measuring antenna for 10 - 30 MHz with a lower antenna factor (i.e. higher output for a given field strength) compared to the tuned loops, a 4.4 m long electrically short dipole has been used. This is designed to resonate slightly above 30 MHz and can be folded or dismantled for easier transport.



As shown in section 6.2 below, antenna modelling of a 4.4 m long dipole at 10 MHz gives a predicted feedpoint impedance of  $4.55 + j1177.84 \Omega$ . In principle, a conjugate impedance matching network could be designed for such a dipole. In practice, this would need to be a remotely controlled antenna matching unit at the feedpoint of the dipole and this would need to be 'track tuned' when swept measurements were made with a measuring receiver. Although such an arrangement would provide optimum matching, a useful EMC measuring antenna that does not require any tuning can be designed using a much simpler matching arrangement.

It can be shown from basic a.c. circuit theory that if an a.c. source with a source impedance of  $4.55 + j1177.84 \Omega$  at 10 MHz is connected directly to a  $50 \Omega$  resistive load, the p.d developed across the load is 0.042 times the source e.m.f, which represents a mismatch loss of 27.44 dB. If a source with an impedance of  $4.55 + j1177.84 \Omega$  at 10 MHz is connected to a  $50 \Omega$  resistive load via a lossless step-down transformer with a 4:1 turns ratio, the load presented to the antenna is  $800 \Omega$  and the p.d developed across the  $50 \Omega$  load is 0.14 times the source e.m.f, which reduces the mismatch loss to 17 dB. Although  $800 \Omega$  is not the optimum load resistance in this case, it has been chosen because of the availability of Mini Circuits T16-6T low loss broad band RF transformers with a 4:1 turns ratio.

It can be shown that the effective height of an electrically short dipole antenna is approximately half its physical length at any frequency that is significantly below resonance. Hence the effective height of a dipole with a length of 4.4 m is approximately 2.2 m. This means that in an E-field strength of 1 V/m, the e.m.f from such a dipole would be 2.2 V. Using 4:1 step-down transformer matching as described above, the p.d delivered to a  $50 \Omega$  load in a 1 V/m field would be  $2.2 \times 0.14 = 0.308$ . This corresponds to an E-field antenna factor of 10.2 dB/m but allowing for losses in the transformer, 12 dB/m would be a more realistic figure.

An antenna factor of 12 dB/m is an improvement of approximately 10 dB compared to the Loop 'C' described in Section 4.2.4 above. Although the use of an  $800 \Omega$  to  $50 \Omega$  matching transformer introduces a mismatch loss of approximately 12 dB at 30 MHz, it improves the matching by approximately 10 dB at 10 MHz, resulting in an antenna factor that is approximately constant from 10 - 30 MHz.

The validity of the above antenna design can also be verified by reference to Fig 55 below, which is reproduced from Fig 13 'Short Dipole Antenna Factors' in BS CISPR 16-1:1999 [66].

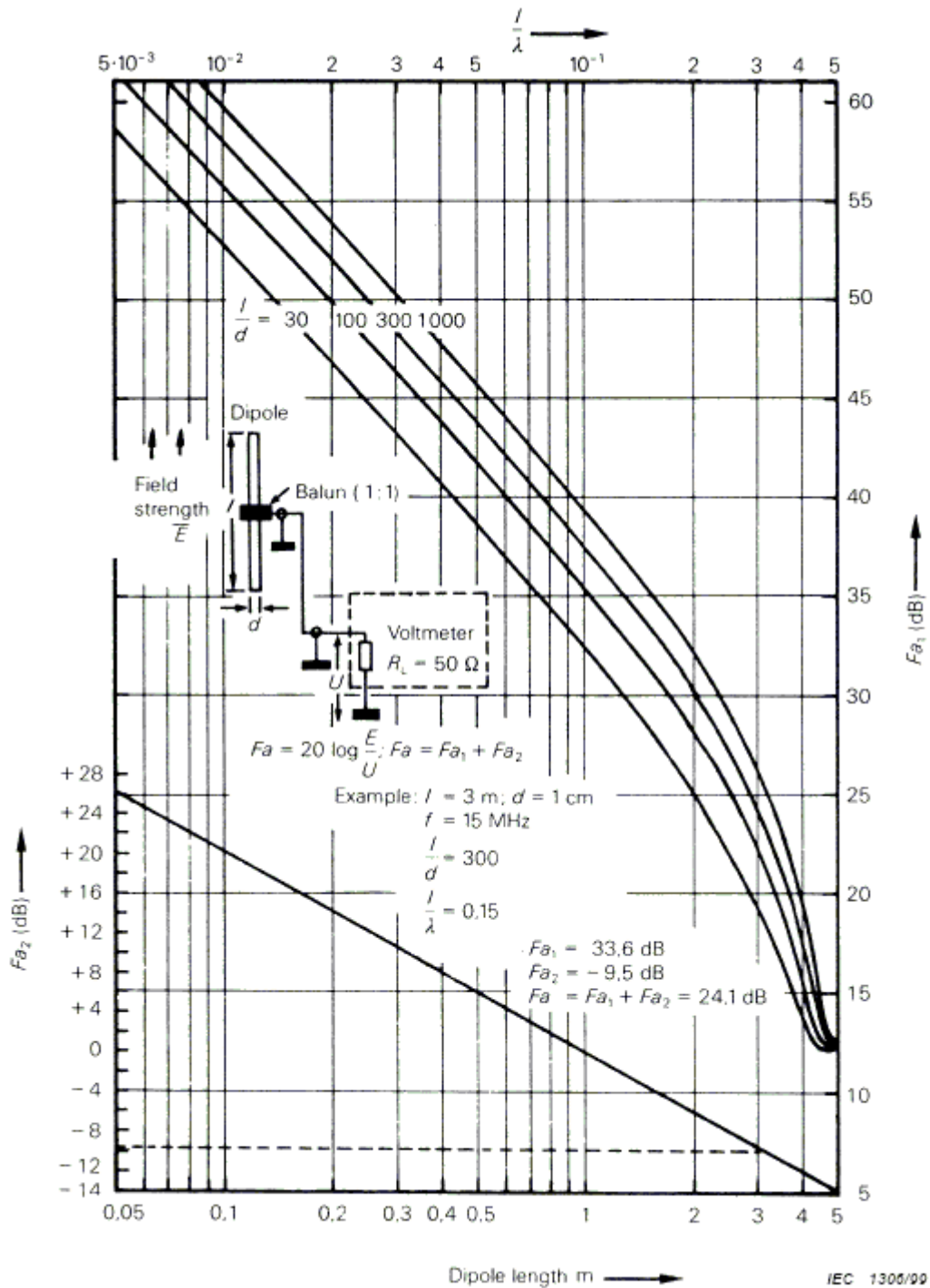


Figure 55. Short dipole antenna factors, reproduced from CISPR 16-1 [66]

According to Fig 55 above, a dipole with a length of 4.4 m with 22 mm diameter elements has an antenna factor of 19.5 dB into a 50  $\Omega$  load. Although [66] does not specify short dipole antenna factors for load impedances other than 50  $\Omega$ , it can be deduced from the curves that the source impedance of such a dipole whose length is of the order of  $0.15 \lambda$  is much higher than

50  $\Omega$  and that transformer matching can yield a reduction in mismatch loss of the order of 10 dB. This would result in an antenna factor of 9.5 dB/m with no transformer loss and this shows close agreement with the figure of 10.2 dB/m calculated above.

A possible further development of the short dipole antenna design described above would be to divide the frequency range 10 - 30 MHz into two or three sub-ranges, using 800  $\Omega$  to 50  $\Omega$  matching in the lower range, 200  $\Omega$  to 50  $\Omega$  matching in the mid range and possibly a direct connection in the upper range. This would improve the antenna factor in the mid and upper ranges.

An alternative type of measuring antenna for 10 - 30 MHz is a monopole with ground radials, that is designed to be a quarter wavelength long at slightly above 30 MHz. Such an antenna is modelled in section 5.3 below. Although the effective height of a monopole is half that of a dipole, the feedpoint impedance of a monopole is also approximately halved so that with suitable matching, a quarter wave monopole and a half wave dipole can achieve a similar antenna factor. A limitation of a vertical monopole is that it can only be used for vertically polarised measurements whereas for EMC measurements, it is often desirable to make both horizontal and vertically polarised measurements. In the case of a dipole, the antenna can be oriented either horizontally or vertically. Although vertical orientation is not ideal due to the unbalance introduced by unequal ground proximity of the two elements, it is considered that this disadvantage is outweighed by the practical advantage of being able to make horizontally and vertically polarised measurements with a single antenna.

For the reasons stated above, the vertical monopole has not been developed further as an EMC measuring antenna for 10 - 30 MHz although it would have significant advantages for background noise measurements if operated with an antenna matching unit.

## **4.6. Conclusions**

A portable measuring system using tuned loop antennas has been designed, modelled and developed for improved sensitivity in LF, MF and HF field strength measurements. The frequency range of 80 kHz - 30 MHz is covered by a set of three tuned loop antennas, each with electronically controlled tuning and integral pre-amplifiers. These functions are controlled remotely via an optical fibre communications link from a PC running LabVIEW™ software which also controls the measuring receiver. The prototype set of loop antennas was delivered to

the Radiocommunications Agency and has been used for field trials by the RA on PLT systems in Crieff and Campbeltown.

One of the remotely tuned loops has been further developed as a 1.6m diameter loop that provides increased sensitivity in the range 1.75 - 10 MHz so that background atmospheric noise rather than receiver or pre-amplifier noise becomes the limiting factor to measuring system noise floor. An improved short dipole antenna for EMC measurements from 10 - 30 MHz has also been designed.

A paper was submitted to the CISPR/A committee that resulted in an amendment to CISPR16-1 to permit the use of tuned loop antennas as well as untuned loops.

A test method has been developed for measurement of common-mode currents in a network cable by means of a small loop located at a specified distance from the cable.

## Chapter 5. Antenna modelling of EMC measuring antennas

This chapter applies antenna modelling software to a loop antenna, an electrically short horizontal dipole antenna and an electrically short vertical monopole antenna in order to determine their radiation patterns and feed point impedances.

### 5.1. Modelling of a loop antenna

The analysis of a receiving loop antenna presented in section 4.2 above (page 93) assumes that the loop is 'electrically small', i.e. the circumference is small compared to a wavelength so that there is no significant phase difference between currents around the circumference of the loop. In order to model a loop that is not 'electrically small', antenna modelling software may be used. Antenna modelling can also predict the polar diagram of a loop for horizontal and vertical polarisation. This was a significant issue when calibrating loop antennas as the polar diagram and angle of polarisation appeared to change with frequency.

Fig 56 shows a 1.6 m diameter loop modelled as 12 straight copper tubes 10 mm in diameter. This is representative of the prototype 1.6 m diameter loop described in Section 4.4 above, which uses 10 mm diameter RG213 type coaxial cable with only the braid connected.

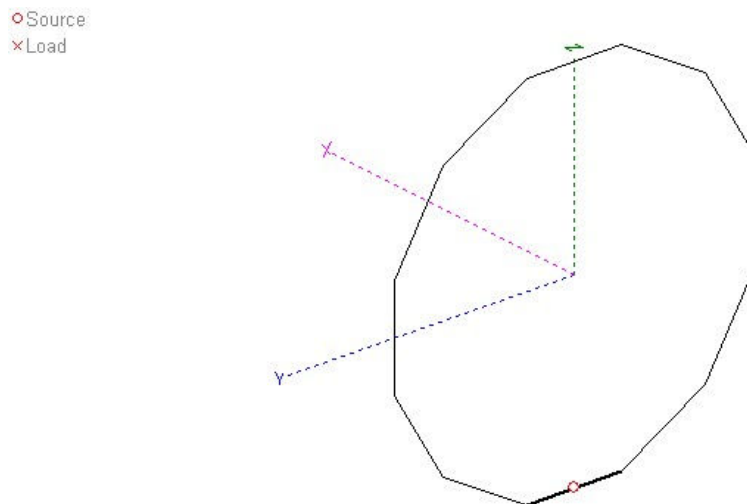


Figure 56. Antenna model of a 1.6 m diameter loop antenna

The loop antenna was modelled with the lowest part 1 m above ground, to represent typical conditions of use. Fig 57 shows the far field plot at 1.75 MHz with horizontal polarisation. It can be seen that the maximum radiation is along the 'X' axis, i.e. perpendicular to the plane of the loop. The real part of the feedpoint impedance,  $0.059 + j54.677 \Omega$  represents radiation

resistance and loss resistance. For an efficient transmitting loop, it would be desirable to use a conjugate impedance matching network which would require a very high 'Q' factor and hence a narrow bandwidth. For a receiving loop, adequate efficiency can be obtained with a much lower 'Q' factor, as explained in Section 5.2 above. Fig 58 shows the far field plot at 1.75 MHz with vertical polarisation. It can be seen that the maximum radiation is along the 'Y' axis, i.e. parallel to the plane of the loop. Figs 59 and 60 show the horizontal and vertically polarised far field plots at 10 MHz. It can be seen that the gain and feed point impedance have increased substantially but the polar diagrams are almost identical.

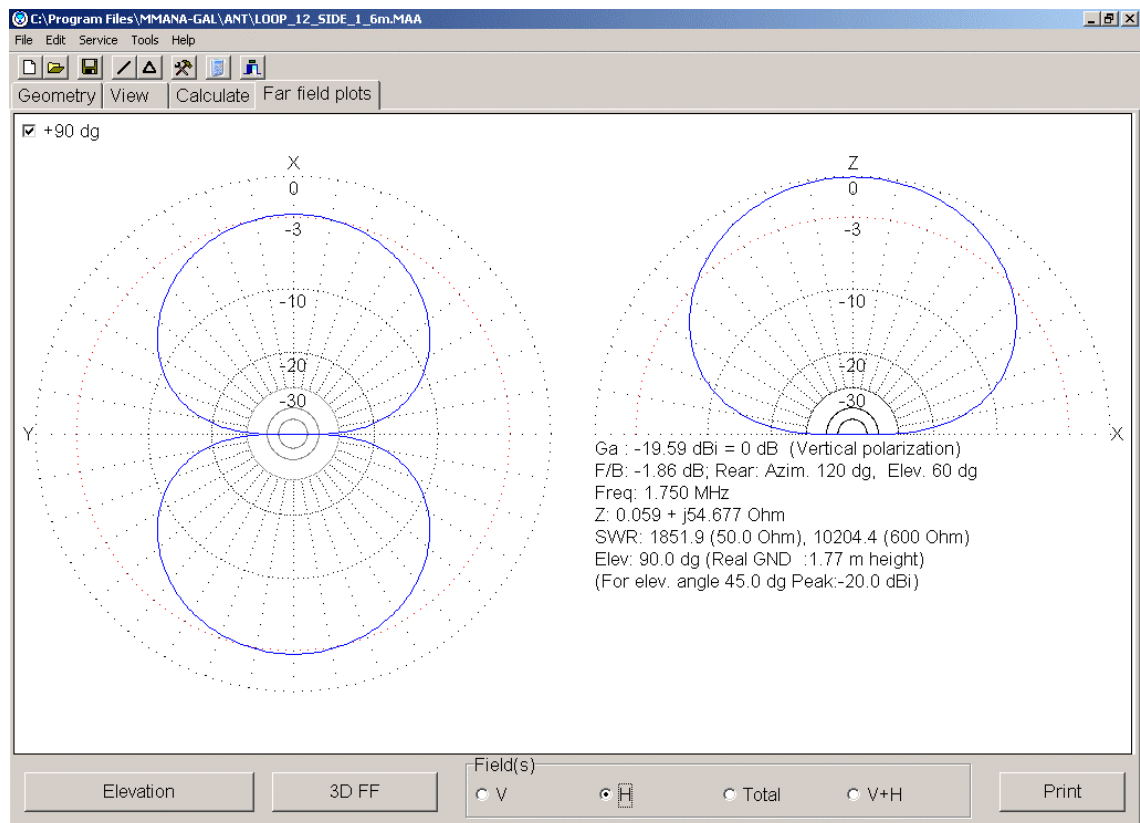


Figure 57. Far field horizontally polarised plot of a 1.6 m diameter loop at 1.75 MHz

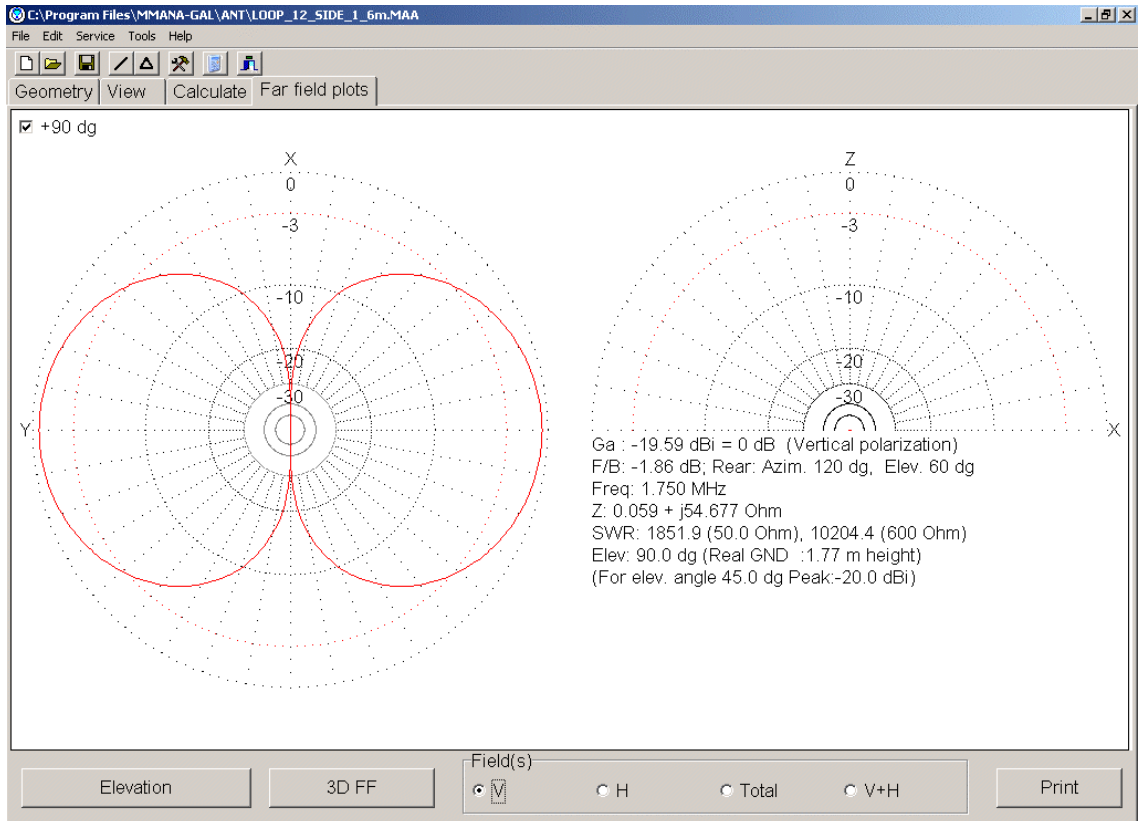


Figure 58. Far field vertically polarised plot of a 1.6 m diameter loop at 1.75 MHz

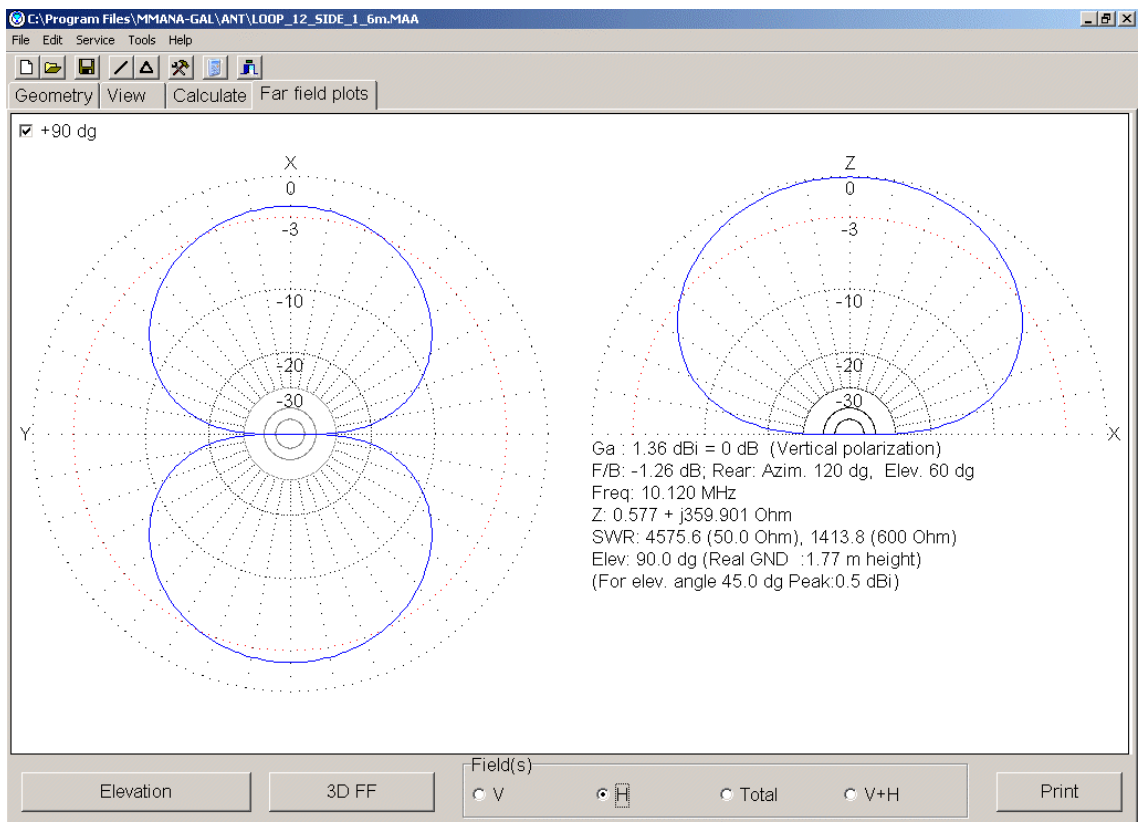


Figure 59. Far field horizontally polarised plot of a 1.6 m diameter loop at 10 MHz

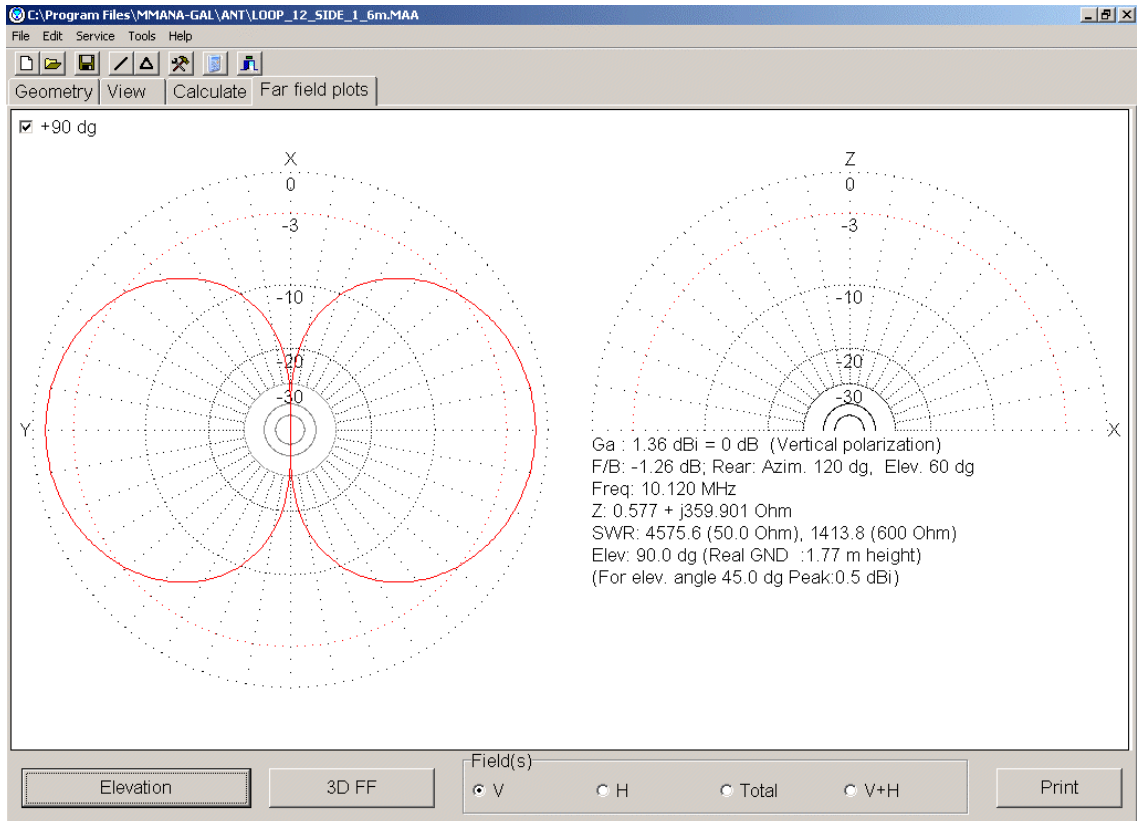


Figure 60. Far field vertically polarised plot of a 1.6 m diameter loop at 10 MHz

## 5.2. Modelling of a short horizontal dipole antenna

A horizontal dipole was modelled for use as an EMC measuring antenna from 10 - 30 MHz, as shown in Fig 61. The total length was 4.4 m and the elements were modelled as 22 mm diameter copper tube.

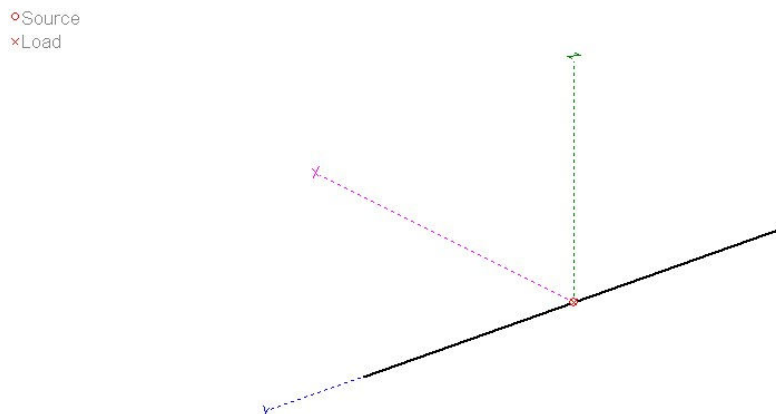


Figure 61. Antenna model of a 4.4 m long horizontal dipole



The dipole in Fig 61 was modelled at a height of 2.5 m above real ground using NEC2. Antenna modelling also shows that the dipole is resonant at 32.2 MHz. The element lengths were chosen so that this resonance is slightly above the highest frequency of operation and hence the antenna is 'electrically short' over the intended operating frequency range of 10 - 30 MHz..

As shown in Figs 62 and 63, the predicted feed point impedance is  $63.995 - j69.727 \Omega$  at 30 MHz. and  $4.55 + j1177.84 \Omega$  at 10 MHz.

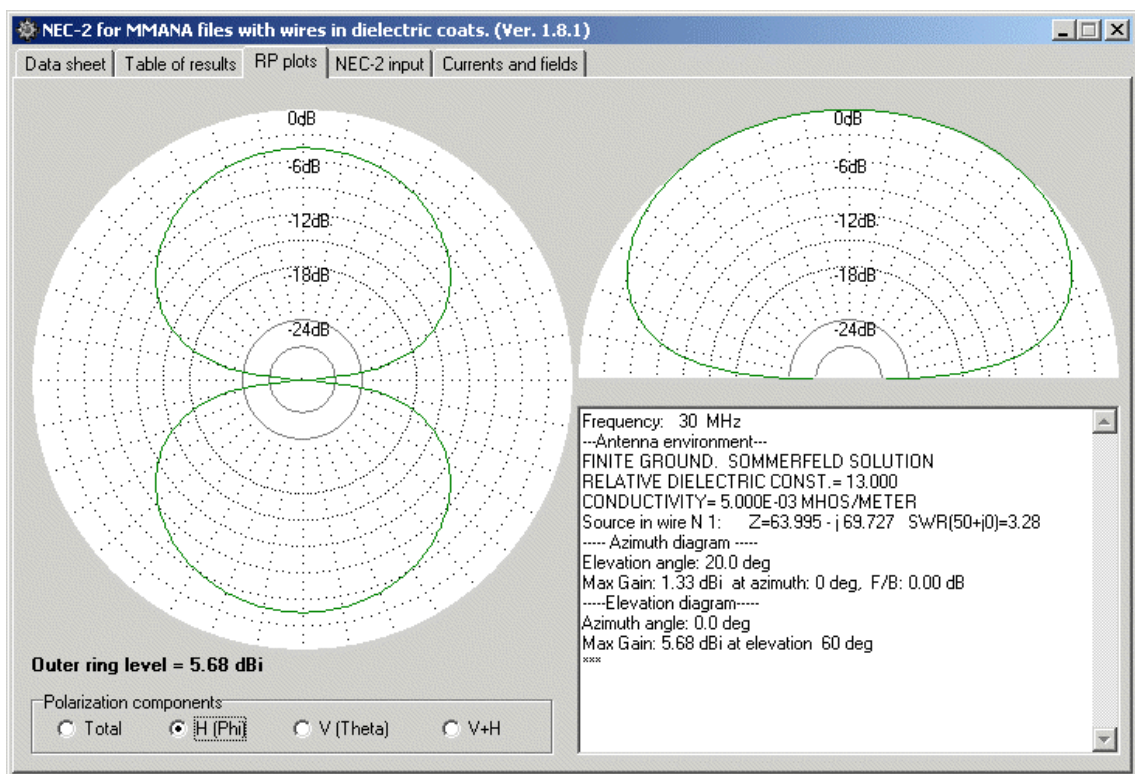


Figure 62. Horizontally polarised far field plot of a 4.4 m horizontal dipole at 30 MHz

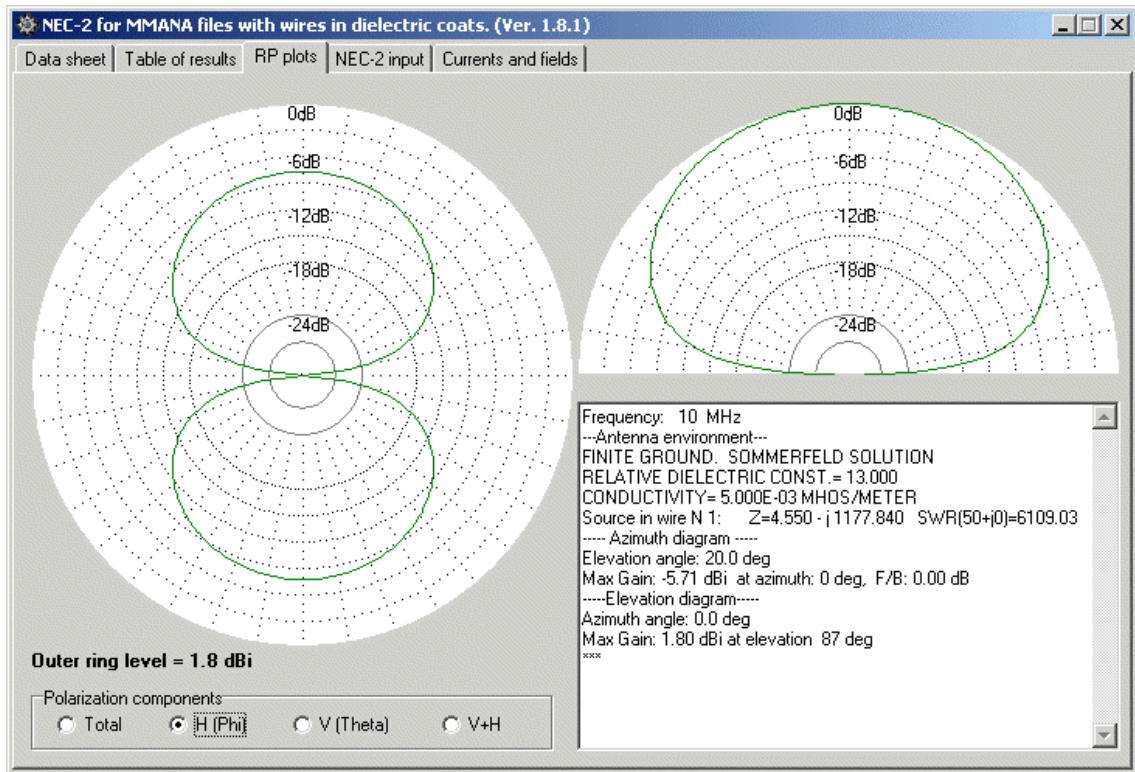


Figure 63. Horizontally polarised far field plot of a 4.4 m horizontal dipole at 10 MHz

### 5.3. Modelling of a short vertical monopole antenna

A short vertical monopole antenna was modelled for use as an EMC measuring antenna from 10 - 30 MHz, as shown in Fig 64 below. The length of the driven element was 2.5 m and the four ground radial elements were also 2.5 m long. All elements were modelled as 22 mm diameter copper tube.

○Source  
×Load

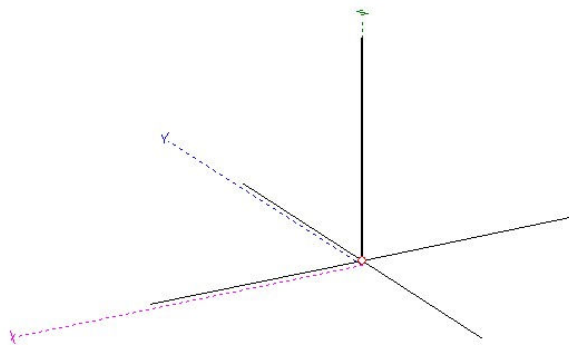


Figure 64. Antenna model of a 2.5 m vertical monopole with ground radials

Figs 65 and 66 show NEC2 far field plots at 10 MHz and 30 MHz respectively. The predicted feedpoint impedance  $Z=6.769 - j 682.434$  at 10 MHz and  $Z=35.783 + j 3.148$  at 30 MHz. The predicted resonant frequency is 30.7 MHz, where  $Z = 41.7 -j0$

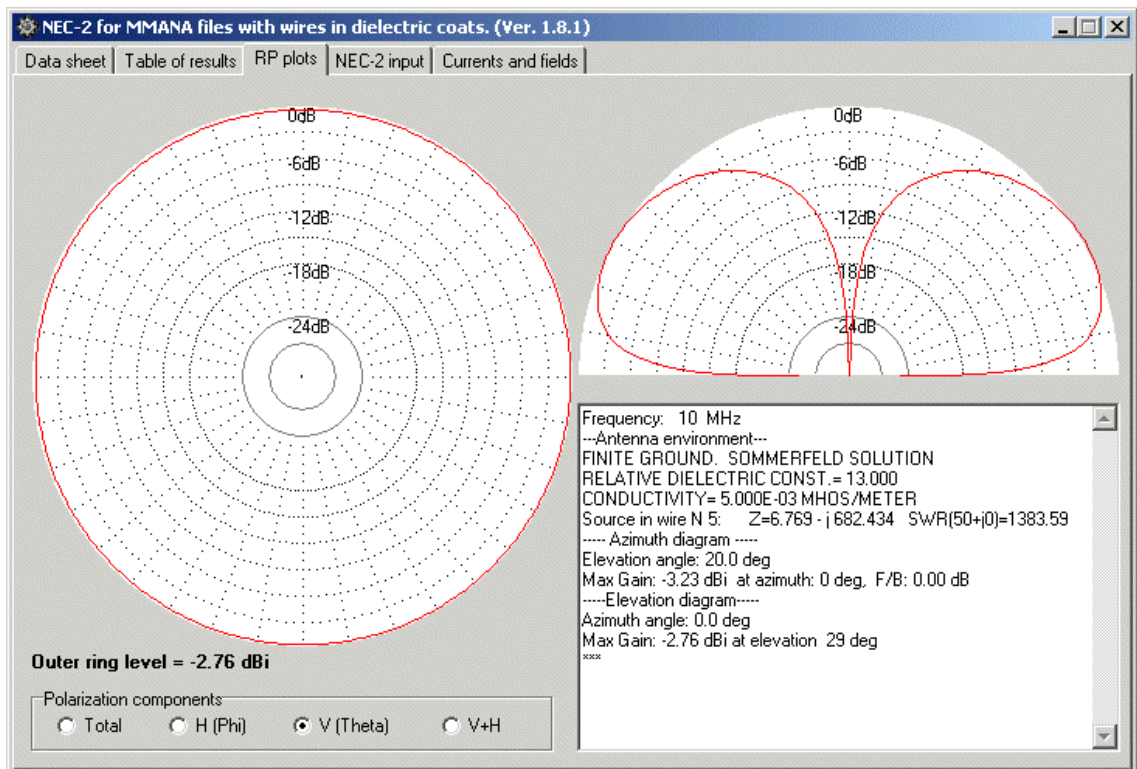


Figure 65. Vertically polarised far field plot of a 2.5 m vertical monopole at 10 MHz

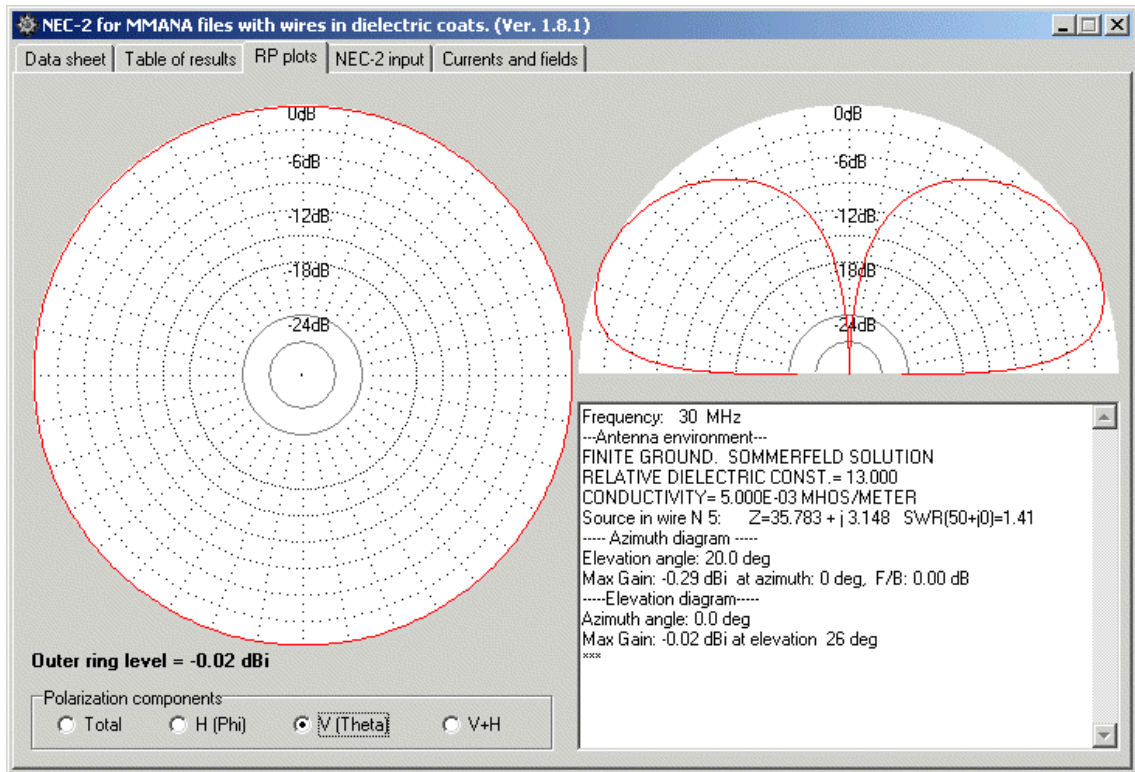


Figure 66. Vertically polarised far field plot of a 2.5 m vertical monopole at 30 MHz

## 5.4. Conclusions

A loop antenna has been modelled using antenna modelling software in order to show the radiation pattern for horizontal and vertical polarisation. An electrically short dipole has been modelled for use as an EMC measuring antenna and the feedpoint impedance has been calculated in order to permit the design of a matching arrangement for a dipole covering 10 - 30 MHz. An electrically short vertical monopole has also been modelled for possible use as an EMC measuring antenna.

## **Chapter 6. Protection of Radio Communication Services**

This chapter studies protection requirements of various HF radio communication services such as analogue and digital broadcasting. Interference models are also presented.

Existing EMC standards for conducted (and radiated) emissions are based on the minimum usable signal levels for certain types of radio communication services. Protection ratios are applied but the limits may then be relaxed to reflect the low probability of worst case conditions. For systems such as PLT which could operate continuously over a wide geographical area and would occupy a wide bandwidth, existing assumptions about the probability of worst case conditions need to be revised. For HF communication systems that operate away from built-up areas or in aircraft, the cumulative effect of many distant xDSL or PLT sources needs to be considered.

It is also necessary to consider the protection requirements of radio communication services that operate in residential areas, e.g. the Amateur Radio service and the DRM (Digital Radio Mondiale) system for digital MF/HF broadcasting [28]. In both services, background man-made and natural noise levels can be a limiting factor. The cumulative effect of many distant xDSL or PLT sources could also be significant even if there were none locally.

PLT systems would need to comply with the existing CISPR 22 Class 'B' conducted emissions from mains ports. The limit is 46 dB( $\mu$ V) from 0.5 - 5 MHz and 50 dB( $\mu$ V) from 5 - 30 MHz, with CISPR average detection. Practical PLT systems would typically require a PSD (Power Spectral Density) of typically -43 dBm/Hz or -3.5 dBm in 9 kHz bandwidth. This corresponds to 103.5 dB( $\mu$ V) p.d. in 50  $\Omega$ , which is 57.5 dB above the EN 55022 Class 'B' conducted limit for mains ports from 0.5 - 5 MHz. It therefore appears that PLT systems can only operate in the HF bands if specific frequencies are assigned to them.

The situation with splitterless xDSL and home phoneline networks is somewhat different however. The CISPR 22 limits for telecommunication ports allow much larger differential mode signal emission levels than for mains ports, provided the specified common mode voltage and current limits are met. In order to determine the maximum permissible level of differential mode signal, a value must be assumed for the worst case LCL of twisted pair cables connected to the port. If this minimum LCL is not achieved in practice, then radiated emissions will be

higher than expected. This is of particular concern with splitterless xDSL and home phoneline networks, where the LCL of the network is poorly defined.

For VDSL, a technical specification [71] has been produced by ETSI. This specifies a launch PSD of -60dBm/Hz. The limit is based on the CISPR 22 limits for telecommunication ports and assumes that an LCL of 30 dB can be achieved. 'Notches' at -80 dBm/Hz are specified in amateur radio bands for countries where overhead telephone distribution is used. The LCL of such overhead cables would generally be better than for the extension telephone wiring tested in Section 3.2 above.

## **6.1. Protection of various radio communication services**

Section 4.9.2 of [72] presents an interference model for the power of the intentional and interfering signals at a victim receiver. Such a model needs to take account of the minimum field strength of the wanted signal and the protection ratio required in order to determine the maximum acceptable field strength of an interfering signal. Some interference models also include a factor that takes account of the relatively low probability of worst-case conditions and thereby relaxes the limit for an interfering signal.

In 2000/2001, various emission limits were considered by the CEPT Working Group SE35 including the German NB30 limit, the NEDAP limit from the Netherlands and MPT1570 from the UK

### **6.1.1. Analogue LF/MF/HF broadcasting**

According to [32], ITU-R recommendation BS 703 specifies the following minimum protected field strength for AM broadcasting:

LF	66 dB( $\mu$ V/m)
MF	60 dB( $\mu$ V/m)
HF	40 dB( $\mu$ V/m)

ITU-R recommendation BS 560 indicates that the minimum field strength for one HF broadcasting planning scenario is chosen so that an RF SNR of 34 dB is achieved and that for LF/MF, these minimum field strengths achieve an RF SNR >40 dB, where RF SNR is defined as follows:

$$RF\ SNR = \frac{\text{mean carrier power}}{\text{mean noise power}} \quad (15)$$

Most proposed emission limits relate to emission measurements made with a peak detector as opposed to a mean or RMS detector but according to [32], if a signal is genuinely noise-like, the RMS noise level is approximately 10 dB less than the peak value indicated on a measuring receiver.

After applying a -10 dB adjustment for peak to RMS and after adjusting the various proposed limits for a distance of 1 m, Stott [32] shows that at LF/MF, the MPT1570 and NB30 limits would only ensure an RF signal to RMS noise ratio of 10 - 20 dB which would result in reception that is of little entertainment value whereas the NEDAP proposed limit provides an RF signal to RMS noise ratio of 27 - 32 dB represents a loss of quality compared to the 40dB target but this might be acceptable as a compromise.

Applying similar considerations at HF, Stott [32] shows that for reception at a distance of 1 m from the interference source, the NB30 limits would only ensure an RF signal to RMS noise ratio of 2 - 12 dB while the NEDAP proposed limit would provide an RF signal to RMS noise ratio of 22 - 32 dB, compared to a target of 34 dB. If the distance of the receiving antenna from the interfering source is increased to 3 m (if this is possible), then the above SNR figures may be increased by approximately 10 dB.

As none of the limits being considered by CEPT SE35 in 2001 was satisfactory in protecting HF broadcasting, Stott made a new proposal [33] for a lower limit based on a 0.5 dB increase in noise floor in a reference scenario where the receiving antenna is 10 m from any potentially interfering cables.

Although the limits considered by CEPT SE35 provided varying levels of protection to radio reception, they were all substantially lower than a practical PLT system could achieve. Various other limits were proposed that allowed PLT systems to operate but were far higher than the NB30 or NEDAP limits. For example, one of the ETSI/CENELEC JWG proposed limits was equivalent to 55.5 dB( $\mu$ V/m) at a distance of 3 m, which would yield a negative SNR for broadcast reception.

### **6.1.2. Digital Radio Mondiale**

According to [32], transmitter powers for DRM are typically 5 - 10 dB lower than for AM broadcasting. This results in a corresponding reduction in RF SNR. DRM field strengths are also considered by Prieto et al [73]

Although DRM may be able to provide high quality reception with a lower RF SNR than for AM broadcasting, DRM, like any digital modulation scheme exhibits a sharp 'threshold' effect where a few dB change in RF SNR results in a transition between near perfect reception and complete loss of reception.

### **6.1.3. Military HF communications**

A report by the Army CIS Engineering Group [24] assessed the potential interference with HF Combat Net Radio (CNR) caused by a PLT system operating in the UK by using the Minimum Wanted Signal (MWS) technique. Increased wanted signal levels of up to 36dB were required in order to overcome interference produced by a nearby PLT system. A typical reduction in range of military land mobile HF communications was from 15 - 20 km down to 7 - 10 km.

## **6.2. Interference models for wireline networks**

In an interference model for a radio communication system, a victim receiver receives a wanted signal from a transmitter and an unwanted or interfering signal from another source such as an unintentional radiated emission from a wireline communication network. In order to calculate the interfering field strength  $E$  at a distance  $d$  from a wireline network, it is necessary to know the power  $P$  of the unintentional radiating source and the effective gain  $G$  of the wireline network as an unintentional radiating antenna.

As the unintentional radiating source in question is typically some form of broad band data communication system that occupies a significantly wider bandwidth than the bandwidth of the victim receiver, it is necessary to consider the power of the interfering signal within the bandwidth of the victim receiver or measuring receiver. If the power spectral density (PSD) of the source in watts per unit bandwidth is known then the power in a given bandwidth (e.g. 9 kHz) can be calculated and vice versa.



Where a wireline network behaves as an unintentional radiating antenna, its gain may be expressed as  $G_i$  relative to an isotropic antenna or  $G_d$  relative to a dipole antenna. The product of the interfering source power in a given bandwidth and the antenna gain gives the Effective Radiated Power (ERP)  $P_d$  or the Effective Isotropic Radiated Power (EIRP)  $P_i$ , depending on whether the antenna gain is expressed as  $G_i$  or  $G_d$ .

The E-field strength  $E$  at a distance  $d$  from an antenna that is radiating  $P_d$  watts ERP is given by [51]:

$$E = \frac{\sqrt{49.15P_d}}{d} \quad (16)$$

In the case of an antenna that is radiating  $P_i$  watts EIRP,  $E$  is given by:

$$E = \frac{\sqrt{30P_d}}{d} \quad (17)$$

In practice, various other factors need to be considered. First, the above expressions for field strength assume 'far field' conditions but in many situations that will be considered at MF/HF, the distance is insufficient to achieve 'far field' conditions. This has several consequences.

- The electric and magnetic fields are not necessarily related by the far field relationship  $E/H = 120\pi$  so that conversion of measured H-field to calculated E-field and vice versa may not be accurate.
- The variation of field strength with distance, sometimes known as the 'regression rate', does not necessarily follow the inverse square law rate of -20 dB per decade.
- A wireline network is a distributed source not a point source, which leads to uncertainty about the distance from the source to the victim and which may also affect the regression rate.

The analysis presented below is therefore only an approximation to the actual situation.

### **6.2.1. Home powerline networking**

Based on the tests performed in home powerline networking products and an in-building power network, the following interference model is proposed.

In Section 2.7 above, two different home powerline networking products were tested on a LISN. They were found to produce broad band conducted emission levels of up to 77 dB $\mu$ V in 9 kHz bandwidth with average detection. Assuming that the amplitude measurement with an average detector is approximately equal to RMS voltage, this corresponds to an average power of 30 dBm in 50  $\Omega$  which corresponds to a PSD of -69.5 dBm/Hz.

If a home powerline networking product is located on a power circuit close to the consumer unit in a house then the antenna characteristics of the wiring could be similar to those shown in Section 2.4 above, where the maximum antenna gain of the power wiring in a particular house was found to be -25 to -28 dBd when measured at an average distance of 14 m. Hence it is considered likely that this gain figure is valid for a distance of 10 m.

Hence the worst-case parameters of this model are as follows:

Source PSD (avg, dBm/Hz)	Source power (dBm in 9 kHz)	Antenna gain of network (dBd)	ERP of network (dBm)	Field strength at 10 m ( $\mu$ V/m)	Field strength at 10 m dB( $\mu$ V/m)	*Field strength at 3 m dB( $\mu$ V/m)	*Field strength at 1 m dB( $\mu$ V/m)
-69.5	-30	-25	-55	39.6	32	42.4	52

Table 6.2.1. Worst case parameters for a home powerline network.

\* Figures at 3 m and 1 m assume a regression rate of -20 dB per decade, rounded to the nearest 1 dB.

It can be seen that the field strengths in Table 6.2.1 above are large in relation to the protection requirements given in Section 6.1 above.

### 6.2.2. Home phoneline networking or splitterless xDSL

Based on the tests performed on in-building telephone networks and connected equipment in Section 2.5 above, the following interference model is proposed.

The specified PSD mask in ITU-T G.989.1 (G.pnt-f) [74] for a home phoneline networking transceiver is specified as -71.5 dBm/Hz into a 100  $\Omega$  load in the range 4 - 10 MHz, with a -10 dB 'notch' to protect the 7 MHz amateur band. As the specified PSD is a peak value, it will be assumed that the average value is 10 dB lower, as explained in section 6.1.1 above.

If a home phoneline networking product is located on UK telephone extension wiring similar to the example tested in section 2.5 above, the maximum antenna gain of the wiring was found to be -20 dBd. Although the impedance varies greatly over the range of the test, it can be seen from Section 2.5 that the magnitude is of the order of  $100\Omega$  over a substantial part of the range.

Hence the worst-case parameters of this model are as follows:

Source PSD (avg, dBm/Hz)	Source power (dBm in 9 kHz)	Antenna gain of network (dBd)	ERP of network (dBm)	Field strength at 10 m ( $\mu\text{V/m}$ )	Field strength at 10 m dB( $\mu\text{V/m}$ )	*Field strength at 3 m dB( $\mu\text{V/m}$ )	*Field strength at 1 m dB( $\mu\text{V/m}$ )
-81.5	-42	-20	-62	17.7	25	35.4	45

Table 6.2.2A Worst case parameters for a home phoneline network

\* Figures at 3 m and 1 m assume a regression rate of -20 dB per decade and are rounded to the nearest 1 dB.

It can be seen that the field strengths in Table 6.2.2A above are large in relation to the protection requirements given in Section 6.1 above.

For a splitterless VDSL scenario, the upstream signals could have a maximum PSD of -60 dBm/Hz [71]. After applying a -10 dB adjustment for peak to average the worst-case parameters of this model are as follows:

Source PSD (avg, dBm/Hz)	Source power (dBm in 9 kHz)	Antenna gain of network (dBd)	ERP of network (dBm)	Field strength at 10 m ( $\mu\text{V/m}$ )	Field strength at 10 m dB( $\mu\text{V/m}$ )	*Field strength at 3 m dB( $\mu\text{V/m}$ )	*Field strength at 1 m dB( $\mu\text{V/m}$ )
-70	-30.5	-20	-50.5	66.5	36.5	46.9	56.5

Table 6.2.2B Worst case parameters for a 'splitterless' VDSL network

\* Figures at 3 m and 1 m assume a regression rate of -20 dB per decade and are rounded to the nearest 1 dB.

It can be seen that the field strengths in Table 6.2.2B above are large in relation to the protection requirements given in Section 6.1 above. Nevertheless, splitterless VDSL may not be a realistic scenario in practice as it would probably be necessary to install a splitter to isolate the VDSL signals from the in-building telephone wiring, which would result in substantially improved balance.

### **6.3. Conclusions**

Protection requirements for several types of HF radio communications have been reviewed and have been compared with some proposed emission limits that would offer varying degrees of protection from interference.

Results of tests in earlier sections have been used to produce interference models for several different scenarios, namely home powerline networking and home phoneline networking and splitterless VDSL.

## Chapter 7. EMC Standards and regulatory issues

This chapter reviews existing EMC standards and standards under development in the context of wireline communication systems.

### 7.1. Legislation

Member states of the EC are bound by the EC EMC Directive 89/336/EEC [75], which requires them to implement measures relating to apparatus which is liable to cause electromagnetic disturbance and to apparatus the performance of which is liable to be affected by such disturbance. In the UK, this Directive is implemented by -

Statutory Instrument - 1992 No. 2372, ELECTROMAGNETIC COMPATIBILITY  
The Electromagnetic Compatibility Regulations. [76]

Part 1, Section 5 (Protection Requirements), Clause 4 of the Statutory Instrument states -

*(4) Without prejudice to the generality of paragraph (2)(a), the electromagnetic disturbance generated by relevant apparatus shall -*

*(a) not exceed a level allowing radio and telecommunications apparatus to operate as intended; and*

*(b) be such as not to hinder the use of apparatus of any of the descriptions listed in Schedule 3 hereto (being descriptions listed in the illustrative list of the principal protection requirements in Annex III of the EMC Directive) where that apparatus has an adequate level of immunity in its usual electromagnetic environment so as to allow its unhindered operation taking into account the levels of electromagnetic disturbance generated by relevant apparatus complying with applicable EMC standards.*

The above regulations impose general requirements that **all** systems must meet in addition to complying with any applicable standards and it appears that PLT in the HF spectrum may not meet the protection requirements of the European EMC Directive 89/336/EEC and UK Statutory Instrument 1992 No. 2372.

As shown in section 2.7 above (page 33), launch powers of some existing PLT systems, such as the home powerline networking products exceed the conducted emission limits of the product standard EN 55022 and it has been shown in Section 6.2.1 above (page 105) that wide band emissions from PLT systems in the HF spectrum from connected domestic wiring may exceed levels allowing radio and telecommunications apparatus to operate as intended. Such products appear to contravene existing product standards and even if a Technical Construction File is used to certify EMC compliance and affix the CE mark, it could be argued that the protection requirements of UK Statutory Instrument 1992 - No.2372, Part 1, Section 5, Clause 4 [76] are not being met. European regulatory authorities would therefore have the power to take enforcement action against such products if they are found to be non-compliant with applicable EMC regulations.

The matter of interference and EMC standards in relation to PLT and DSL has also been raised in the House of Commons [77] and has been the subject of EC Mandate M/313 on EMC of telecom networks [78]. There has been some opposition to Mandate M/313 from industry due to claimed difficulties in making measurements.

## **7.2.Applicable EMC standards**

### **7.2.1. A review of existing EMC standards**

BS EN 50065-1 + AMD.3. 1996 CENELEC. GENERAL REQUIREMENTS. SIGNALLING ON LOW VOLTAGE INSTALLATIONS 3kHz - 148.5kHz - ELECTROMAGNETIC INTERFERENCE.

EN 50083-8 : 2000 CENELEC. CABLED DISTRIBUTION SYSTEMS FOR TELEVISION, SOUND AND INTERACTIVE MULTIMEDIA SIGNALS - PART 8: ELECTROMAGNETIC COMPATIBILITY FOR INSTALLATIONS.

EN 50083-8 is a relatively new European Standard that covers the frequency range 300 kHz - 3.0 GHz and cross references to numerous 'Normative references' (other related CENELEC or IEC standards) quoting them where appropriate throughout the text. It further recognises in Section 1, Scope, the risk of interference to other radio services from cabled distribution systems -

*“To minimise the risk of interference to other radio services caused by possible radiation from a cabled distribution system and to limit the possible penetration of external signals which may interfere with the operation of a system, it is necessary not only to use equipment which satisfies the requirement regarding limits of radiation and of immunity to external fields but also to ensure the integrity of all cable connections on each item of active or passive cabled distribution system equipment.”*

The standard further lays down the maximum allowed radiation levels together with methods of measurement. Annex A (informative) additionally makes specific reference to the Radiocommunications Agency standard MPT 1510 which pre-dated the European Standard. Existing emission standards for cable TV networks are based on single carrier modulation techniques such as Vestigial Sideband (VSB). Consequently, emissions may approach the limit only at a relatively small number of vision carrier frequencies. The same limit is not appropriate for multi-carrier modulation where a large number of sub-carriers could all approach the limit and the probability of interference to other radio services is increased.

MPT 1520 - RADIOCOMMUNICATIONS AGENCY: RADIATION LIMITS AND MEASUREMENT STANDARD; ELECTROMAGNETIC RADIATION FROM CABLED DISTRIBUTION SYSTEMS OPERATING IN THE FREQUENCY RANGE 300 KHZ - 30 MHZ; JULY 1984 (REVISED 1989).

MPT 1520 is similar in scope to prEN 50083-8 and specifies radiation limits from cabled distribution systems in the frequency range 300 kHz - 30 MHz but development of this standard has been suspended.

IEC 61000-3-8 - (1997-08) ELECTROMAGNETIC COMPATIBILITY (EMC) - PART 3: LIMITS - SECTION 8: SIGNALLING ON LOW-VOLTAGE ELECTRICAL INSTALLATIONS - EMISSION LEVELS, FREQUENCY BANDS AND ELECTROMAGNETIC DISTURBANCE LEVELS.

IEC 61000-3-8 (1997) applies to mains signalling in the 3kHz to 525kHz range and specifies disturbance limits in the frequency range 3kHz up to 400GHz.

EN 50065-1 applies to mains signalling at frequencies from 3 kHz - 148.5 kHz.



Although not applicable in Europe, US FCC 47CFR Part 15.3 defines a 'Current-Carrier system' as:

*"A system, or part of a system, that transmits radio frequency energy by conduction over the electric power lines. A carrier current system can be designed such that the signals are received by conduction directly from connection to the electric power lines (unintentional radiator) or the signals are received over-the-air due to radiation of the radio frequency signals from the electric power lines (intentional radiator)."*

Part 15.3 defines an 'Unintentional Radiator' as:

*"A device that intentionally generates radio frequency energy for use within the device, or that sends radio frequency signals by conduction to associated equipment via connecting wiring, but which is not intended to emit RF energy by radiation or induction."*

The FCC rules that allow 'current carrier devices' were introduced in the early 1950s when only narrow band systems were in use

Part 15, Section 15.209 (1st October 1999 edition) defines a radiated field strength limit of 30  $\mu\text{V}/\text{m}$  at 30 m. This is equivalent to 29.5 dB( $\mu\text{V}/\text{m}$ ) at 30 m or 39.5 dB( $\mu\text{V}/\text{m}$ ) at 10 m.

The FCC rules state the operators of Part 15 devices must ensure that they do not cause harmful interference to radio services. The operator of a radio frequency device is required to cease operating the device upon notification by an FCC representative that the device is causing harmful interference. Operation is not allowed to resume until the condition causing the harmful interference has been corrected. This contrasts with the situation that would exist in Europe if a harmonised European standard were introduced for PLT.

### **7.2.2. A review of EMC standards development for wireline communications**

A draft CENELEC document on PLT, prES 59013 was circulated for comment in December 2000 but was withdrawn and a revised January 2001 version was circulated. ETSI also worked

Electromagnetic Compatibility In Wireline Communications, Rev. 3 Page 113

on developing a System Reference Document (SRD) for PLT. The draft included specifications for radiated emission limits that were claimed to protect radio services against interference from PLT. These limits were 50 dB( $\mu$ V/m) in the range 1.6 - 30 MHz, measured at 10 m. There was an option to implement 'notches' which reduce the Power Spectral Density (PSD) by 20 dB in specified amateur radio bands where the radiated emission limit would therefore be 30 dB( $\mu$ V/m).

A similar proposal was contained in CENELEC SC205A (Sec)75, 'Proposal for a CENELEC ES: Power Line Communication on Low Voltage Installations in the frequency range 1.6 MHz - 30MHz - Radiation and Power Spectral Density Levels'. In the CENELEC proposal, the depth of the 'notches' for the amateur bands followed a sloping characteristic that was claimed to follow the German NB30 limits [79] for protection of radio services. The NB30 limits are numerically equal to the RegTP 322MV05 limits [80]. The 322MV05 limits are measured at 3m distance whereas in the SC205A (Sec)75 proposal, the measurement distance for outdoor devices was 10 m. Hence the SC205A (Sec)75 proposed limit was effectively 10 dB higher than the 322MV05 limit. See also Hansen [81].

Section 6 of CENELEC SC205A (Sec)75 quotes coupling factors of about 50 (dB( $\mu$ V/m)-dBm) for PLC outdoor devices and about 60 (dB( $\mu$ V/m)-dBm) for PLC indoor devices in the middle of rooms, where the measurement distance would be less than 3m. These results are said to be derived from measurements by the PLCforum [82] but no further details are given. There is a large discrepancy between these PLCforum results and the results of a comprehensive study performed by the Technical University of Dresden [8]. In section 8.1.8 of the TU Dresden report, the field strength resulting from injecting 105 dB( $\mu$ V) was found to be 77 (dB( $\mu$ V/m)) from 500 kHz - 5MHz at a distance of 3 - 5 m. This corresponds to a coupling factor of 79 (dB( $\mu$ V/m)-dBm) compared to a figure of 60 (dB( $\mu$ V/m)-dBm) quoted in CENELEC SC205A (Sec)75 for indoor measurements.

Section 1 of CENELEC SC205A (Sec)75 states that operation of a PLC system would be subject to conditions that no harmful interference is caused to any radio service. Nevertheless, there is no definition of 'harmful interference'. For example, even a radiated emission level of 30 dB( $\mu$ V/m) for broad band signals would be regarded as 'harmful interference' by various radio users such as HF broadcasting and amateur radio. The level required to avoid 'harmful

interference' is therefore significantly lower and may not be achievable by a practical PLT system.

Fig 67 shows the proposed radiated limits from the draft ETSI PLT SRD and CENELEC SC205A (Sec)75 in relation to background noise levels at frequencies up to 30 MHz.

Tests by the RSGB [83] have shown that the background noise levels in the HF band are lower than is generally realised. In particular, it is understood that the levels in ITU-R report PI 372/6 are based on measurements made in the USA and are higher than the man-made noise levels in the UK and elsewhere in Europe. A possible reason for the difference is that LV electricity distribution in the US uses predominantly overhead wiring whereas UK LV distribution wiring is predominantly underground. Some RSGB background noise level measurements are shown in Fig. 67. RSGB have argued that intentional broad band emissions from PLT in amateur bands should not exceed 0 dB( $\mu$ V/m) in 9 kHz bandwidth at a distance of 10 m.

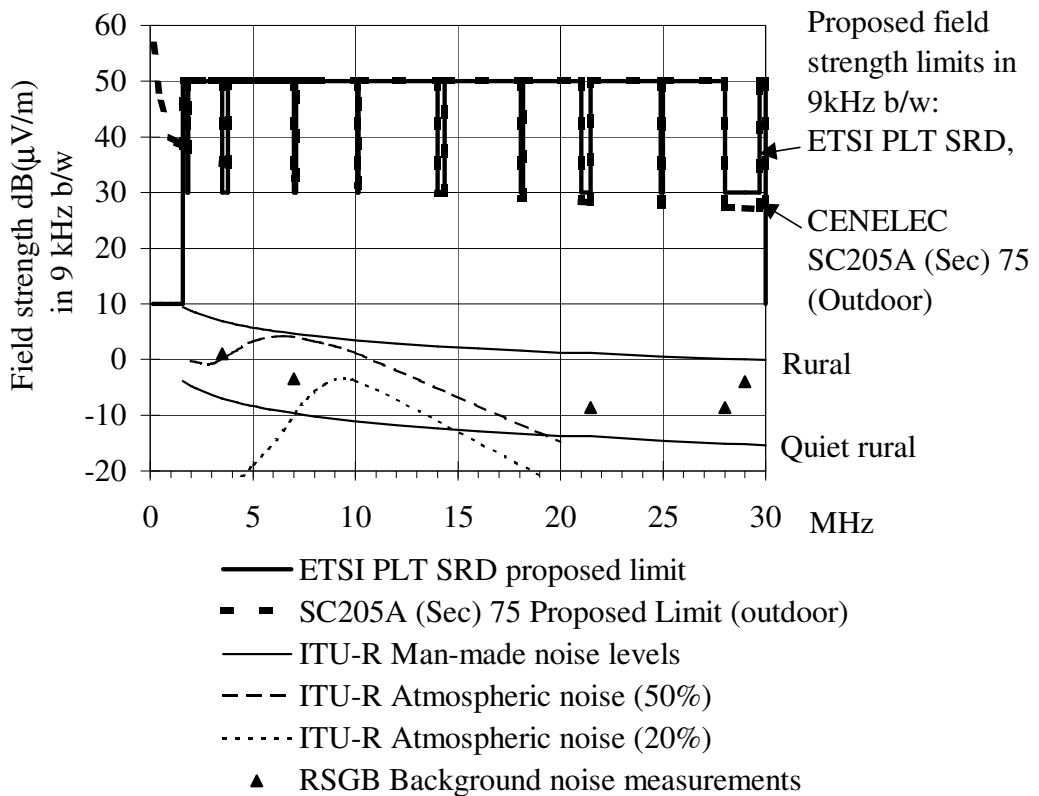


Figure 67. The proposed radiated limits from the draft ETSI PLT SRD and CENELEC SC205A (Sec)75 in relation to background noise levels at frequencies up to 30 MHz.

The draft ETSI PLT SRD also specified a maximum PSD that PLT systems may transmit into the mains power network. This limit was  $-40$  dBm/Hz outside the 'notches', which is equivalent to  $-0.5$  dBm in 9 kHz bandwidth or  $106.5$  dB( $\mu$ V) in  $50 \Omega$ . Fig 68 shows the proposed conducted emission levels in relation to the EN 55022 Class 'B' conducted emission limits, which are generally applicable to domestic rather than industrial situations.

Another ETSI document, TS 101867 includes information on the average 'noise floor' that may be expected on mains power distribution networks. This 'noise floor' has been converted to dB( $\mu$ V) in  $50 \Omega$  in 9 kHz bandwidth and is also shown on Fig 68. The fact that this 'noise floor' falls by 20 dB from 1.6 - 30 MHz indicates that in practice, the conducted noise level on typical mains power distribution networks is far below the EN 55022 'B' limit over much of the HF band.

This result is consistent with measurements of radiated emissions generated by typical electronic equipment such as switch-mode power supplies. Such emissions may be within a few dB of the EN 55022 'B' limit at frequencies below 1 - 2 MHz but are normally far below the EN 55022 Class 'B' limit in the higher parts of the HF band.

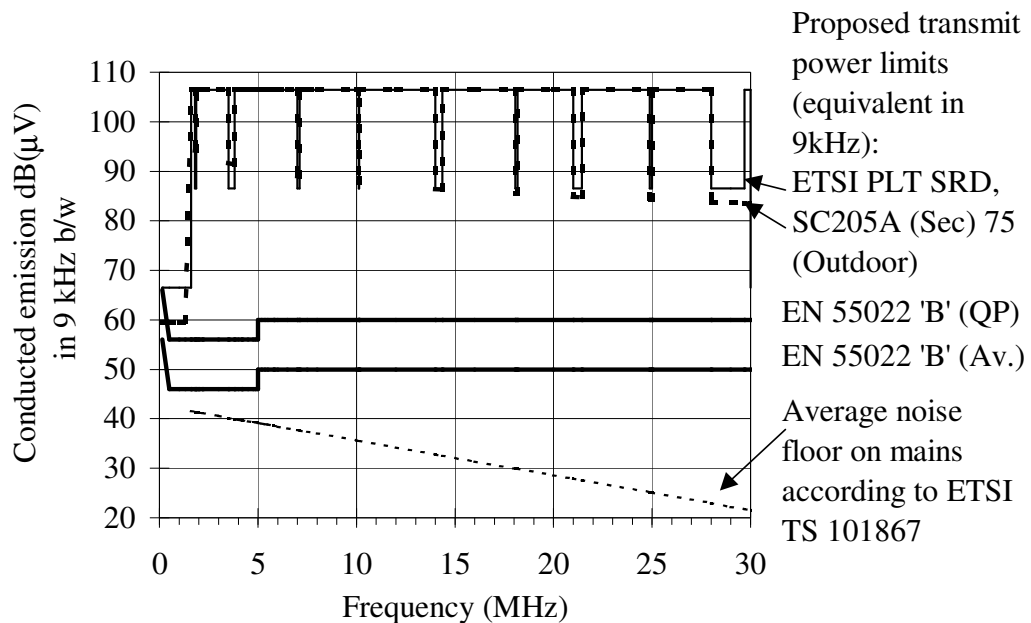


Figure 68. A proposed PLT transmit power limit from the ETSI PLT SRD and CENELEC SC205A (Sec) 75 in relation to EN 55022 Class 'B' conducted emission limits and background noise levels on mains power networks at frequencies up to 30 MHz.

PLT is a cabled distribution system and it could be argued that it should be subject to limits that are no higher than those for other cable distribution systems such as cable television networks. Even the cable TV emission limits could be considered to be too high because they were not intended for broad band multi-carrier modulation techniques. RSGB has expressed the view [84] that broad band emissions from PLT in amateur bands should not exceed 0 dB( $\mu$ V/m) in 9 kHz bandwidth at a distance of 10 m.

### 7.2.3. Recent standards work on PLT/PLC

A summary of the current standards situation in Europe with respect to ETSI and CENELEC standards as of March 2007 is included in a report by the Radio Spectrum Committee of the European Commission Information Society and Media Directorate-General [85], which states,

#### *"Power Line Telecommunications*

*ETSI and CENELEC have been working under mandate to find a single harmonized standard for radiated emissions from networks, including CATV, PLT and xDSL. After considerable work in a joint CENELEC/ETSI working group, it had become clear that it was not possible to achieve consensus at this stage. The work items for the Harmonized Standards are therefore on hold, while practical experience of networks is gathered in the field.*

*The Joint Working Group is developing a Code of Practice covering engineering guidelines and field trial reporting of Powerline access networks, in line with Commission Recommendation on broadband electronic communications in powerlines 2005/292/EC.*

*In parallel, ETSI Technical Committee Power-Line Telecommunications (PLT) is developing a specification TS 102 578 including a "smart notching" mechanism to reduce the potential of PLT modems to interfere with short-wave radio broadcasting. The mechanism operates by detecting SW radio broadcasts and applying selective notching into the PLT modem signal to limit interference."*

The ETSI document TS 102 578 mentioned above is still under development in July 2007 and is not publicly available. Nevertheless, it is understood that a recent draft includes a definition of the so-called "noise floor" and that the test procedure specified involves measuring the energy in adjacent bands above and below a particular short wave radio band. Nevertheless, the specified test procedure does not appear to distinguish between intentionally transmitted signals and background noise in the adjacent bands. This could lead to misinterpretation of the

apparent 'noise floor' and has major significance as some measurements of emissions are made in relation to the so-called 'noise floor'.

Another technique that has been proposed for reduction of interference is called 'smart notching' where a PLT modem attempts to detect the presence of intentional HF broadcasts by their ingress into power wiring. If such transmissions are detected, the PLT modem then applies an adaptive 'notch' to its frequency spectrum to avoid the frequencies that appear to be in use [36], [86]. Although such a technique may appear to work for strong AM broadcast signals on the HF bands, it may not be able to detect all receivable broadcast signals because the power wiring is likely to have lower gain and higher interference levels than the antenna of a radio receiver. There is also a question of whether the noise-like signals of DRM broadcasts could be detected, other than by actually demodulating the DRM data.

Another group working on EMC standardisation is CISPR/I/PT PLT, which is working with the COST 286 project, Electromagnetic Compatibility (EMC) in Diffused Communications Systems under Joint Technical Action 2 (JTA2). The CISPR/I/PT PLT/JTA2 group is working on measurement and characterisation of various parameters including K-factor of power wiring, characterising radiated emission from BPL, regression values [87], LCL and/or MDF of BPL systems, common mode impedance of mains wiring up to 30 MHz and above and ingress noise levels.

It is argued in some quarters that there should be a single international standard for PLT/BPL under CISPR 22, which would be a combination of a product standard and a radiated emission standard. This contrasts with the existing situation where CISPR 22 defines conducted emission limits below 30 MHz that are lower than those emitted by practical PLT systems.

It is understood that the US FCC part 15 rules are due to be reviewed and there is a possibility that the limit for BPL systems in the US may be reduced in order to align with any future international standard.

### **7.3. Conclusions**

PLT Emissions in the radio spectrum cannot be confined to the mains power distribution cables. Proposed PLT radiated emission levels may conflict with the EC EMC Directive

89/336/EEC and UK Statutory Instrument 1992 No. 2372, The Electromagnetic Compatibility Regulations.

A great deal of work has been done in the past 8 years or more on EMC standards for PLT, DSL and other wireline communication systems. Nevertheless, it has not been possible to agree on emission limits for PLT that provide a level of protection that is acceptable to radio users whilst also allowing PLT systems to achieve the range and data rates that their designers desire.

A compromise that has been proposed is to use 'smart notching' where PLT equipment detects whether a particular range of HF spectrum is in use by broadcast signals and avoids using such frequencies.

## **Chapter 8. Final analysis of research programme and recommendations for further investigations**

### **8.1. EMC measurements - conclusions**

A portable measuring system consisting of a set of three tuned loop antennas covering frequency range of 80 kHz - 30 MHz has been designed and developed. These antennas offer significantly improved sensitivity in LF, MF and HF field strength measurements compared to untuned loops. The tuning of each loop can be controlled remotely by a PC via an optical fibre communications link and software has been developed that controls the antennas and an EMC measuring receiver, thereby permitting swept frequency measurements to be made. The prototype set of remotely tuned loop antennas was used by the Radiocommunications Agency for field trials on PLT systems in Crieff and Campbeltown.

One of the remotely tuned loop antennas has been further developed as a 1.6m diameter loop that provides increased sensitivity in the range 1.75 - 10 MHz so that background atmospheric noise rather than receiver or pre-amplifier noise becomes the limiting factor to measuring system noise floor. An improved short dipole antenna for EMC measurements from 10 - 30 MHz has also been designed.

A paper was submitted to the CISPR/A committee in 2000 that resulted in an amendment to CISPR16-1 to permit the use of tuned loop antennas as well as untuned loops.

A test method has been developed for measurement of common-mode currents in a network cable by means of a small loop located at a specified distance from the cable.

### **8.2. EMC measurements - suggestions for further work**

The 1.6 m diameter loop could be further developed to provide full software control using LabVIEW™ software in order to allow HF background noise levels to be measured. A further development would be to develop an algorithm that searches for frequencies that appear to be free of intentional signals and then reduces the resolution bandwidth and logs background noise on 'quiet' frequencies, i.e. frequencies that appear to be free of intentional signals.



The short dipole for 10 - 30 MHz could be further developed and calibrated. An improved remotely tuned matching network could be developed, either for a dipole or for a monopole.

### **8.3. Emissions from wireline networks - conclusions**

Tests have been performed on various data communication networks that use existing cable infrastructure. These include Power Line Telecommunication (PLT) and home networks using domestic mains electricity wiring or indoor telephone wiring. The tests on indoor telephone wiring are also applicable to splitterless xDSL.

Tests performed include complex impedance, effective antenna gain and LCL. The validity of an LCL test method used by other researchers for in-building power wiring has been questioned.

Tests were performed to measure the radiated emissions of a test signal from a dipole and a buried power cable with signals being received via an NVIS ionospheric propagation path with an estimated length of 600 km.

Some antenna modelling of networks was also performed although it was found to be difficult to model mode conversion from differential mode to common mode by means of antenna modelling software.

### **8.4. Emissions from wireline networks - suggestions for further work**

Further work on LCL test methods could compare the results from various different methods of grounding the LCL probe, as described in Section 2.3 above, in order to establish the validity of various LCL test methods for measuring in-building powerline networks in-situ. It may also be useful to submit a paper on the results of this work to a relevant EMC standards working group.

Further work on antenna modelling of various wireline networks could be performed with a view to developing a method of modelling mode conversion from differential mode to common mode.

## **8.5. Protection of radio communications - conclusions**

The protection requirements of various radio communication services from emissions from telecommunication networks have been studied in relation to unintentional emissions from wireline networks. It has been shown that emission limits that give adequate protection to radio communications are too low to allow some wireline communication systems, particularly PLT, to operate. Conversely, emission limits that allow PLT systems to operate fall short of protecting radio communications by a large margin.

There is therefore no emission limit that could permit PLT to operate while also protecting radio services. This leads to the conclusion that PLT and radio communication services are electromagnetically incompatible with each other if they operate at the same time, on the same frequency and in the same location.

## **8.6. Protection of radio communications - suggestions for further work**

ITU-R publication PI 372-6 [69] gives details of natural and man-made noise levels in the RF spectrum. There is evidence that certain values listed in PI 372/6, such as man-made HF noise levels for residential areas, may be significantly higher than levels that are found in the UK in practice. There is scope for further work to make measurements of man-made and natural background noise levels in the UK and to compare these results with the data in PI 372-6. Such measurements would need to be made over a swept range of frequencies up to 30 MHz at various times of the day and at various seasons. It would be necessary to use an antenna with a known gain that is sufficiently high to ensure that the noise floor of the receiving system would not be the limiting factor to measurements. The tuned loop antennas described in section 4 above offer a possible solution. This type of measurement is of particular significance in view of confusion that exists in some quarters about the meaning of atmospheric 'noise floor', for example in the current draft of ETSI Technical Specification TS 102 578.

Automatic swept measurement and logging under software control is required and can be implemented using LabVIEW software.

## **References**

- [1] P. Brown, "Power line communications - past, present and future," presented at 3rd IEEE International Symposium on Power-Line Communications and its Applications, Lancaster, UK, 1999,
- [2] Ofcom Office of Communications, "Ascom PLT measurements in Winchester," 11 May 2005  
<http://www.ofcom.org.uk/research/technology/archive/cet/powerline/ascom.pdf>.
- [3] Ofcom Office of Communications, "DS2 PLT measurements in Crieff," 11 May 2005  
<http://www.ofcom.org.uk/research/technology/archive/cet/powerline/ds2.pdf>.
- [4] J. H. Stott, J. E. Salter, "The effects of power-line telecommunications on broadcast reception: Brief trial in Crieff," BBC Research & Development Ref. White Paper WHP067, September 2003.
- [5] J. Newbury, "Technical developments in power line communications," presented at 3rd IEEE International Symposium on Power-Line Communications and its Applications, Lancaster, UK, 1999,
- [6] F. Issa, D. Chaffanjon, and A. Pacaud, "Outdoor radiated emission associated with power line communications systems," presented at 2001 IEEE International Symposium on Electromagnetic Compatibility, 2001,
- [7] R. V. Womersley, R. D. Simmons, and C. V. Tournadre, "Final report on a study to investigate PLT radiation," The Smith Group Ltd. Ref. HA134D009-1.1 (RA Ref AY3062), 1998  
[http://www.ofcom.org.uk/static/archive/ra/topics/research/topics/emc/plt/plt\\_intr.htm](http://www.ofcom.org.uk/static/archive/ra/topics/research/topics/emc/plt/plt_intr.htm).
- [8] Technical University of Dresden, "Abschlussbericht zur Power-Line Studie," 27 January 2000 [http://www.regtp.de/tech\\_reg\\_tele/start/in\\_06-03-02-03-00\\_m/index.html](http://www.regtp.de/tech_reg_tele/start/in_06-03-02-03-00_m/index.html).
- [9] L. S. Cohen, J. W. de Graaf, A. Light, and F. Sabath, "The measurement of broad band over power line emissions," presented at International Symposium on Electromagnetic Compatibility, 2005,
- [10] E. Hare, "Measurements and calculations of BPL emissions," presented at EMC 2005. IEEE International Symposium on Electromagnetic Compatibility, 2005,
- [11] Ofcom Office of Communications, "Amperion PLT measurements in Crieff," 20 September 2005  
<http://www.ofcom.org.uk/research/technology/archive/cet/powerline/amperion.pdf>.

- [12] J. Newbury, "Measurement of LV PLC Channels," presented at Power Line Communications and Its Applications, 2006 IEEE International Symposium on, 2006,
- [13] G. Young, K. T. Foster, and J. W. Cook, "Broadband multimedia delivery over copper," *BT Technology Journal*, vol. 13, pp. 78-96, 1995.
- [14] K. T. Foster, et al, "Realising the potential of access networks using DSL," *BT Technology Journal*, vol. 16, pp. 34-47, 1998.
- [15] F. Amemiya, et al, "Estimation of electromagnetic interference field emitted from telecommunications line," *IEICE Transactions on Communications*, vol. E78, pp. 159-67, 1995.
- [16] L. De Clercq, et al, "Mitigation of radio interference in xDSL transmission," *IEEE Communications Magazine*, vol. 38, pp. 168-173, 2000.
- [17] K. Foster, "On the subjective effect of RF emissions from VDSL - a practical comparison between transmissions from two laboratory demonstrators," American National Standards Institute (ANSI), Ref. T1E1.4/96-191, July 1996.
- [18] K. T. Foster, et al, "The radio frequency environment for high speed metallic access systems," presented at IEEE Globecom '96 VDSL Workshop, London, 1996,
- [19] D. W. Welsh, "Investigation of Impedance and Mode Conversion of Telecommunications Cables for xDSL Systems, Final Report AY3944," York EMC Services Ltd. Ref. 5051CR, June 2001  
<http://www.ofcom.org.uk/static/archive/ra/topics/research/topics/emc/ay3944/ay3944.htm>.
- [20] A. R. Bullivant, "Continuation of Investigations into the Possible Effect of DSL Related Systems on Radio Services," ERA Technology Ltd. Ref. 2001-0333, RA Ref. AY3949, May 2001  
<http://www.ofcom.org.uk/static/archive/ra/topics/research/topics/emc/ay3949/ay3949.htm>.
- [21] M. Darnell, N. Pem, "OFDM Using Complementary Sequences for Data Transmission Over Non-Gaussian Channels," presented at 3rd IEEE International Symposium on Power-Line Communications and its Applications, Lancaster, UK, 1999,
- [22] S. Battermann, H. Garbe, "Influence of PLC transmission on the sensitivity of a short-wave receiving station," presented at International Symposium on Power Line Communications and Its Applications, 2005, 2005,

- [23] Royal Air Force Signals Engineering Establishment, "Investigation into threat to HF communications from digital signalling over power cables," Ministry of Defence (Air), Henlow, Beds. UK. Ref. RAFSEE Tech Report 99022, 1999.
- [24] I. D. Park, "EMC assessment of Digital Powerline (DPL) Communications System," Army CIS Engineering Group, EMC Division, Blandford, Dorset, UK. Ref. ENG/EMC/MI/6049 (Restricted - commercial), 10 Sept 1998.
- [25] J. H. Stott, "Protection of 'sensitive' receiving sites, paper for RA Working Group on HF mains signalling," BBC Research & Development. Ref. t1282, 21 Oct 1999  
<http://www.bbc.co.uk/rd/pubs/papers/pdffiles/t1282.pdf>.
- [26] M. H. Capstick, I. D. Flikntoft, and A. D. Papatsoris, "Specification of the Scope of Work Needed to Determine the Technical and Operational Impact of Emissions from Unstructured Telecommunications Transmission Networks Interfering with Aeronautical and Maritime Radio Services in the UK, Final Report (AY4075) for Radiocommunications Agency," York EMC Services, Report Ref. 4206CR3, April 2002  
<http://www.ofcom.org.uk/static/archive/ra/topics/research/topics/emc/ay4075final.pdf>.
- [27] J. H. Stott, "DRM - key features," *EBU Technical Review*, vol. 286, March, 2001.
- [28] J. H. Stott, "Digital Radio Mondiale: key technical features," *Electronics & Communication Engineering Journal*, vol. 14, pp. 4-14, 2002.
- [29] J. Briggs, "DRM - a summary of the field tests," *EBU Technical Review*, October 2003.
- [30] J. H. Stott, "The threat to new radio systems from distributed wired-communication installations," presented at IEE Eighth International Conference on HF Radio Systems and Techniques IEE Conf. Publ.No.474. 2000: 385-9, London, UK, 2000,
- [31] J. H. Stott, "Cumulative effects of distributed interferers," BBC Research & Development Ref. White Paper WHP004, August 2001.
- [32] J. H. Stott, "AM broadcasting and emissions from xDSL/PLT/etc. Compatibility analysis of various proposals for limits," BBC Research & Development Ref. White Paper WHP012, November 2001.
- [33] J. H. Stott, "Emission limits - A new proposal based on a limited increase in the noise floor," BBC Research & Development Ref. White Paper WHP013, November 2001.
- [34] J. H. Stott, "Do EMC limits protect broadcasting as intended?," BBC Research and Development Ref. White Paper WHP055, February 2003.
- [35] J. H. Stott, "How best to protect radio services as intended?," BBC Research & Development Ref. White Paper WHP063, 2003.

- [36] J. H. Stott, "PLT and broadcasting - can they co-exist?," BBC Research & Development Ref. White Paper WHP099, November 2004.
- [37] J. H. Stott, "Co-existence of PLT and Radio Services - A Possibility?," BBC Research & Development Ref. White Paper WHP114, June 2005.
- [38] D. Lauder, J. Moritz, "Design of a portable measuring system capable of quantifying the LF and HF spectral emissions from telecommunications transmission networks at field strengths of 1 microvolt/metre and below," University of Hertfordshire, Report Ref. RA project AY3430, 1999  
<http://www.ofcom.org.uk/static/archive/ra/topics/research/topics/emc/measure/measure.htm>.
- [39] D. Lauder, "Development of Practical Methods and Equipment to Facilitate Detection and Measurement of Radiation From, and Wideband Radio Frequency Currents in, Unstructured Distribution Networks," University of Hertfordshire, Report Ref. RA project AY3920, 5 Jan 2003  
<http://www.ofcom.org.uk/static/archive/ra/topics/research/topics/emc/ay3920.pdf>.
- [40] D. Ball, J. Loughlin, "PLT Measurements at Crieff," Radiocommunications Agency, Baldock Radio Station Ref. Report ML2 014/02, 25th November 2002  
[http://www.ofcom.org.uk/static/archive/ra/topics/research/topics/emc/edcrie\\_2.pdf](http://www.ofcom.org.uk/static/archive/ra/topics/research/topics/emc/edcrie_2.pdf).
- [41] D. Lauder, "EMC and Interference Issues Related To Networking Systems Used In The Home - Examining Compatibility Issues and Worldwide Standards That May Impact Home Phonenumber And Powerline Networks.," presented at 3rd Home Networks Congress, London, 2001,
- [42] T. Hahner, B. Mund, "EMC-performance of balanced (symmetrical) cables," presented at IEE Colloquium on Screening Effectiveness Measurements (Ref. No. 1998/452), 1998,
- [43] I. P. Macfarlane, "A Probe for the Measurement of longitudinal conversion loss (LCL) and transverse Conversion Loss (TCL) in the frequency range 0.04-30 MHz," Ref. CISPR/G/WG2 (Macfarlane) 3, November 1998.
- [44] I. P. Macfarlane, "A probe for the measurement of electrical unbalance of networks and devices," *IEEE Transactions on Electromagnetic Compatibility*, vol. 41, pp. 3-14, 1999.
- [45] CCITT (now known as ITU-T), "Recommendation G.117, Transmission Aspects of unbalance about earth,," in *Blue Book*, vol. Fascicle III.1. Geneva, Switzerland: CCITT, 1989.

- [46] CCITT (now known as ITU-T), "Recommendation O.9, Measuring arrangements to assess the degree of unbalance about earth," in *Blue Book*, vol. Fascicle IV.4. Geneva, Switzerland: CCITT, 1989.
- [47] A. Stuart, "EMC in data communications using unscreened cables," School of Electronic, Communication and Electrical Engineering, University of Hertfordshire, Hatfield, Herts, UK, BEng final year project report 2003.
- [48] J. Catrysse, K. Vantomme, "White Paper on CISPR/I/PLT," presented at COST 286 Workshop at EMC Europe 2006, Barcelona, 2006,  
[http://www.emc.york.ac.uk/cost286/Technical%20reports/BarcelonaSept2006/white\\_paper\\_CISPR\\_I\\_PLT\\_WG\\_version\\_15052006.pdf](http://www.emc.york.ac.uk/cost286/Technical%20reports/BarcelonaSept2006/white_paper_CISPR_I_PLT_WG_version_15052006.pdf)
- [49] D. Lauder, Y. Sun, "Modelling and measurement of radiated emission characteristics of power line communications systems for standards development," presented at 3rd IEEE International Symposium on Power-Line Communications and its Applications, Lancaster, UK, 1999,
- [50] D. Lauder, Y. Sun, "Radiated emission characteristics of communication systems using unscreened cables," presented at IEE 11th International Conference on Electromagnetic Compatibility, York, UK, 1999,
- [51] T. Williams, *EMC for Product Designers*, 4th ed: Elsevier, 2006.
- [52] HomePNA, "HomePNA Home Networking," HomePNA Alliance, Web pages <http://www.homepna.org>, Accessed: July 2007
- [53] D. Griffith, "Surface Transfer Impedance of Cable Shields Having a Longitudinal Seam," *IEEE Transactions on Communications*, vol. 19, pp. 517-522, 1971.
- [54] P. Martinez, "Using Doppler DSP to study HF Propagation," *Radio Communication*, vol. 74, pp. 16-20, 1998.
- [55] D. W. Welsh, I. D. Flintoft, and A. D. Papatsoris, "Cumulative Effect Of Radiated Emissions From Metallic Data Distribution Systems On Radio Based Services (AY3525) for Radiocommunications Agency," York EMC Services Ltd. Ref. R/00/0026, 2 May 2000  
<http://www.ofcom.org.uk/static/archive/ra/topics/research/topics/emc/ay3525/intro.htm>  
 .
- [56] HomePlug, "HomePlug Powerline Alliance," Web pages [www.homeplug.org](http://www.homeplug.org), Accessed: July 2007
- [57] R. W. Lewallen, *Software manual for EZNEC Antenna Modelling Software, Version 2.0*, 1998.

- [58] L. B. Cebik, "Antenna Modeling," Web site,  
<http://www.cebik.com/amod/modeling.html>, Accessed: July 2007
- [59] I. Flintoft, A. D. Papatsoris, D. W. Welsh, and A. C. Marvin, "Modelling of the Cumulative Emissions of Unstructured Telecommunications Transmission," presented at Cost 286 Workshop - Liege, March 2004, Liege, Belgium, 2004,  
[http://www.emc.york.ac.uk/cost286/Technical%20reports/Liege%20March%202004/Cost286\\_Liege\\_IFlintoft.pdf](http://www.emc.york.ac.uk/cost286/Technical%20reports/Liege%20March%202004/Cost286_Liege_IFlintoft.pdf)
- [60] D. M. Hockanson, et al, "FDTD modeling of common-mode radiation from cables," *IEEE Transactions on Electromagnetic Compatibility*, vol. 38, pp. 376 -387, 1996.
- [61] E. Hare, "Methods of Feeding Overhead Electrical Power-Line Distribution Lines With BPL Signals and the Relationship of These Methods to the Radiated Emissions of the Conductors," American Radio Relay League, Online report, 7th July 2003,  
[http://www.arrl.org/announce/regulatory/et03-104/bpl\\_feed\\_methods\\_analysis.pdf](http://www.arrl.org/announce/regulatory/et03-104/bpl_feed_methods_analysis.pdf),  
 Accessed: July 2007
- [62] E. Hare, "NEC Analysis of Power Lines as Radiators," Report by American Radio Relay League, Newington, CT, USA 22 June 2004  
<http://www.arrl.org/announce/regulatory/et04-37/reply-comments/reply-comments-exhibit-a.pdf>.
- [63] "Characteristic Impedance," in *Radio Communication Handbook, Sixth Edition*, D. Biddulph, Ed.: Radio Society of Great Britain, 1994, pp. 12.18-12.20.
- [64] British Standards Institute, "BS EN 55022 : 2000, EMC standard for Information technology equipment (ITE)," 2000.
- [65] R. Collin, F. Zucker, "The Shielded Loop, section 11.8," in *Antenna Theory Part 1*,: McGraw-Hill, 1969.
- [66] British Standards Institute, "BS CISPR 16-1:1999 Specification for radio disturbance and immunity measuring apparatus and methods. Radio disturbance and immunity measuring apparatus," 1999.
- [67] British Standards Institute, "BS EN 55016-1-1:2004 Specification for radio disturbance and immunity measuring apparatus and methods. Radio disturbance and immunity measuring apparatus," 2004.
- [68] M. Kanda, "Standard Antennas for Electromagnetic Interference Measurements and Methods to Calibrate Them," *IEEE Transactions on Electromagnetic Compatibility*, vol. 36, no. 4, pp. 261-273, 1994.



- [69] International Telecommunications Union, "ITU-R Recommendations, 1994 PI Series Volume, 'Propagation in Ionized Media' Recommendation," International Telecommunications Union Ref. ITU-R PI.372-6, 1994.
- [70] D. Lauder, "EMC - Measuring background noise," in *Radio Communication*, vol. 83, No. 6, 2007, pp. 45-45.
- [71] ETSI, "Technical Specification TS 101 270-1 V1.1.2 (1998-06) Transmission and Multiplexing (TM); Access transmission systems on metallic access cables; Very high speed Digital Subscriber Line (VDSL); Part 1: Functional requirements," 1998.
- [72] A. J. Rowell, I. D. Flintoft, "Development of improved test methods for assessing the EMC emissions from luminaires and ancillary devices, AY4125 for Radiocommunications Agency," York EMC Services Ltd. 2002.
- [73] G. Prieto, M. Velez, P. Angueira, D. Guerra, and D. de la Vega, "Minimum ON requirements for DRM reception based on field trials," *Communications Letters, IEEE*, vol. 9, pp. 877-879, 2005.
- [74] International Telecommunications Union, "Phone-line networking transceivers - Foundation," Specification Ref. G.989.1 (G.pnt.f), 2001.
- [75] European Commission, "Council Directive 89/336/EEC of 3 May 1989 on the approximation of the laws of the Member States relating to electromagnetic compatibility.," *Official Journal of the European Communities*, vol. L139, 1989.
- [76] HMSO, "The Electromagnetic Compatibility Regulations," Ref. UK Statutory Instrument, SI 1992 No. 2372, 1992.
- [77] P. Hewitt, "Broadband Telecommunications, House of Commons Hansard Written Answers for 9 Nov 2000 (pt 4)," 2000.
- [78] European Commission Enterprise Directorate-General, "Mandate M/313 (Telecommunication Networks)," Brussels Ref. M 313 EN, 7 August 2001 [http://europa.eu.int/comm/enterprise/electr\\_equipment/emc/m313\\_en.pdf](http://europa.eu.int/comm/enterprise/electr_equipment/emc/m313_en.pdf).
- [79] RegTP (Regulierungsbehörde für Telekommunikation und Post), "Nutzungsbestimmung (Usage Provision) regulations NB 30," Ref. NB30-07/01, 2001.
- [80] German Regulatory Authority for Telecommunications and Posts, "Radio Monitoring and Inspection Service Measurement Specification for Disturbance Field Measurements on Telecommunications Equipment and Lines in the Frequency Range from 9 kHz - 3 GHz," Ref. Reg TP 322 MV 05., January 2000.

- [81] D. Hansen, "Update on power line telecommunication (PLT) activities in Europe," presented at Electromagnetic Compatibility, 2002 IEEE International Symposium on, 2002,
- [82] PLCforum, "PLC Forum," Web site 2007, <http://www.plcforum.org/>, Accessed: July 2007
- [83] D. Lauder, "EMC - PLT," in *Radio Communication*, vol. 77, No. 4, 2001, pp. 90-90.
- [84] D. Lauder, R. Page-Jones, F. Robins, and H. Clayton-Smith, "Compatibility between radio communications services and power line communication systems - A position paper prepared by the RSGB EMC Committee for the PLC Workshop in Brussels, 5-Mar-2001," 2001 <http://www.rsgb.org/emc/pdfs/plt/emcplc.pdf>.
- [85] European Commission - Information Society and Media Directorate-General, "Radio Spectrum Committee, Working Document. Subject: ETSI Report to RSC#19," Brussels Ref. DG INFSO/B4, RSCOM07-19 Rev1, 2007  
[http://ec.europa.eu/information\\_society/policy/radio\\_spectrum/docs/ref\\_docs/rsc19\\_public\\_docs/rscom07\\_19\\_r1\\_etsi\\_report\\_RSC19.pdf](http://ec.europa.eu/information_society/policy/radio_spectrum/docs/ref_docs/rsc19_public_docs/rscom07_19_r1_etsi_report_RSC19.pdf).
- [86] J. H. Stott, "PLT and broadcasting - can they co-exist?," *EMC & Compliance Journal*, Issue 55, pp. 16-26, 2004.
- [87] J. Newbury, "The assessment and Measurement of the signal Regression of Broadband Power Signals in the frequency range 1.6MHz to 30MHz over the low voltage distribution Network," presented at Power Line Communications and Its Applications, 2007. ISPLC '07. IEEE International Symposium on, Pisa, Italy, 2007,

## **Bibliography**

Stolle R, *Electromagnetic coupling of twisted pair cables*, IEEE Journal on Selected Areas in Communications, June 2002; 20(5): 883-92

Nobesawa M, et al, *Induced voltage on a communication cable caused by incoming radio waves*, Electronics and Communications in Japan, Part 1 Communications. 2002; 85(4): 10-22

Harlacher B L; Stewart R W, *Common mode voltage measurements comparison for CISPR 22 conducted emissions measurements*, IEEE International Symposium on Electromagnetic Compatibility, 2001, Pages: 26 -30 vol.1

Mardiguian M; Raimbourg J, *Shielded (STP) versus unshielded (UTP) twisted pairs: an EMC comparison*, IEEE International Symposium on Electromagnetic Compatibility, 2001, Pages: 43 -46 vol.1

Maki M, et al, *Immunity of communications systems using a balanced cable*, IEEE International Symposium on Electromagnetic Compatibility 2001, Pages: 37 -42 vol.1

Harlacher B L; Stewart R W, *Comparison of common mode impedance measurements using 2 current probe technique versus V/I technique for CISPR 22 conducted emissions measurements*, IEEE International Symposium on Electromagnetic Compatibility, 2001, Pages: 17 -20 vol.1

Rannou V.; Brouaye F. et al, *Statistical analysis of the end current of a transmission line illuminated by an elementary current source at random orientation and position*, IEEE International Symposium on Electromagnetic Compatibility, 2001, Pages: 1078 -1083 vol.2

Yamamoto N, et al, *Prediction of electromagnetic noise induced on unshielded twisted pair cable for high speed LAN*, Proceedings of the 2000 International Symposium on Antennas and Propagation ISAP2000, 21-25 Aug. 2000 Fukuoka, Japan, Pages 1577-80 vol. 4

Stecher M, *Limits Test methods and ISNs for emission and immunity on unshielded telecommunication ports*, IEEE International Symposium on Electromagnetic Compatibility, 1999, Pages: 71 -74

Hiroshima Y, et al, *Method of measuring conducted disturbance using both capacitive voltage probe and current probe*. IEEE International Symposium on Electromagnetic Compatibility, 1999, Page: 798

Hahner T, Mund B, *EMC-performance of balanced (symmetrical) cables*, IEE Colloquium on Screening Effectiveness Measurements, 1998 (Ref. No. 1998/452), Pages: 8/1 -8/7

Shimoshio Y et al, *LCTL characteristics of twisted pair cable represented by varying lumped elements*, 1998 Asia Pacific Microwave Conference Proceedings. APMC'98. 1998: 1207-10 vol.3

Shimoshio Y et al, *A new calculation method of LCTL for balanced pair cable with partial unbalance*, Proceedings of 14th International Symposium on Electromagnetic Compatibility. 23-25 June 1998 Wroclaw, Poland, Pages 175-9

Ehrich M, et al, *Models of a cable bunch formed by twisted three-phase cables*, Proceedings of IEEE International Symposium on Electromagnetic Compatibility, 1997, Pages: 463 -466

Harms P, et al, *Simulating measurements for a cable radiation study*, IEEE Transactions on Electromagnetic Compatibility, Volume: 38 Issue: 1, Feb. 1996, Pages: 25 -30

Hockanson D M, et al, *FDTD modeling of thin wires for simulating common-mode radiation from structures with attached cables*, IEEE International Symposium on Electromagnetic Compatibility, 1995. Symposium Record, Pages: 168 -173

Yanagawa K, *A measurement of balanced transmission lines using S-parameters*, Proceedings of IEEE Instrumentation and Measurement Technology Conference - IMTC '94. vol. 2 10-12 May 1994 Hamamatsu, Japan

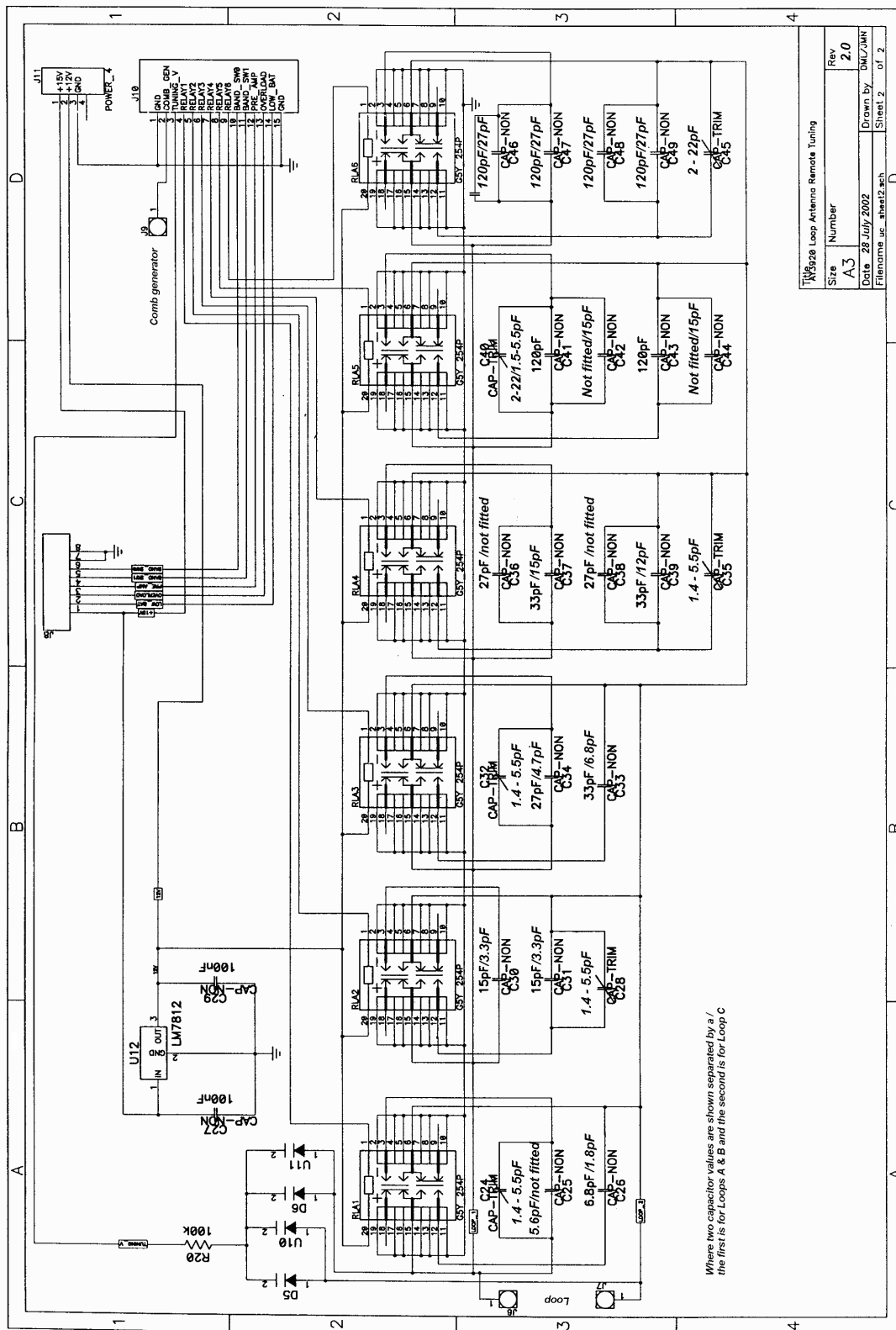
Bromley K, *Electromagnetic compatibility of building cables*, IEE Proceedings on Science, Measurement and Technology, Volume: 141 Issue: 4, July 1994 Pages: 263 -265

Gisin F, *Using the method of moment NEC code to solve EMC problems*, IEEE International Symposium on Electromagnetic Compatibility, 1993. Symposium Record, Aug. 1993 Pages: 275 -278

Arafiles V P; Valdez I, *Power line noise effects and new radio noise models*, IEEE International Symposium on Electromagnetic Compatibility, 1993. Symposium Record., 1993 , Aug. 1993, Pages: 51 -52

Millen E, *A comparison of loop antennas*, IEEE International Symposium on Electromagnetic Compatibility, 1990, Symposium Record., Pages: 451 - 455





Title		Rev
TK3928 Loop Antenna Remote Tuning		2.0
Size	Number	
A3		
Date	Drawn by	
28 July 2002	DMU/JMN	
Filename uc_a3st22.sch	Sheet 2	of 2

Figure 70. Schematic diagram of loop remote tuning switched capacitor board





## Appendix C. Scattering or 's' Parameters

**Scattering** or 's' parameters are used at RF where they describe a component or device in terms of the effect it has on waves incident on it and reflected from it.

$S_{mm}$  = reflection parameter at port 'm'

$S_{mn}$  = transmission parameter to port 'm' from port 'n'

Where 'm' and 'n' are integers corresponding to the numbered ports of the device.

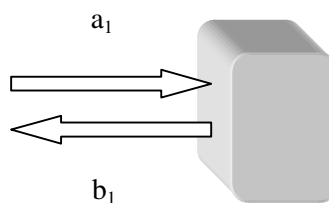
For example:

$S_{11}$  is the complex reflection parameter at port 1.

$S_{21}$  is the transmission parameter to port 2 from port 1.

### Single Port Device

Consider the following *single port device* (e.g.; load impedance) with incident wave  $a_1$  and reflected wave  $b_1$  ;



The following can be written;

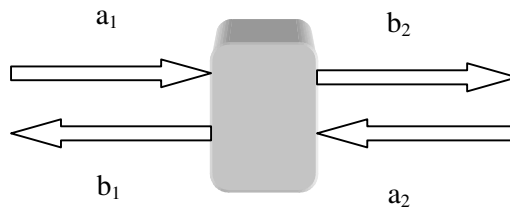
$$b_1 = s_{11}a_1$$

or as a simple matrix;

$$[b_1] = [s_{11}][a_1]$$

## Two Port Device

Consider the following *two port device* (e.g.; amplifier) with incident waves **a<sub>1</sub>** and **a<sub>2</sub>** and reflected waves **b<sub>1</sub>** and **b<sub>2</sub>**;



The following can be written;

$$\begin{aligned} b_1 &= s_{11}a_1 + s_{12}a_2 \\ b_2 &= s_{21}a_1 + s_{22}a_2 \end{aligned}$$

or as a simple matrix;

$$\begin{bmatrix} b_1 \\ b_2 \end{bmatrix} = \begin{bmatrix} s_{11} & s_{12} \\ s_{21} & s_{22} \end{bmatrix} \begin{bmatrix} a_1 \\ a_2 \end{bmatrix}$$

## Scattering Parameters and Reflection Coefficient

By definition, the reflection coefficient  $\Gamma$  at any point is the ratio of the net reflected wave to the forward wave. The reflection coefficient  $\Gamma_n$  at any port can therefore be evaluated in terms of the 's' parameters of the device;

$$\Gamma_1 = \frac{b_1}{a_1} = s_{11} + \frac{s_{12}a_2}{a_1}$$

and

$$\frac{1}{\Gamma_2} = \frac{b_2}{a_2} = s_{22} + \frac{s_{21}a_1}{a_2} \Rightarrow \frac{a_2}{a_1} = \frac{s_{21}\Gamma_2}{1 - s_{22}\Gamma_2}$$

hence;

$$\Gamma_1 = \frac{b_1}{a_1} = s_{11} + \frac{s_{12}a_2}{a_1} = s_{11} + \frac{s_{12}s_{21}\Gamma_2}{1 - s_{22}\Gamma_2}$$

The above demonstrates that the reflection coefficient at a port (in this case port 1) may be influenced by that at another port (in this case port 2).

**NOTE: If port 2 is matched, then  $\Gamma_2 = 0$  hence  $\Gamma_1 = s_{11}$**

### Important Points about S-Parameters

- Scattering parameters can be used to describe a device no matter how many ports it has
- Waves **a** and **b** have magnitude and phase and so may be represented as complex numbers. These could either be in polar form, e.g.  $Ve^{j\theta}$  or rectangular form  $V(\cos \theta + j \sin \theta)$ .

## **Appendix D. The author's research papers and reports**

The following research papers and reports are included in this appendix (not included in the electronic copy of this thesis):

D. Lauder and Y. Sun, "Modelling and measurement of radiated emission characteristics of power line communications systems for standards development," presented at 3rd IEEE International Symposium on Power-Line Communications and its Applications, Lancaster, UK, 1999.

D. Lauder and Y. Sun, "Radiated emission characteristics of communication systems using unscreened cables," presented at IEE 11th International Conference on Electromagnetic Compatibility, York, UK, 1999.

D. Lauder and J. Moritz, "Design of a portable measuring system capable of quantifying the LF and HF spectral emissions from telecommunications transmission networks at field strengths of 1 microvolt/metre and below," University of Hertfordshire Report for RA, Ref. AY3430, 1999. (excluding appendices containing full details of electronic design which are commercially confidential to Ofcom and are not published)

D. Lauder and Y. Sun, "Prediction and measurement of HF radiated emissions from communication networks that use unscreened cables," presented at HF Radio Systems and Techniques, 2000. Eighth International Conference on (IEE Conf. Publ. No. 474), Guildford, UK, 2000.

D. Lauder, "EMC and Interference Issues Related To Networking Systems Used In The Home - Examining Compatibility Issues and Worldwide Standards That May Impact Home Phoneline And Powerline Networks" presented at 3rd Home Networks Congress, London, 2001.

D. Lauder, "EMC - PLT," in Radio Communication, vol. 77, No. 4, 2001, pp. 90.

Lauder D, Page-Jones R, Robins F and Clayton-Smith H "Compatibility between radio communications services and power line communication systems - A position paper prepared by the RSGB EMC Committee for the PLC Workshop in Brussels, 5-Mar-2001,"

D. Lauder, "Development of Practical Methods and Equipment to Facilitate Detection and Measurement of Radiation From, and Wideband Radio Frequency Currents in, Unstructured Distribution Networks," University of Hertfordshire, report for RA Ref. AY3920, 5 Jan 2003 (excluding appendices containing full details of electronic design and program source code which are commercially confidential to Ofcom and are not published)

Lauder D, Sun Y, "EMC Measurements of Radiated Emissions up to 30 MHz from Installed Communication Cables", IEE Symposium, "EMC - It's Nearly All About the Cabling", IEE Savoy Place, London, UK. 22 Jan 2003.

Lauder D, Sun Y, "Modelling and Measurement of Radiated Emission Characteristics of In-building Power and Telecommunications Cables", IEE Symposium, "EMC and Broadband - The Last Mile" IEE, Savoy Place, London, UK. 17 May 2005

Lauder, D "EMC - Measuring background noise," in Radio Communication, vol. 83, No. 6, 2007, pp. 45.